The Dissertation Committee for Misti Caudle White Certifies that this is the approved version of the following dissertation:

A MECHANISM FOR SCA10 NEURODEGENERATION DUE TO INTRONIC REPEAT EXPANSION

Committee:

Tetsuo Ashizawa, M.D. Supervisor

Joel Gallagher, Ph.D.

Ralf Krahe, Ph.D.

Golda Leonard, Ph.D.

Giulio Taglialatela, Ph.D.

Dean, Graduate School of Biomedical Sciences

A MECHANISM FOR SCA10 NEURODEGENERATION DUE TO INTRONIC REPEAT EXPANSION

by

Misti Caudle White, B.S.

Dissertation

Presented to the Faculty of the Graduate School of

The University of Texas Medical Branch

in Partial Fulfillment

of the Requirements

for the Degree of

Doctor of Philosophy

The University of Texas Medical Branch

March 26, 2007

Dedication

This work is dedicated to my continually supportive family. Without your encouragement, I could not have done this.

Acknowledgements

First, I would like to thank the UTMB community. I truly appreciate the willingness to help and the expertise each of the core facilities provides, specifically the Quantitative RT-PCR core lab and Dr. Huiping Guo as well as the histopathology core lab. We would like to thank Dr. Claudio Soto and Dr. Ana Tari for their valuable suggestion and Dr. Jeffery White for his help in critical reading in the second chapter of the manuscript. I would like to take this opportunity to thank my committee members. They have gone above and beyond to offer support as I forged through the normal time constraints of a PhD student and had multiple committee meetings within months of each other. Dr. Leonard, thank you for your continuous support as an advisor, a committee member, and a friend. Dr. Taglialatela, thank you for your expertise in cell culture and apoptosis. Dr. Gallagher, thank you for the knowledge you gave me in Cell Excitability and Synaptic Transmission, as well as your endless words of encouragement. Dr. Krahe, thank you for the many trips from Houston, and for your expertise within the repeat field. I would also like to thank Dr. Kelly Dineley and Dr. Dale Hogan. They offered extensive knowledge in the transgenic mice characterization. Also, Dr. Partha Sarkar, my guide and philosopher, thank you for teaching me how to think scientifically and ethically. Dr. Rui Gao, thank you for your perfect hands; if I can do half of what you do, I will be doing well. And lastly, thanks to Dr. Tetsuo Ashizawa, my mentor, for his continuous motivation and for teaching me to think and write scientifically. What a great experience. This work was supported by grant NS041547 from NIH to TA and grant NS27699 to HYZ.

A MECHANISM FOR SCA10 NEURODEGENERATION DUE TO INTRONIC REPEAT EXPANSION

Publication No._____

Misti Caudle White, Ph.D.

The University of Texas Medical Branch, 2007

Supervisor: Tetsuo Ashizawa

Spinocerebellar ataxia type 10 (SCA10) is the second most prevalent ataxia in Mexico and Brazil. Phenotype of the disorder first occurs around the third to fourth decade, generally after procreation, resulting in a highly transmissible autosomal dominant disease. SCA10 begins as gait ataxia, but as the cerebellum degenerates, progresses to difficulties swallowing, loss of limb coordination, ocular abnormalities, and a basic inability to perform daily tasks. The disorder is due to an intronic repeat expansion, ATTCT, in the gene *Ataxin 10*. Ataxin 10 is a protein of unknown function. However, *Ataxin 10* from SCA10 patient samples is known to be fully transcribed and properly spliced, resulting in a normal, but expanded transcript. The results presented here demonstrate that the AUUCU transcript is the toxic species in SCA10. A ubiquitous protein within the cell, heterogeneous nuclear ribonucleoprotein kinase (hnRNP K), important for basic cellular function, binds the AUUCU expansion in *in vitro* binding experiments as well as within cell culture and in the brain of SCA10 transgenic animals.

The loss of function of hnRNP K is hypothesized to induce SCA10 phenotypes by resulting in the translocation of Protein Kinase C δ (PKCδ) to mitochondria, where it is known to activate apoptosis. Both induction of this mechanism through endogenous expression of expanded repeat and inactivation of hnRNP K, as well as rescue of the mechanism via reduced levels of *Ataxin 10* transcript and overexpression of hnRNP K, are utilized to validate the proposed SCA10 mechanism. The data presented in this dissertation provides a mechanism for possible therapeutic intervention into SCA10. Additionally, many similarities exist between SCA10 and other repeat expansion disorders such as myotonic dystrophy, the most common form of muscular dystrophy, other Spinocerebellar ataxias, Freidreich's Ataxia, and Fragile-X mental retardation, the most commonly inherited genetic disease. The results presented here provide a mechanism that can be utilized in the listed disorders to further understand the mechanism for therapeutical intervention.

Table of Contents

List of Tables

List of Figures

Chapter I:

Introduction

Neurodegeneration is defined by a progressive loss of structure and function of neurons. Generally, the word "neurodegeneration" is associated with well-known disorders such as Alzheimer's disease (AD), Parkinson's disease (PD), Huntington's disease (HD), and amyotrophic lateral sclerosis (ALS). Yet, hundreds of other neurodegenerative disorders exist. The most common risk factor for neurodegeneration is increasing age (Przedborski et al., 2003), although some of the genetically inherited disorders occur at a younger age. By looking at the etymology, "neuro" has Greek lineage, and literally means "from the nerve." Degeneration comes from the Latin derivative "degeneratus," meaning "to fall from ancestral quality." Degeneratus can be broken into two roots, one being "genus," where the word genetics was derived three centuries later by Thomas Carlyle, a Victorian era satirist and historian. Combined, the phrases come to mean a disorder affecting the nerves resulting in a disdained condition that should not be genetically continued. The word neurodegeneration stems from the 15th century when life expectancy was around 48 years (Lancaster, 1990). Given the current life expectancy has climbed to 79 years and the average population of elderly is increasing, the incidence of neurodegeneration is likely to increase.

Finding a molecular explanation for neurodegeneration has been quite difficult due to variability within the disorder. Degeneration of different regions of the central nervous system results in varied symptoms between and within disorders. Histopathological changes of these disorders often show misfolding and aggregations of various proteins such as β–amyloid, hyper-phosphorylated tau, and poly glutamine

aggregates, occurring both intra- and extracellularly. Despite concerted efforts to find an effective prevention or treatment, therapies have been hindered due to the limited knowledge of mechanisms by which neurons die in these debilitating disorders (Przedborski et al., 2003).

Spinocerebellar Ataxia Type 10 is an autosomal dominant neurodegenerative disorder in the category of spinocerebellar ataxias. The spinocerebellar ataxias (SCA) are dominantly inherited disorders of known genetic loci, which are broken into approximately three categories, autosomal dominant cerebellar ataxia I (ADCAI), ADCAII, and ADCAIII. All three groups manifest with cerebellar ataxia, but ADCAI and ADCAII have additional symptoms. ADCAI is variably associated with dysarthria, opthalmoplegia, pyramidal and extrapyramidal signs, sensory loss, and dementia. ADCAII is associated with progressive macular degeneration. More than twenty SCAs have been described, with degeneration primarily affecting the cerebellum, although other regions of the brain are also targeted in some of the SCAs. Though the mechanism of degeneration is not fully understood, some themes occur within the class of disorders. Most SCAs occur due to expansion of a repeat, typically CAG, though an expansion of pentanucleotide repeats and point mutations also are represented. The broad spectrum of this work encompasses the search for a mechanism for SCA10, the only pentanucleotide repeat expansion disease known to date.

CELL DEATH IN NEURODEGENERATION

In the vast majority of neurodegenerative disorders, drastic differences in normal and degenerating affected neurons are seen histopathologically. Generally, degenerating neurons show shape and size changes of cell body and nucleus, organelle fragmentation,

cytoplasmic vacuolization, chromatin condensation, and proteinaceous inclusion (Przedborski et al., 2003). Degeneration in brain is usually obvious and widely considered to represent programmed cell death. Programmed cell death is a planned course of action, thought of as an active "suicide" process, that can be subdivided in three categories. The first category is nuclear or apoptotic cell death, the second is autophagic cell death, and the third is cytoplasmic cell death (Bredesen et al., 1996). Several cellular mechanisms trigger programmed cell death, including misfolded proteins, reactive oxygen species, mitochondrial damage, and death receptor activation, all of which are known to occur in neurodegenerative diseases (Bredesen et al., 1996).

Fortunately, apoptosis is a well-researched cellular process, and is known to be executed in two major pathways: extrinsic and intrinsic. The extrinsic pathway originates through activation of cell-surface death receptors and activates caspase-8 or 10 (Salvesen and Dixit, 1997), while the intrinsic pathway originates from mitochondrial release of cytochrome c and activates caspase-9, and results in activation of caspase-3 (Yuan and Yankner, 1999). Biochemical responders such as Bcl-2 and Bax are either pro- or anti-apoptotic, and when pro-apoptotic activators outnumber the anti-apoptotic activators, the cell executes suicide. The pro-apoptotic biochemical responders are known to be activated by misfolded proteins and protein aggregations through the unfolded-protein response (UPR) (Taylor et al., 2002). The UPR is a stress response that postpones cell death temporarily, but the cell is eventually overwhelmed by the damage and results in apoptosis. The majority of the neurodegenerative disorders contain lesions resulting from misfolded, or aggregated proteins, resulting in a widely researched mechanism for activation of apoptosis (Taylor et al., 2002).

Autophagy is the second form of programmed cell death and the second most common implicated form of neurodegeneration and literally means self-eating. First studied as a starvation mechanism, autophagy also occurs as a prolonged stress response. Autophagy can be subdivided into macro- and micro-autophagy, and chaperone-mediated autophagy (Larsen and Sulzer, 2002). It accompanies the proteasomal degradation pathway, but includes protein degradation, protein aggregate degradation, and organelle degradation through lysosomal digestion. Literature debates the prevalence of autophagy versus apoptosis in neurodegenerative disorders, but the current opinion is that autophagy may provide protection in neurodegenerative disorders for many years, but eventually the cell toxicity becomes so prevalent that apoptosis occurs (Chu, 2006; Cuervo, 2004; Larsen and Sulzer, 2002).

Cytoplasmic cell death is also known as "necrosis-like" cell death, and is less accepted in the scientific community as programmed. Swelling of the ER and mitochondria occurs absent of typical apoptotic features such as apoptotic bodies and nuclear fragmentation (Bredesen et al., 1996).

REPEAT EXPANSION DISORDERS

SCA10 is caused by expansion of a microsatellite repeat within an intron, which should be excised and degraded during post-transcriptional events. While the mechanism of a non-coding repeat disorder is intriguing, it is not an isolated concept. Several other neurological disorders result from repeat expansion within an untranslated region. Friedreich's Ataxia (FRDA) is an autosomal recessive disorder resulting from an unstable GAA repeat within the first intron of the *frataxin* gene. The mutation results in *frataxin* loss-of-function due to transcription hindrance (Montermini et al., 1997). Fragile X

Syndrome (FMR1) and FRAXE mental retardation are other untranslated disorders resulting from CGG/CCG repeats within the promoter region of the *FMR1* and *FMR2* gene, respectively (Gunter et al., 1998). The mutation leads to hypermethylation of the repeat tract and an upstream CpG island, resulting in transcription silencing and loss of

Figure 1.1. Mechanisms of Repeat Expansion Disorders.

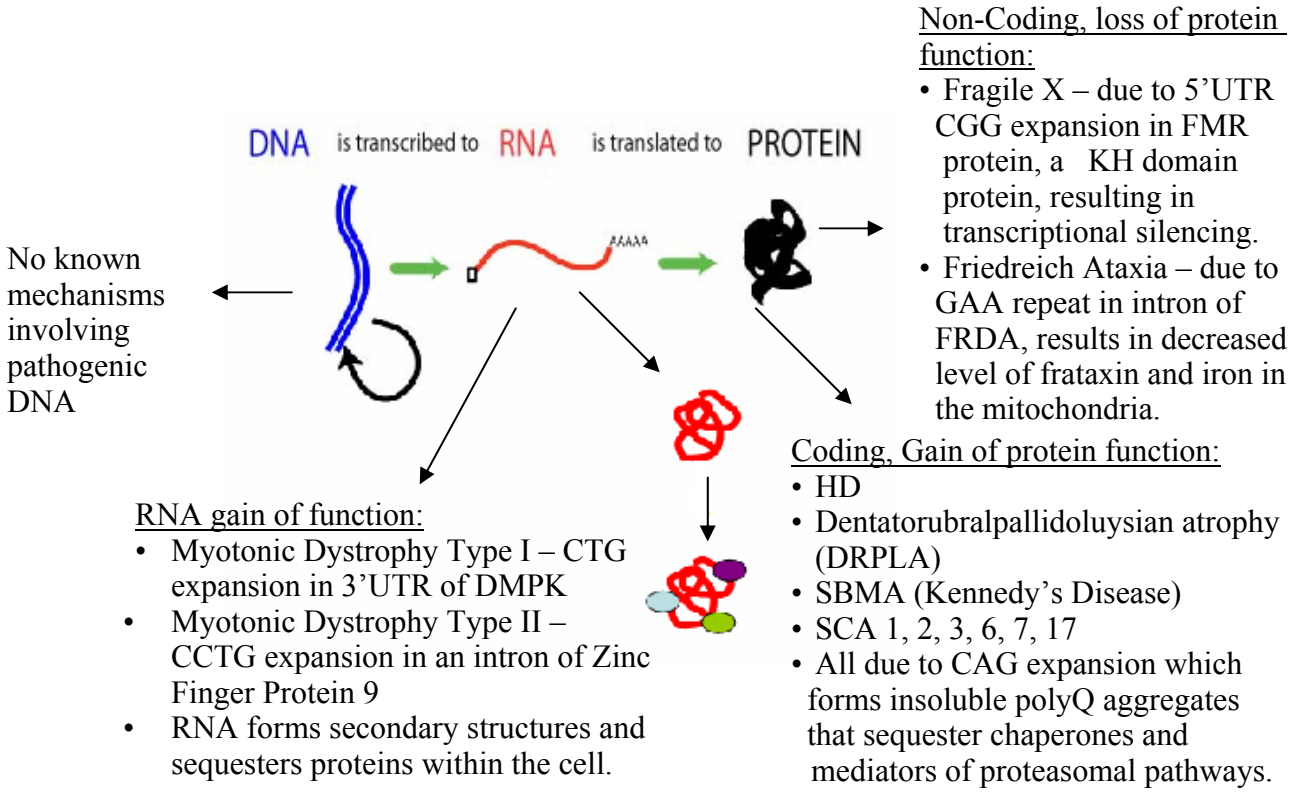

FMR1/FMR2 protein. FMR1 protein is an RNA-binding protein which contains two heterogeneous nuclear ribonucleoprotein kinase (hnRNP K) homology (KH) domains and an RGG box. CGG expansion of greater than 200 repeats in FMR1 results in fragile X

syndrome, but permutation of 55-200 CGG repeats results in fragile X tremor ataxia syndrome (FXTAS). In SCA8, a CUG repeat expansion occurs in the 3' UTR of the *SCA8* gene. Initially, CUG repeat-containing RNA was reported to bind to the gene Kelch-like 1(KLH1), and inhibits translation of the gene (Mosemiller et al., 2003). More recent reports suggest that the CUG repeat is translated on the opposite strand as a CAG repeat expansion, acting as a polyglutamine repeat expansion (Moseley et al., 2006). SCA12 results from a CAG repeat in the 5'UTR of a proteinphosphatase gene. The repeat expansion is thought to incur increased expression of this gene (Holmes et al., 1999) (Figure 1.1).

Two variations of myotonic dystrophy, myotonic dystrophy type 1 (DM1) and myotonic dystrophy type 2 (DM2), occur from a CTG expansion in the 3' UTR of the *DMPK* gene and a CCTG repeat expansion in the first intron of the *ZNF9* gene, respectively. DM1 and DM2 also represent diseases caused by a trans-dominant RNA gain of function. The repeat expansions sequester muscleblind proteins and form RNA-protein complexes in intranuclear foci. The sequestration results in pathogenesis by preventing the muscleblind proteins from performing their normal tasks. In DM1, CTG repeat expansion adversely affects upstream *(DMWD)* and downstream *(SIX5)* gene transcription (Klesert et al., 2000) . Expanded repeat in DM1 also has been associated with increased CUG-binding protein 1 (CUG-BP1) activity, with evidence that transgenic mice overexpressing CUG-BP1 show DM1-like phenotypes (Ho et al., 2005). The over-expression of CUG-BP1 is thought to disrupt splicing regulation and lead to DM1 pathogenesis. The disorders which most parallel SCA10 are the myotonic dystrophies, DM1 and DM2. In the majority of the other repeat expansion disorders, short, coding, trinucleotide repeats result in disease pathogenesis. DM1, DM2, and SCA10 all represent

repeat disorders with a non-triplet repeat, which is untranslated and extensively expanded.

SPINOCEREBELLAR ATAXIA TYPE 10

In 1999, a clinically and genetically new ADCA characterized with cerebellar ataxia and motor seizures was first described (Matsuura et al., 1999; Zu et al., 1999). The locus of mutation was narrowed down by linkage analysis to an 8.8 cM interval on chromosome 22, and the disease locus was designated SCA10. Several trinucleotide repeats were analyzed for expansion, but none were found. In the wildtype population, an ATTCT repeat in this region showed length polymorphism with heterozygosity in 87% of individuals, while patients showed hemizygosity at this locus by PCR analysis. Expansion of the second allele was identified by Southern blot (Matsuura and Ashizawa, 2002) and was subsequently deemed unamplifiable by PCR due to the large expansion. At the time, chromosome 22 almost had been fully sequenced by the Human Genome Project. The locus was later identified as *Ataxin 10 (ATXN10)*, so named after SCA10.

Initial identification of SCA10 occurred in two large Mexican families with a relatively pure cerebellar ataxia disorder with seizures (Matsuura et al., 1999; Zu et al., 1999). SCA10 is now the second most common ataxia in Mexico and Brazil, has recently been reported in Argentina, and new patients have been found from Guatemala. Mexican SCA10 patients typically demonstrate cerebellar atrophy, gait, dysarthria, dysphagia, ophthalmoplegia, dysdiadokinesis, and seizures (Figure 1.2). Seizures are reported in approximately 70% of the affected Mexican population (Rasmussen et al., 2001), but among the hundreds of Brazilians diagnosed with SCA10, only one Brazilian patient has been reported to suffer from seizures (Raskin, In press). Additional

symptoms seen in SCA10 Mexican patients not typical of the disorder included cognitive and psychiatric impairment, polyneuropathy, and pyramidal signs (Rasmussen et al., 2001). Brazilian

Figure 1.2. Clinical Symptoms of Spinocerebellar Ataxia Type 10.

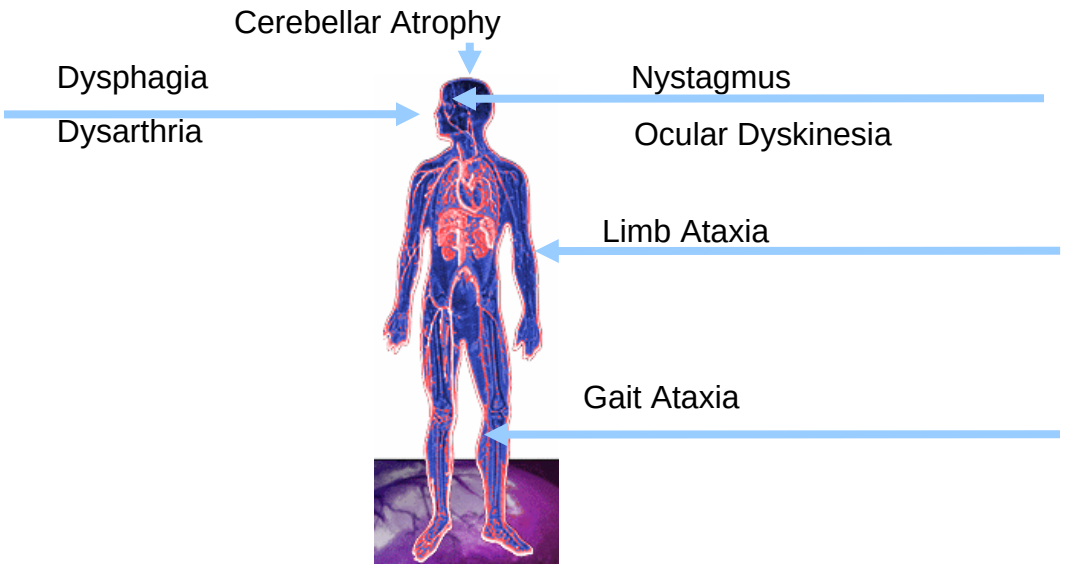

patients did not have seizures, showed no signs of polyneuropathy, or neuropsychologic abnormalities (Teive et al., 2004). Neurological MRI showed significant atrophy of the cerebellum in both Mexicans and Brazilians, with minimal or absent cortical or brain stem atrophy (Rasmussen et al., 2001; Teive et al., 2004). The sole Brazilian patient with seizures has an ethnic background including Italian, Portuguese, Spanish, and South American Indian ancestries, with this patient being the first and only Brazilian SCA10

patient known to have Spanish ancestry and suffer from abnormally aggressive phenotypes and seizures (Raskin, In press). Ethnicities of the Mexican, Argentinean, and Guatemalan SCA10 families all include Spanish and South American Indian ancestries, while Brazilian ancestries contained Portuguese and South American Indian ancestries. SCA10 is thought to be the result of the founder effect, linked primarily to South American Indian ancestries, but the variability between the ancestries in the patients who have the additional seizure phenotype with SCA10 is intriguing. While the Spanish ancestry poses a possibility for the additional seizure phenotype, the Amerindian ancestry in the Brazilian families could be different as well.

Ataxin 10

Ataxin-10 is a 55 kDa protein of unknown function, containing 476 amino acids, and 12 exons. Sequence similarity between murine and rat genomes is 94%, and 86% similarity occurs between human and rat, suggesting a high level of evolutionary conservation, particularly at the C-terminus (Marz et al., 2004). Ataxin-10 is expressed primarily in brain, but is also detectable in heart, liver, and hematopoeitic cells with high expression in testis (Marz et al., 2004; Matsuura et al., 2000; Rasmussen et al., 2001). Within the brain, ATXN10 is highly expressed in deep cerebellar nuclei, nucleus cuneatus, nucleus pontis, vestibular nucleus, olivary nucleus, hypoglossal nucleus, Purkinje cells, and the midbrain/ Raphe nucleus (Marz et al., 2004). Mostly cytoplasmically expressed, ATXN10 does not contain subcellular localization signals. Fold recognition analysis to determine the secondary structure of ATXN10 shows clear similarities to the armadillo repeat protein family, specifically β-catenin and importin- β, suggesting importance in protein-protein interactions. Knockdown of ATXN10 by

small interfering RNA results in increased apoptosis in rat primary cerebellar neurons, suggesting that ATXN10 is vital for cell survival in the CNS (Marz et al., 2004). To determine molecular partners of ATXN10, Waragai et al conducted a yeast-two hybrid analysis, where G-protein β2 was identified as an ATXN10 interacting protein which activates neuritogenesis through the Ras-MAP kinase cascade (Waragai et al., 2006). Recently, ATXN10 was reported to be constitutively bound to O-linked-β-N-Acetylglucosamine Transferase p110, a protein containing an armadillo-like domain that has previously shown importance in Alzheimer's and in Diabetes type II, specifically in hyper or hypoglycosylation of target proteins (Marz et al., 2004).

Expanded ATTCT Repeat

The mutation responsible for SCA10 is an expansion of ATTCT repeats within the 65kb, ninth intron of *ATXN-10* (Matsuura et al., 2000). Due to the autosomal dominant nature of SCA10, only one allele requires repeat expansion to induce a disease state. In normal individuals, alleles are approximately 80% heterozygous and range from 10 – 29 repeats. In affected individuals, allele size is variable with the smallest disease-producing allele being 280 repeats, and the largest described being 4500 repeats. Alleles up to 850 repeats appear to have reduced penetrance, based upon a mother-daughter case with both patients containing 280 repeats and only the daughter showing SCA10 phenotypes (Matsuura et al., 2006) and a Brazilian family with expanded alleles of 850 repeats scattered throughout the family, with only one patient showing SCA10 phenotypes and seizures (Raskin, In press).

Stability of the expanded repeat is sex-dependent with paternal inheritance of the expanded allele resulting in either shrinkage or expansion. However, when maternally

inherited, the repeat remains remarkably stable. The unstable expansion of the repeat, when paternally inherited, has been correlated to an earlier onset in offspring, resulting in anticipation based upon the size of the repeat (Matsuura et al., 2004). Instability of the repeat in germline tissues is likely the reason for variable paternal transmission (Matsuura et al., 2004). Somatic tissues also display variable instability, with blood samples being relatively stable, while buccal samples are somewhat unstable, leaving the stability of the repeat questionable within the brain.

The abnormally small nature of the repeat in the Mexican family with reduced penetrance (280 repeats ~ approximately 6kb) was subjected to PCR amplification and sequencing. Extensive interruption was found in the ATTCT repeat expansion, and contained novel repeated sequences within the expansion (Matsuura et al., 2006). Somatic cell hybrids and cloning experiments in our lab have illustrated that many of the Mexican families contain interruptions within the repeat expansion, some with recurring interrupted patterns. In contrast, to date, cloning and sequencing data of the Brazilian repeats shows pure ATTCT's (unpublished data). Purity differences between the Mexican and Brazilian patients provide an interesting correlation with the disparate phenotype of SCA10 between Mexican and Brazilian patients.

How the expansion of the repeat occurs is not understood, just as the mechanism is unknown in many of the other repeat expansion disorders. However, the SCA10 repeat forms abnormal, unpaired structures at high superhelical densities in repeat lengths up to 43 ATTCT's (Potaman et al., 2003). The normal allele size ranges from 10 – 29 repeats, with large, normal alleles (>17 repeats) generally containing an interrupting sequence before the final repeat (Matsuura et al., 2006). The unpaired region of DNA is accessible to small molecules and can serve as an aberrant origin of replication in HeLa cell extract

(Potaman et al., 2003). Aberrant activation of replication at regions of unpairing perhaps could help explain the mechanism for expansion. Slippage, speculated in other CAG repeat disorders, is not likely to occur in SCA10, due to minimal slipped strand DNA being detectable (Potaman et al., 2003). Subsequent studies suggest that the propensity for the repeat to unpair is due to the relatively low GC content and abnormally high superhelical stress, not present at physiological conditions (Handa et al., 2005). However, this report found an unusual tendency for the transcribed form of the repeat, AUUCU, to form RNA hairpins at physiological conditions. RNA hairpins are characteristic of repeat disorders (FRDA, fragile-X, DM1 and DM2) known to form "toxic RNA" and result in RNA-mediated gain of functions. Double stranded RNA is known to sequester proteins and cause activation of various RNA-dependent protein kinases which can activate various cell-signaling pathways and expression of genes (Handa et al., 2005).

The Search for a Mechanism

To further substantiate the possibility that RNA hairpins could have a toxic role in SCA10 pathogenesis, Wakamiya et al.. investigated the efficiency of transcription of the expanded repeat. The *ATXN10* transcript was measured in lymphoblasts, fibroblasts, and myoblasts from SCA10 patients by Northern blot and found to occur at the same level and concentration as normal adult tissues, suggesting the mRNA is properly transcribed and spliced (Wakamiya et al., 2006). By RT-PCR, wildtype alleles also were found to be transcribed at the same level as expanded alleles without abnormal isoforms of alternatively spliced *ATXN10*. Neighboring genes were tested for altered transcription and found to be transcribed normally (Wakamiya et al., 2006). Additionally, the

epilepsy phenotype prompted analysis of the calcium channel gene *CACGN2*, also located on chromosome 22q13. Voltage-dependent calcium channel mutations have previously been associated with a variety of neurological phenomenon including spinocerebellar ataxia (SCA6), epilepsy, and cerebellar degeneration (Burgess et al., 2000). However, the *CACGN2* gene was studied prior to the discovery of the expanded ATTCT repeat and found to be distal to the region defined by linkage mapping.

Finally, in the search for a mechanism leading to neurodegeneration in SCA10, the level of ATXN10 protein was evaluated. Marz et al. previously found that knock-down of ATXN10 by siRNA was toxic to primary cerebellar neurons from rat (Marz et al., 2004). Initially, the induction of apoptosis due to decreased levels of ATXN10 was thought to provide the foundation in the hunt for a mechanism. However, upon generation of ATXN10 knockout mice, homozygous mice were found to be embryonic lethal prior to implantation, but heterozygotes were overtly normal (Wakamiya et al., 2006). Heterozygotes performed normally on rotating rod test (RotaRod), showing no cerebellar defects, and showed no histological changes in cerebellum (Wakamiya et al., 2006). Taken together, these results argue against a simple loss or gain of *ATXN10* as the pathogenic mechanism of SCA1O, with *ATXN10* being transcribed and spliced normally into a functioning protein.

Expanded AUUCU RNA

Exclusion of the ATXN10 protein abnormalities from the mechanism of SCA10, along with aberrant transcription of *ATXN10* gene partners, leaves a possible toxic DNA or RNA species. Based upon the report from Handa suggesting that AUUCU repeat forms RNA hairpins at physiological levels, and the mechanism of other repeat expansion

disorders involving RNA secondary structures (Fragile X syndrome, CUG repeat disorders), toxic RNA aggregates remain a plausible mechanism for SCA10 pathogenicity (Handa et al., 2005; Koch and Leffert, 1998; Weisman-Shomer et al., 2000). Moreover, DNA toxicity has not been previously reported in the repeat expansion disorders. Repeat Expansion Detection (RED) analysis on normal individuals has shown ATTCT expansion at loci other than *ATXN10*, suggesting that expansion of ATTCT is not toxic. Since the DM2 repeat expansion most closely parallels SCA10, and the DM2 repeat expansion is transcribed and sequesters muscleblind protein, MBNL, we wanted to investigate sequestration of proteins to the transcribed AUUCU expansion. To determine the fate of the expanded AUUCU repeat after transcription, *fluorescent in situ hybridization (FISH)* was performed on primary fibroblasts derived from SCA10 patients. The AUUCU expansion was found to aggregate as foci within the SCA10 cells. While the intron containing expanded AUUCU repeat was shown to be excised properly, normal degradation does not occur and results in insoluble inclusions of expanded RNA repeat. Eventually, preliminary data suggested the repeat bound *in vitro* and *in vivo* to an RNA-binding protein, heterogeneous nuclear ribonucleoprotein kinase (hnRNP K). Based upon this preliminary data, the hypothesis was formulated that the expanded ATTCT repeat in the mutant allele is transcribed into an expanded AUUCU repeat, which sequesters nuclear protein(s) (hnRNP K), resulting in loss of function of the sequestered protein(s).

HETEROGENEOUS NUCLEAR RIBONUCLEOPROTEIN KINASE

Few proteins are as ubiquitous within the cell as hnRNP K, or K protein. Four alternatively spliced transcripts have been described for this gene. As a member of the

hnRNA complex, it is essential in mRNA processing. Evolutionary conservation of hnRNP K, with 93% between human and mouse, suggests importance of this protein. Significantly conserved are the three K homology (KH) domains, which are RNA and DNA binding domains. HnRNP K is known to bind both single and double stranded DNA, RNA, and poly-C motifs within proteins. K protein also contains a KI region with proline rich docking sites which bind to SH3 domains, specifically the Src-family kinases. HnRNP K localizes in the cytoplasm and the nucleus, and is also found in the mitochondria where it functions as a transcription activator of many genes (Ostrowski et al., 2001). Both a nuclear localization signal (NLS) and a nuclear shuttling domain (KNS) are found in hnRNP K.

K protein is involved in activation and repression of signal transduction, gene expression through chromatin remodeling, transcription, RNA processing, mRNA stability, translation, and response to DNA damage. In transcriptional regulation, hnRNP K directly interacts with histone methyltransferases and DNA methyltransferases (Shnyreva et al., 2000). Additionally, hnRNP K enhances expression of transcription factor c-myc through interaction of TFIID TATA box-binding protein (TBP) (Michelotti et al., 1996). hnRNP K also interacts with the c-src promoter cooperatively with transcription factor Sp1 and represses Sp1 and Sp3 activation of neuronal nicotinic acetylcholine receptor β4 subunit (Du et al., 1993). HnRNP K binds multiple transcription factors including translation elongation factor-1 α (EIF-1 α), and translation initiation factor 4E (eiF4E). hnRNPK interacts with factors in RNA splicing and has been shown to bind enhancers in alternative splicing processes (Lee et al., 1996). As for mRNA stability, hnRNP K protein binds to the 3' UTR of renin and regulates its stability (Skalweit et al., 2003). The effects of hnRNP K on translation have been studied fairly

extensively. The protein is essential to mitigate extracellular changes, such as signals through various phosphorylation sites, allowing regulation of the cell by extracellular signals and providing accessibility to SH2 docking domains (Bomsztyk et al., 2004). HnRNP K is activated through two extracellularly activated signaling pathways, the Src-kinase pathway, and the PKCδ pathway. Additionally, hnRNP K is activated by ERK-1/2, which both binds and phosphorylates the TATA box binding protein (TBP). TBP, in turn, binds hnRNP K and adjoins the hnRNP K binding site of ERK 1/2, suggesting a possible role of a docking platform for hnRNP K (Bomsztyk et al., 2004). When hnRNP K interacts with hnRNP E1/2, an internal ribosome entry site is created within c-myc mRNA, a protein important in cell-cycle progression and transcriptional regulation. In addition, hnRNP K is equally important in repression of translation. By binding DICE elements in the 3'UTR of the 15-liposygenase (LOX) gene, blocking of the 60s ribosomal subunit occurs. It seems that the biological function of hnRNP K is multifaceted.

While hnRNP K is not essential for growth in yeast, embryonic lethality was seen in loss-of-function mutants in *C. elegans* (Piano et al., 2002). Point mutations in the *Drosophila* ortholog *bancal* resulted in extremely low viability (1-5%) (Charroux et al., 1999). Knockouts showed impaired development of appendages due to decreased cell proliferation. Moreover, over-expression of *bancal* resulted in apoptosis. These studies suggest that levels of *bancal*, or hnRNP K, are tightly controlled and are essential to determine cell fate. Mouse hnRNP K knockout has not been reported.

Several interesting pathways leading to cell death involve hnRNP K. hnRNP K binds a protein kinase, PKCδ, at a low constitutive level within the cell (Schullery et al., 1999). However, when hnRNP K binds RNA, PKCδ can no longer bind or phosphorylate hnRNP K (Bomsztyk et al., 2004; Schullery et al., 1999). Studies in

monocytes show that overexpression of PKCδ results in increased apoptosis, while inhibition of PKCδ decreases apoptosis. Apoptosis is mediated by PKCδ through phosphorylation of caspase-3, rendering caspase-3 more susceptible to proteolytic cleavage by caspase-9 (Voss et al., 2005). Additionally, PKCδ increases DNA fragmentation, leading to increased activation of caspase-3. If expanded AUUCU repeats prevent hnRNP K from binding with PKCδ, excess free PKCδ may accumulate within the cell. The free PKCδ may increase DNA fragmentation and phosphorylate caspase-3, leading to neuronal death in SCA10. Moreover, both PKCδ and hnRNP K are known to interact with p53. hnRNP K is rapidly induced by DNA damage through activation of known DNA-damage signaling kinases, ataxia telangiectasia mutated (ATM) and Rad3 related (ATR). A depletion in hnRNP K results in abrogated induction of p53, leading to faulty cell-cycle arrest points (Moumen et al., 2005). Furthermore, proteolytic activation of PKCδ is reportedly required for activation of p53 (Johnson et al., 2002). Both PKCδ and p53 have been implicated in genotoxic stress induction of mitochondrial-activated apoptosis (Lasfer et al., 2006). Given the consistent relationship between hnRNP K and PKCδ, and apoptosis, it seems likely that these proteins somehow may be working together to bring about apoptosis in SCA10.

Protein kinase C δ is a member of the protein kinase C family, which can be divided into three categories: classical PKCs (α, β1, β2, and γ) activated by diacylglycerol (DAG) and calcium, the novel PKCs (δ, ε, η, and θ) activated by DAG, and the atypical PKCs (ξ, and λ/ι) that do not respond to DAG or calcium. PKCδ is 78 kDa and contains a regulatory domain at the amino terminus and a catalytic domain at the carboxy terminus. Three phosphorylation sites are thought to prime the enzyme for activation by cofactors (Basu, 2003). PKCδ is a substrate for caspase-3, which cleaves

PKCδ, and results in activation of programmed cell death via apoptosis. Overexpression of the cleaved, catalytic domain of PKCδ has been shown to induce nuclear fragmentation and apoptosis (Brodie and Blumberg, 2003). When PKCδ is activated, it translocates from the cytoplasm to the plasma membrane (Szallasi et al., 1996), or translocates to mitochondria (Li et al., 1999). The chicken or the egg conundrum exists with PKCδ and caspase-3 activation. It is not fully understood whether caspase-3 first cleaves PKCδ, or PKCδ first translocates to mitochondria and results in cleavage of caspase-3. PKCδ inhibitors and PKCδ dominant negative mutants result in inhibition of activation of caspase-3 and cleavage of PKCδ (Brodie and Blumberg, 2003). However, caspase-3 and PKCδ are thought to act in a positive regulatory loop, with PKCδ being cleaved by caspase-3, and activated PKCδ cleaving caspase-3 (Brodie and Blumberg, 2003). Recently, a novel inhibitor targeted to PKCδ cleavage site of caspase-3 was shown to inhibit degeneration of dopaminergic neurons in Parkinson's disease (Kanthasamy et al., 2006). These results suggest that cleavage-specific interference of PKCδ may be therapeutical for Parkinson's Disease, and possibly SCA10.

In the study of SCA10, we hope to establish a mechanism for the disorder, as well as gain knowledge into the instigation of neurodegeneration. While SCA10 is the second most common ataxia in Mexico and Brazil and increasingly being diagnosed, the number of people affected is not expansive. However, several disorders similar to SCA10 result from repeat expansion and are highly prevalent, with the combined population affected by Huntington's, Parkinson's, Fragile X Mental Retardation, and the combined autosomal dominant cerebellar ataxias being vast. The pathogenic mechanism of SCA10 may have close similarity with the RNA gain of function of Myotonic Dystrophies, the most prevalent muscular dystrophy. Efforts placed in finding the

mechanism for neurodegeneration in SCA10 can be applied to other repeat expansion disorders, hopefully leading to insight to provide treatment.

The objective of this work is to determine a mechanism by which repeat expansion leads to neuronal death and pathogenesis. The central hypothesis is that the expanded ATTCT repeats encoded in the mutant allele are transcribed, and the transcripts encoding expanded AUUCU repeat sequester nuclear protein(s) which results in loss of function of the sequestered protein(s). The loss of function of sequestered proteins is projected to be the primary mechanism in SCA10. Preliminary data illustrated that the expanded AUUCU repeat binds heterogeneous nuclear ribonucleoprotein kinase (hnRNP K) both *in vitro* and *in vivo*. Preliminary data also suggested that inactivation of hnRNP K results in caspase-3 mediated apoptosis. To test the central hypothesis, two specific aims were established: to evaluate the extent of toxicity associated with expanded AUUCU repeat, and to determine the mechanism by which repeat expansion leads to neuronal death. These aims were investigated through *in vitro* experiments, in cell culture and in transgenic mice. Endogenous induction of the proposed mechanism by overexpressing AUUCU repeat or inactivating hnRNP K, as well as rescue of the proposed mechanism by inactivating *ATXN10* or overexpressing hnRNP K in fibroblasts derived from SCA10 patients, was used to validate the proposed mechanism. The data presented in this dissertation supports an RNA gain of function for SCA10, and sequestration of the protein hnRNP K. Similar sequestration of K homology domain proteins and RNA binding proteins can be evaluated in methods similar to the ones employed in this dissertation to provide a mechanism for degeneration in other repeat expansion and aggregation disorders.

Chapter II:

Expanded AUUCU RNA in SCA10 Facilitates Mitochondrial Translocation of PKCδ, Activating Apoptosis

SUMMARY

The genetic mutation in spinocerebellar ataxia type 10 (SCA10), an autosomal dominant neurodegenerative disorder, is an expansion of ATTCT repeats within intron 9 of *ATXN10* on chromosome 22q13.31. The mechanism for manifestation of SCA10 phenotypes due to the ATTCT expansion is currently unknown. Previous results have shown that neither a gain nor a loss of function of ataxin-10 protein is likely the pathogenic mechanism of SCA10. Our findings suggest that the mutant *ATXN10* transcripts encoding expanded AUUCU sequences are the principal pathogenic molecules that trigger neuronal apoptosis in SCA10. The expanded AUUCU RNA complexes with an RNA-binding protein, hnRNP K, and diminished cellular hnRNP K activity results in massive migration of PKCδ to mitochondria and activation of apoptosis. Together, these results provide a key mechanism for neuronal apoptosis and neurological deficiencies in SCA10 and clues for development of therapeutic strategies.

INTRODUCTION

Spinocerebellar ataxia type 10 (SCA10) is the second most common autosomal dominant cerebellar ataxia in Mexico and Brazil (Lin and Ashizawa, 2003; Rasmussen et al., 2001; Teive et al., 2004). The disorder first presents as an impaired gait, followed by progressive pan-cerebellar ataxia which leads to total disability (Lin and Ashizawa, 2003;

Lin and Ashizawa, 2005; Rasmussen et al., 2001; Teive et al., 2004). Additionally, approximately 60% of Mexicans with SCA10 also suffer from epilepsy with complex partial seizures and generalized tonic clonic seizures, which can become life-threatening due to development of status epilepticus (Matsuura et al., 2000; Rasmussen et al., 2001). The disease-causing genetic mutation is an expansion of a pentanucleotide repeat, ATTCT, present within the ninth intron of the *Ataxin 10* (*ATXN10*) gene on chromosome 22q13.31 (Matsuura et al., 2000). The ATTCT repeat is polymorphic in length, with the number of repeats in normal alleles ranging from 10 to 29, whereas the repeat lengths associated with SCA10 are expanded up to 4,500 repeats with intermediate alleles up to 850 repeats possibly showing reduced penetrance in rare SCA10 patients (Matsuura et al., 2006; Raskin, In press; Raskin, 2006). Thus, the SCA10 repeat expansion represents one of the largest microsatellite expansions known to occur within the human genome.

The *ATXN10* gene consists of 12 exons spanning 172.8 kb of genomic DNA, and encodes a novel protein, ataxin 10, which has no homology to other human proteins and contains no recognizable sequence domains except for two armadillo repeats. The presence of the armadillo repeats suggests a potential importance of ataxin 10 in cellular processes through interactions with other proteins. Marz and colleagues have shown that a knock-down of ataxin 10 with small interfering RNA (siRNA) causes neuronal death in primary cerebellar neurons (Marz et al., 2004). We recently demonstrated that ataxin 10 interacts with G-protein β2 subunit and increases differentiation of PC12 cells through activation of the Ras-MAPK pathway (Waragai et al., 2006). While *ATXN10* is expressed in a wide variety of tissues, the expression is especially strong in brain, heart and muscle. Although these data suggest that ataxin 10 may play a role in neuronal survival and differentiation, the exact function of ataxin 10 remains unknown.

Currently it is unknown how the massive expansion of the ATTCT repeats within the intronic region of the SCA10 gene results in neurodegeneration and manifestation of SCA10 phenotypes. Recently we demonstrated that neither a gain nor a loss of the physiological function of *ATXN10* is likely to be the primary pathogenic mechanism of SCA10 (Wakamiya M, 2006). Analyses of SCA10 patient-derived fibroblasts and lymphoblasts showed that the overall steady-state level of the *ATXN10* mRNA remains normal (Matsuura et al., 2004; Wakamiya M, 2006), and transcription of the mutant alleles, as well as splicing of the mutant *ATXN10* transcripts, is largely unaltered in SCA10 patients (Wakamiya M, 2006). These studies suggest that the ataxin 10 protein is unlikely to play a major role in the pathogenic mechanism of SCA10.

In the present study, we report experimental results supporting the hypothesis that the mutant *ATXN10* transcripts containing the expanded AUUCU sequences are the principal pathogenic molecules triggering neuronal death in SCA10. These results demonstrate that the expanded AUUCU RNA complexes with an RNA-binding protein, heterogeneous nuclear ribonucleoprotein kinase (hnRNP K), leading to reduced hnRNP K activity within SCA10 cells. We further show that the inactivation of hnRNP K in these cells results in translocation of Protein Kinase C δ (PKCδ) to mitochondria, where PKCδ is known to be an apoptotic activator (Schullery et al., 1999). Taken together, these results support our hypothesis and define a key pathogenic mechanism of SCA10.

RESULTS

The Mutant *Ataxin10* Transcripts are Accumulated in SCA-10 Cells as Discrete Aggregates

Since we have already shown that a gain or a loss of the function of the ataxin 10 protein is unlikely to be the major disease mechanism in SCA10 (Wakamiya M, 2006), we examined alternative disease mechanisms focusing on the pathogenic role of the mutant RNA transcript. We hypothesized that the mutant *ATXN10* transcripts containing expanded AUUCU repeats are the primary toxic molecules that trigger neuronal death leading to SCA10 disease phenotypes. We first carried out RNA fluorescent *in situ* hybridization (*FISH)* with a Cy3-labeled $(AGAAU)_{10}$ riboprobe on SCA10 fibroblasts containing a repeat expansion of approximately 2000 ATTCT repeats to detect the expanded AUUCU repeat transcripts. The SCA10 fibroblasts, but not normal fibroblasts, contained bright and distinct nuclear and cytoplasmic foci (Figure 1.1A), suggesting that the transcripts containing expanded AUUCU repeats are transcribed and deposited as distinct aggregates in SCA10 cells.

Ectopically Expressed Expanded AUUCU Repeats form Nuclear Aggregates

To ascertain whether the expanded AUUCU repeat sequences are sufficient to form aggregates, we transiently transfected PC12 cells with two different plasmids expressing either 12 or 500 AUUCU repeats. The plasmids contained a PrP promoter, a *LacZ* reporter gene, BGH poly-A sequences, and minimal *ATXN10* flanking sequences (Figure 1.1B). RNA *FISH* with the Cy3-labeled $(AGAAU)_{10}$ riboprobe revealed a large number of aggregates similar to those observed in SCA10 fibroblasts in the PC12 cells expressing between 400 and 500 ATTCT repeats (Figure 1.1C). In contrast, PC12 cells

Figure 2.1. Expanded AUUCU Transcripts form Discrete Cellular Aggregates.

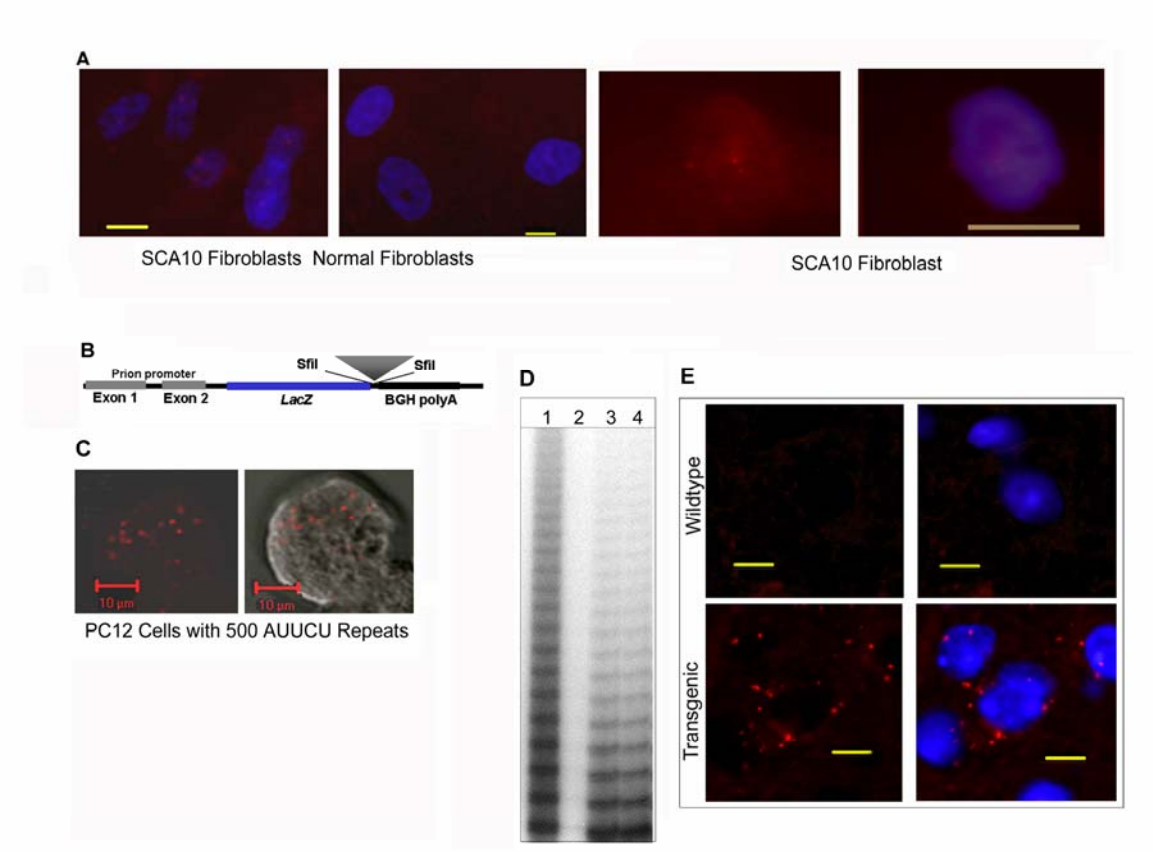

A. FISH on SCA10 fibroblasts and normal control fibroblasts hybridized with Cy3-$(AGAAU)_{10}$ probe and DAPI counterstain. Bottom two figures illustrate multiple, bright aggregates in the nucleus and in the far nuclear boundary, perhaps outside the nuclear membrane. Bars represent 10 µm. B. Schematic drawing of the transgene including a prion promoter (PrP), *LacZ* gene, expanded 500 ATTCT repeats (or normal range of 12 repeats for control), and BGH polyA signal. This construct was used in cell culture and in transgenics. C. *FISH* with Cy3-$(AGAAU)_{10}$ riboprobe on PC12 cells overexpressing the transgene in figure 1B. Distinct aggregates are seen nuclearly when compared to phase contrast. D. Ladder PCR of mouse genomic DNA showing expanded ATTCT repeats, lane 1 – Expanded transgene from Figure 1B (positive control), lane 2 – mouse negative for transgene, lane 3, 4 – two transgenic founders. E. FISH using Cy3-$(AGAAU)_{10}$ riboprobe and DAPI (blue) on sagittal brain sections of transgenic mice. Top boxes show pontine nuclei in normal, age-matched control; bottom boxes show AUUCU aggregates in pontine nuclei of 3 month old transgenics. Bars represent 20 µm.

expressing 12 ATTCT repeats did not contain any detectable aggregates (data not shown). These results support the idea that the expanded AUUCU RNA is necessary and sufficient to form RNA aggregates similar to those present in SCA10 cells.

To investigate whether expanded AUUCU RNA forms similar aggregates when expressed in mouse brain, novel transgenic mouse lines using the construct described in Figure 1B were developed. The repeat-primed PCR (RP-PCR) analysis of genomic DNA isolated from the transgenic mice showed an expanded smear of amplification products when analyzed on acrylamide gel, confirming the presence of expanded repeats (Figure 2.1D). Expanded AUUCU RNA is expressed predominantly in brain within these mouse lines since the transgene is driven by a rat prion promoter (PrP) (Boy et al., 2006). The transgenic mice develop structural and functional abnormalities characteristic of SCA10 (detailed characterization of the transgenic mouse is presented in Chapter 3). Open field analysis of the transgenic mouse shows that transgenics move at a significantly slower speed (n=5, p=0.006) for a significantly shorter distance (n=5, p=0.007) than wildtype littermates (see Chapter 3), suggesting that the transgenic mice may recapitulate the motor deficit seen in SCA10 patients. In sagittal sections of transgenic mouse brain, the RNA *FISH* showed distinct nuclear and cytoplasmic aggregates reminiscent of SCA10 cells most prominently in pontine nuclei and pyramidal and granular hippocampal neurons (Figure 2.1E). Similar aggregates were not found in wild type, age-matched control mice (Figure 2.1E). The formation of discrete aggregates in cells transfected with expanded AUUCU repeat as well as in transgenic mouse brain confirms that the expanded AUUCU repeat is sufficient to form RNA foci. Moreover, the formation of discrete foci suggests that the expanded AUUCU repeat may aggregate

as RNA-protein complexes, as described in other repeat expansion disorders (Gatchel and Zoghbi, 2005).

Expanded AUUCU RNA Activates Apoptosis

Analysis of PC12 cells transfected with plasmid expressing 500 AUUCU repeats by light microscopy showed that expression of expanded AUUCU repeats resulted in a dramatic increase in cell death, whereas cells transfected with normal-size repeats showed virtually no cell death. To determine whether the observed cell death involved activation of apoptosis, we performed a TUNEL assay. More than 70% of the PC12 cells expressing the expanded AUUCU repeat underwent apoptosis, while significantly fewer numbers (<20%) of cells expressing normal-size repeat underwent apoptosis, 48 hours after transfection ($p < 0.0001$) (Figure 2.2A and 2.2B). To determine whether the observed apoptosis is induced via the caspase-3 pathway, we measured caspase-3 activity in the PC12 cells expressing expanded AUUCU RNA. caspase-3 activity was significantly higher in cells expressing expanded AUUCU RNA compared to the control ($p < 0.0001$) (Figure 2.2C). These results suggest that the expanded AUUCU RNA repeat activates caspase-3-mediated apoptosis.

Expanded AUUCU RNA Binds hnRNP K *in Vitro*

Dissection of the molecular composition of the AUUCU RNA aggregates is an important step for identifying pathogenically relevant molecules interacting with the expanded repeat RNA. The expanded AUUCU RNA is likely to form complexes with proteins, seen as distinct aggregates in SCA10 cells. To identify proteins which potentially aggregate with the repeat expansion, we pulled down proteins from mouse

Figure 2.2. Expanded AUUCU Repeat Induces Apoptosis.

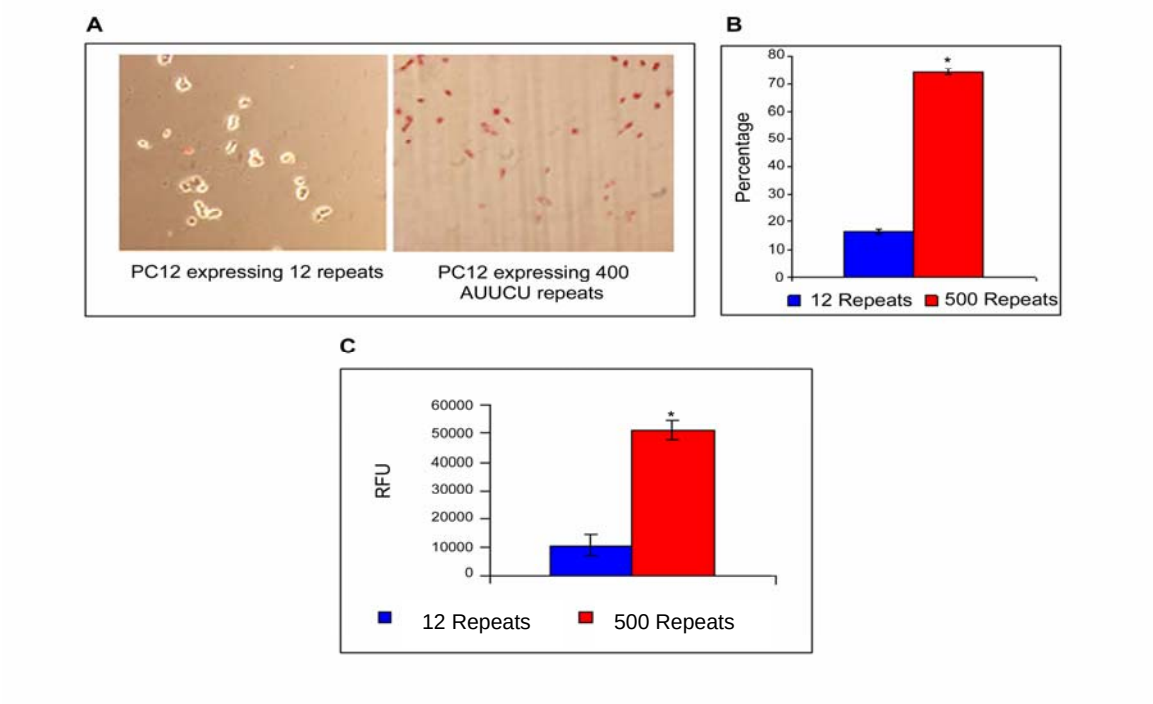

A. Percentage of cells in TUNEL assay undergoing apoptosis when PC12 cells were treated with either normal repeat (blue) or expanded repeat (red) (*n=6, $p<0.0001$). B. Caspase-3 assay showing percentage of cells undergoing apoptosis as counted by TUNEL assay when PC12 cells were transfected with short repeat (blue) and expanded repeat (red) (*n=3, $p<0.0001$). C. Caspase-3 assay showing relative fluorescent units (RFU) when PC12 cells are transfected with short repeat (blue) or expanded repeat (red) (*n=3, $p<0.0001$).

brain extract that interact with the AUUCU RNA repeat using biotin-labeled AUUCU repeat RNA (Figure 2.3). Polyacrylamide gel electrophoresis (PAGE) of the biotin-labeled repeat showed multiple, distinct bands suggesting that the single-stranded

AUUCU RNA formed different secondary structures with varying electrophoretic mobility (Figure 2.4A).

Figure 2.3. Method of Biotin Labeling Pull-Down Experiment.

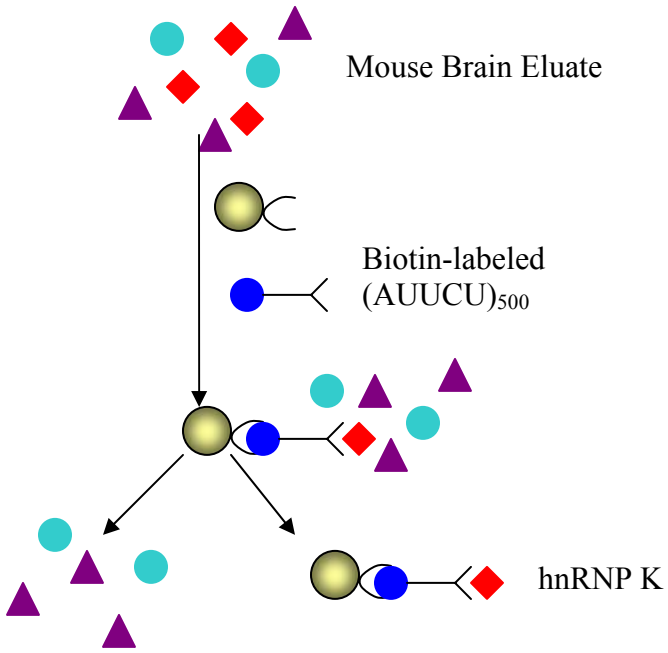

Biotin beads were labeled with expanded AUUCU and exposed to mouse brain eluate. Magnetic separation pulled down the protein hnRNP K.

The proteins that were pulled down with repeat RNA were further analyzed on SDS PAGE (Figure 2.4B). The protein that was specifically and reproducibly pulled down by repeat RNA (n=6) was analyzed by Mass Spectrometry as heterogeneous nuclear ribonucleoprotein kinase (hnRNP K) (shown in blue arrow). hnRNP K is a polypyrimidine binding protein containing three homology (KH) domains that mediate its

interactions with RNA and DNA, and a K interactive (KI) region with proline-rich docking sites important for sarc-homology domain (SH) binding. hnRNP K mediates multiple cellular processes such as transcription, cell proliferation, and regulatory processing, and constitutively binds an apoptotic activator, protein kinase C δ (PKCδ) (Schullery et al., 1999). The identification of hnRNP K as a protein partner of expanded AUUCU repeat provides a possibility that RNA-protein complexes of AUUCU RNA and hnRNP K might exist as aggregates in SCA10 cells as well as in transgenic mouse brain.

HnRNP K Complexes with the Expanded AUUCU Repeats *in Vivo*

Thus far, we have demonstrated that the expanded AUUCU repeat accumulates as bright foci in SCA10 cells and in the brain of transgenic mice expressing expanded AUUCU repeats, and the expanded AUUCU RNA specifically and reproducibly binds with hnRNP K *in vitro.* To investigate the possible *in vivo* interaction of the expanded repeat with hnRNP K, we investigated the co-localization of hnRNP K with AUUCU RNA in the transgenic mouse brain. The RNA *FISH* analysis showed a significant overlap between the red fluorescence from the AUUCU repeats and green fluorescence from hnRNP K both in the neurons of the hippocampus and the pontine nuclei, as well as in other regions of the brain (Figure 2.4C). A high degree of co-localization suggests that hnRNP K interacts with the expanded AUUCU RNA *in vivo.*

Figure 2.4. Expanded AUUCU RNA Binds hnRNP K *in Vitro* and *in Vivo*.

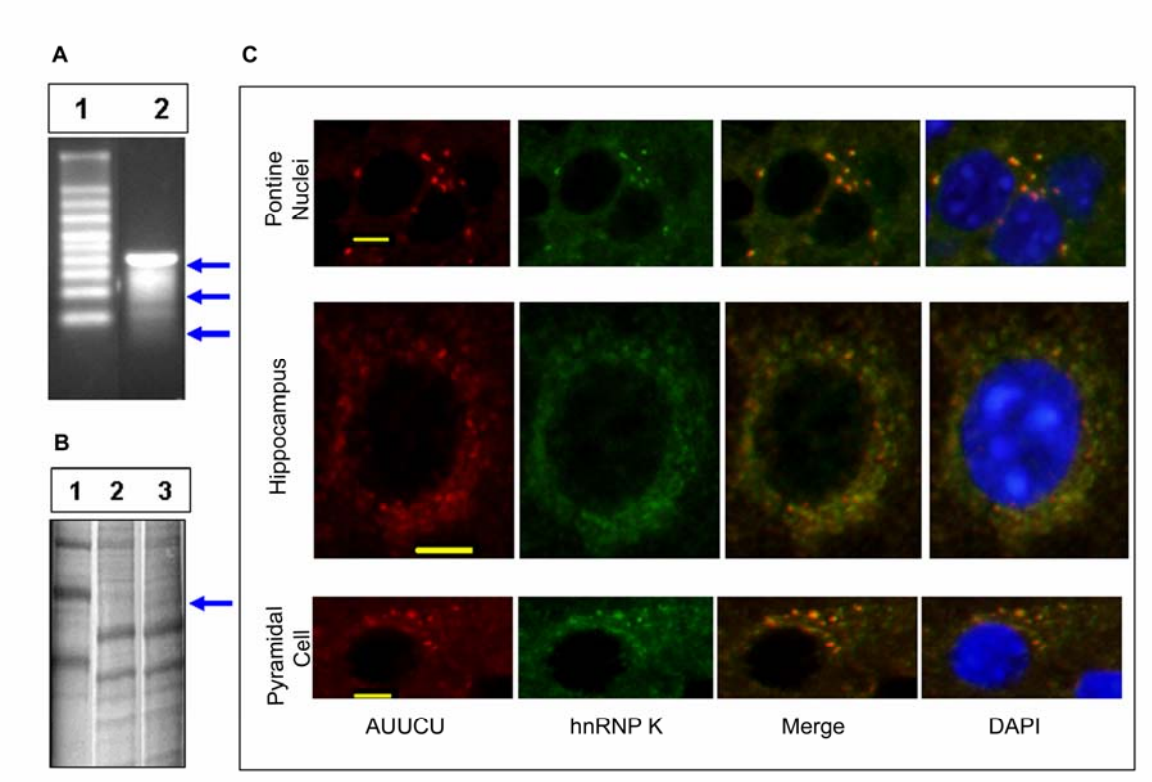

A. PAGE of AUUCU expansion bound to biotin-labeled bead showing different secondary structures with variable electrophoretic mobility (arrows), Lane 1 – marker, Lane 2 – Expanded AUUCU bound to biotin beads. B. SDS PAGE of proteins pulled down from mouse brain eluate through binding to AUUCU-biotin beads. Lane 1 – Marker, Lane 2- Beads bound to Transgene containing short AUUCU repeat (Figure 1B) and flanking regions, Lane 3 – Expanded AUUCU repeat (500 repeats) and flanking regions (Figure 1B). Arrow shows protein band of hnRNP K only present in the third lane. C. *FISH* using Cy3-$(AGAAU)_{10}$ riboprobe and immunodetection of hnRNP K in sagittal sections of transgenic mouse brain. Top three boxes show AUUCU aggregates (red) and hnRNP K (green) overlap (yellow) in the pontine nuclei (DAPI-blue) mostly perinuclearly and cytoplasmically. Center three boxes show hnRNP K and AUUCU colocalization in CA1 of the hippocampus and bottom three boxes show co-localization in the pyramidal cells of the dentate gyrus. Co-localized aggregates are seen in the nucleus, perinucleus and cytoplasm. Bars represent 10 μm.

Down-regulation of hnRNP K Triggers Apoptosis

The above results led to the idea that the formation of hnRNP K-AUUCU RNA aggregates may result in a change of hnRNP K function in SCA10. To understand the possible pathogenicity of either a diminished or complete loss of hnRNP K function in SCA10, we treated PC12 cells with siRNA designed to target hnRNP K transcripts specifically. The Western blot analysis showed that siRNA treatment resulted in >55% reduction of the hnRNP K protein level, compared with the level in cells treated with control siRNA (Figure 2.5A). We detected no significant cell death up to 48 hours after siRNA treatment, in accordance with previous studies (Lynch et al., 2005; Moumen et al., 2005; Svitkin et al., 1996). However, we observed a large amount of dying cells 72 hours after transfection with the hnRNP K siRNA; in contrast, cells treated with control siRNA did not show any significant cell death. Activation of cell death pathways was verified with caspase-3 assay, and significant caspase-3 activation occurred at 72 hours in PC12 cells with hnRNP K inactivation ($n=3$, $p<0.001$) (Figure 2.5B). We also detected significantly increased TUNEL-positive cells among PC12 cells transfected with hnRNP K-siRNA compared to a control siRNA treatment 72 hours post-transfection ($n=6$, $p < 0.0001$) (Figure 2.5C). Concentration of hnRNP K siRNA sufficient to activate apoptosis at 72 hours was evaluated and 100pM was deemed sufficient to significantly activate apoptosis ($n=3$, $p=0.0001$) (Figure 2.5D). Thus, down-regulation of hnRNP K produces caspase-3-mediated apoptotic cell death similar to cells expressing expanded AUUCU repeat.

Down-Regulation of hnRNP K Results in Massive Accumulation of PKCδ in Mitochondria

In vivo studies have shown that hnRNP K and PKCδ not only interact, but remain constitutively bound together within the cell (Bomsztyk et al., 2004; Idriss et al., 1994; Ostrowski et al., 2004; Schullery et al., 1999). Studies also show that hnRNP K, when bound to nucleic acids, cannot be phosphorylated and cannot interact with PKCδ (Bomsztyk et al., 2004). Overexpression of PKCδ has been shown to activate apoptosis through a positive regulatory loop, with caspase-3 activating PKCδ, and activated PKCδ cleaving caspase-3 (Voss et al., 2005). Subsequent studies show that a secondary activation mechanism of caspase-3 exists with PKCδ overexpression resulting in the translocation of PKCδ to mitochondria and activation of caspase-3 through the release of cytochrome c (Brodie and Blumberg, 2003; Majumder et al., 2000; Voss et al., 2005). Since aggregation of hnRNP K and the expanded AUUCU repeat is expected to minimize the formation of hetero-dimeric complexes of hnRNP K and PKCδ and mimic PKCδ over-expression, we investigated the ramifications of hnRNP K down-regulation on PKCδ expression and their sub-cellular localization in primary fibroblasts. We targeted the hnRNP K transcripts with siRNA and then studied the cellular localization of PKCδ. The results revealed that when hnRNP K function is attenuated, the majority of the PKCδ translocates to the mitochondria and a negligible amount of PKCδ is detected outside mitochondria (Figure 2.6A). In normal fibroblasts, or in fibroblasts treated with

Figure 2.5. Down-regulation of hnRNP K triggers apoptosis

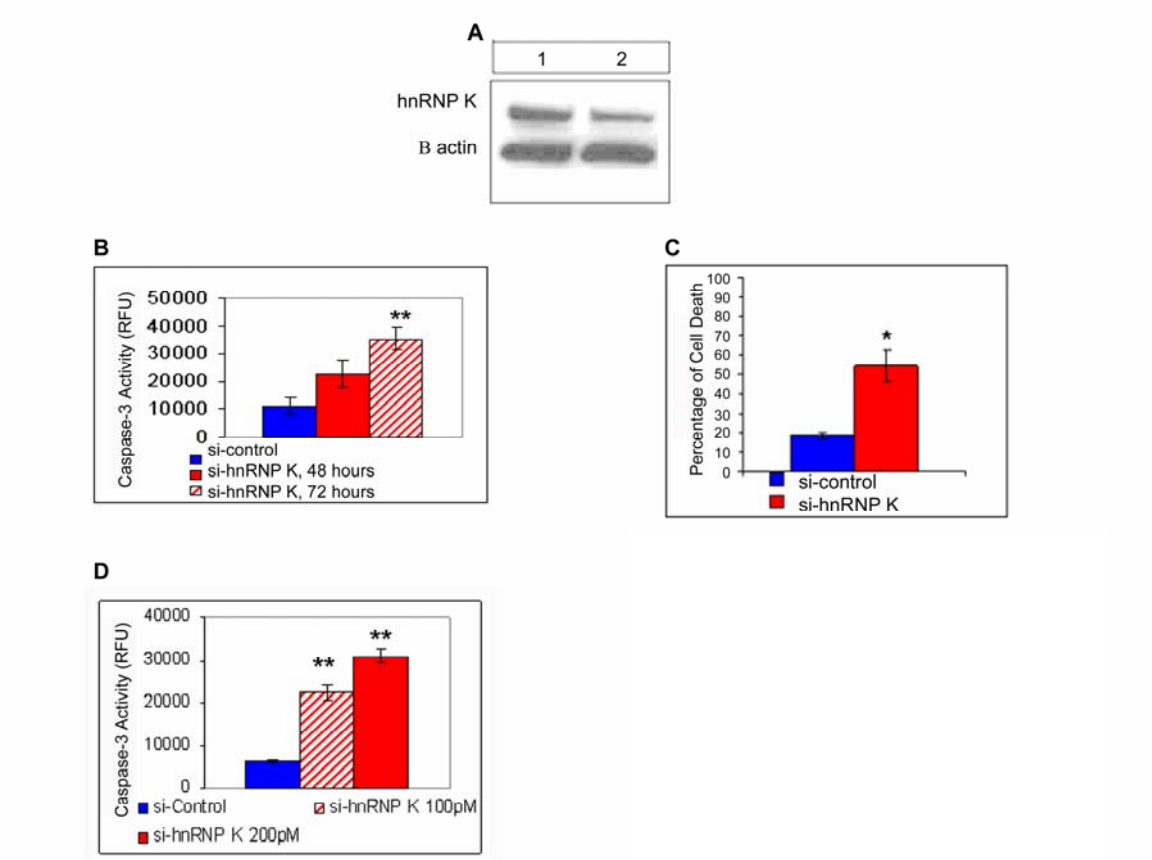

A. Detection of decreased hnRNP K in PC12 cells after treatment with siRNA. No change in hnRNP K levels was seen in PC12 cells not treated with siRNA (not shown). Lane 1 – 72 hours after PC12 cells were treated with si-control, Lane 2 - 72 hours after PC12 cells were treated with 100pM si-hnRNP K showing a 55% decrease (top band) and β-actin loading control (bottom band). B. Caspase-3 assay showing relative fluorescent units (RFU) 48 and 72 hours after treatment with 100 pM si-hnRNP K (*n=3, $p<0.0001$) and 72 hours after treatment with si-control. C. Percentage of cells undergoing apoptosis as assayed using TUNEL with control siRNA (blue) and si-hnRNP K (red) (n=6, $p<0.0001$). D. Caspase-3 Assay showing relative fluorescent units (RFU)_when PC12 cells were treated with either 100 pM (*n=3, p= 0.0001) or 200pM si-hnRNP K .

control siRNA, most of the PKCδ is detected within the cytoplasm and nuclei, with no detectable presence of PKCδ within mitochondria (Figure 2.6B). These findings support the hypothesis that migration of PKCδ to mitochondria is the likely mechanism by which reduced hnRNP K levels induce neuronal apoptotic programs in SCA10.

Expression of Expanded AUUCU RNA is Sufficient to Facilitate Migration and Accumulation of PKCδ in Mitochondria

The results described thus far support the hypothesis that expanded AUUCU RNA complexes with hnRNP K, and the consequent loss of hnRNP K function results in massive translocation and accumulation of PKCδ in mitochondria and induces apoptosis. To test whether expanded AUUCU RNA is sufficient to facilitate translocation of PKCδ to mitochondria, we transfected primary human fibroblasts with plasmids that express expanded AUUCU RNA (~500 repeats) and studied the cellular localization of PKCδ in the transfected cells. As we expected, the red fluorescence from mitochondria showed significant overlap with the green fluorescence from the PKCδ in fibroblast expressing expanded AUUCU sequences (Figure 2.6C), suggesting that PKCδ translocates to mitochondria in response to the expression of expanded AUUCU repeats. In contrast, a negligible overlap of mitochondria with PKCδ was observed in fibroblasts expressing 12 AUUCU repeats (Figure 2.6D). These results demonstrate that expression of the expanded AUUCU repeats is sufficient to promote translocation of PKCδ to mitochondria and activate the apoptotic program.

Figure 2.6. Transfection of Normal Fibroblasts with hnRNP K siRNA or Expanded AUUCU Repeat Results in Mitochondrial Localization of PKC δ.

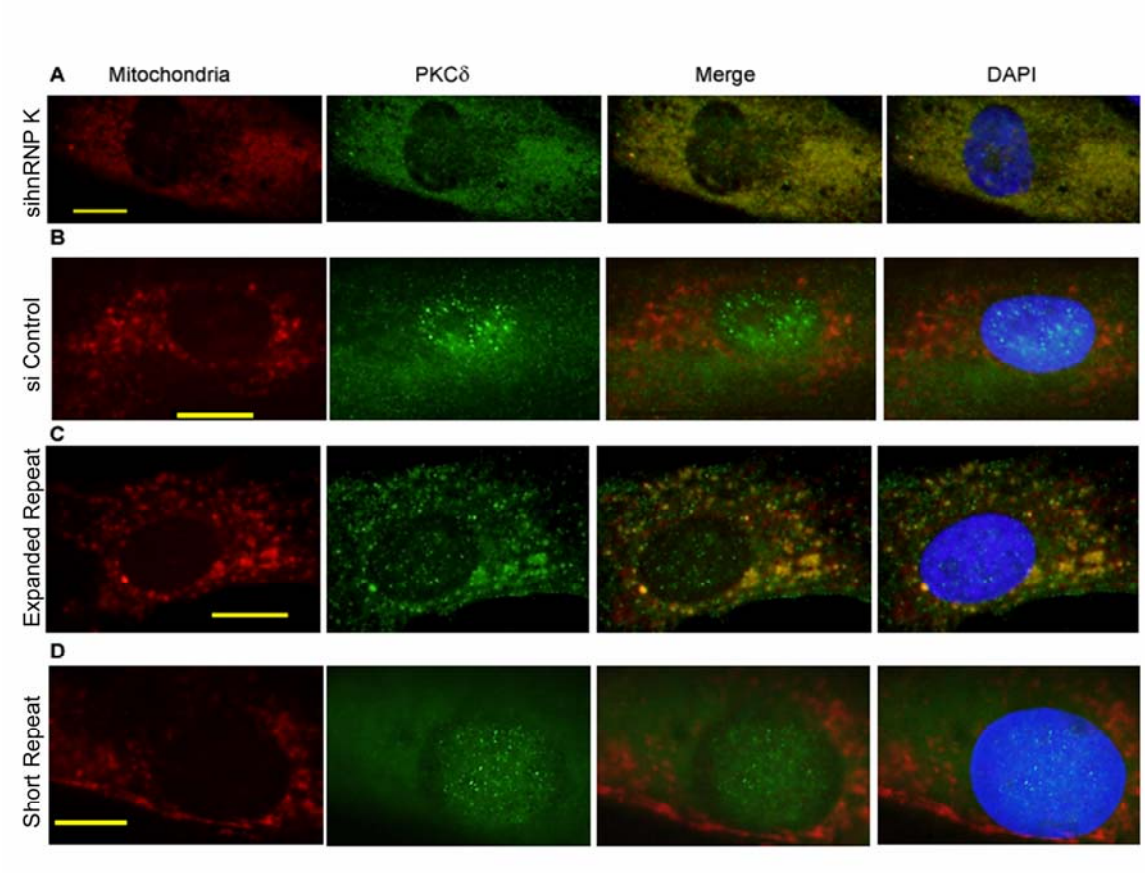

A. Normal fibroblasts transfected with hnRNP K-siRNA and stained with mitotracker (deep red) and immunodetection of PKCδ (green). Superimposition shows localization of PKC δ in the mitochondria. Bar represents 10 μm. B**.** Normal fibroblasts transfected with control siRNA show negligible PKCδ in the mitochondria. C. Normal fibroblasts transfected with expanded AUUCU transgene (figure 1B) and stained with mitotracker (deep red) and immunodetection of PKCδ (green). Superimposition shows localization of PKC in the mitochondria. Bar represents 10 μm. D. Negligible localization of PKCδ in mitochondria is seen in fibroblasts transfected with the 12 repeat transgene. Bar represents 10 μm.

Protein Kinase C δ (PKCδ) is Accumulated within SCA10 Patient and Transgenic Mitochondria

Since previous experiments have shown that down-regulation of hnRNP K, as well as the expression of expanded AUUCU repeats, results in the accumulation of PKCδ into mitochondria, we tested whether cellular localization of PKCδ is significantly altered in SCA10 cells. We immunostained SCA10 fibroblasts and normal age-matched control fibroblasts for PKCδ. PKCδ is present in the cytoplasm and the nuclei of the normal fibroblasts, but no significant co-localization of PKCδ and mitochondria is seen (Figure 2.7A). In contrast, the green fluorescence from PKCδ significantly and reproducibly overlaps with the red fluorescence from mitochondria in SCA10 fibroblasts as punctate staining around the nucleus (Figure 2.7B), suggesting that PKCδ is translocated into mitochondria in SCA10 cells. Moreover, sagittal sections of transgenic mouse brain demonstrate similar mitochondrial localization of PKCδ in regions previously shown to contain AUUCU foci (Figure 2.7C). Negligible mitochondrial localization of PKCδ was seen in wildtype age-matched mice (data not shown). These results further substantiate our previous results that expanded AUUCU RNA facilitates massive translocation of PKCδ into mitochondria, triggering programmed cell death.

DISCUSSION

Multiple inherited human neurological disorders are now attributed to expansion of short tandem repeats either in coding or non-coding regions of genes (Gatchel and Zoghbi, 2005). Genetic and molecular analysis of these disorders have revealed that the repeat expansion can result in either a loss of function of the gene (as in the non-coding

Figure 2.7. PKC δ is Localized in the Mitochondria in SCA10 Fibroblasts and Transgenic Mouse Brain

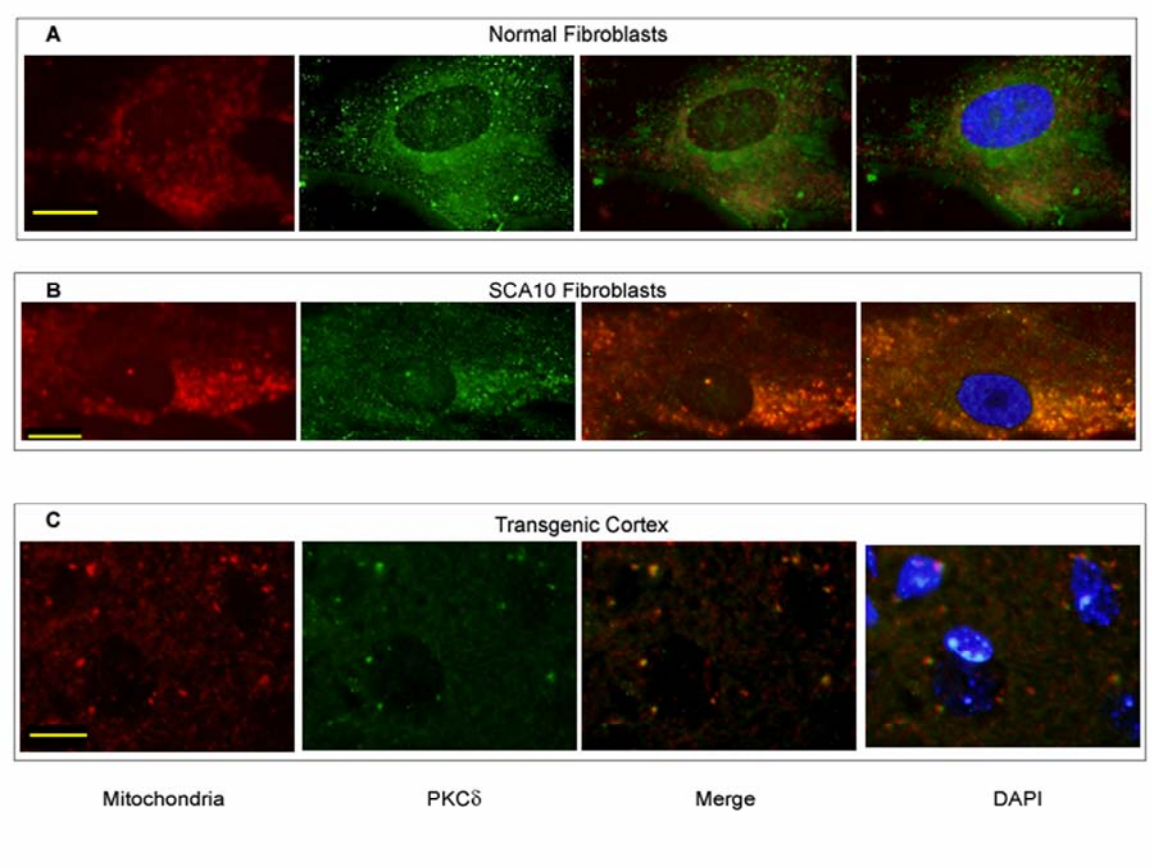

A. Immunodetection of PKCδ (green) and staining of mitochondria (deep red) in normal age-matched control fibroblasts. PKC δ staining is seen mostly within the cytoplasm. Superimposition in normal fibroblasts shows relatively no localization in mitochondria. Bar represents 10 μm. B. Immunodetection of PKCδ (green) and staining of mitochondria (deep red) in SCA10 derived fibroblasts. PKC δ staining is seen primarily as punctate staining outside the nucleus. Superimposition shows virtually complete localization of PKC δ in the mitochondria. Bar represents 10 μm. C. Immunodetection of PKCδ (green) and mitochondrial immunodetection with CoxIVa (red) in sagittal brain section. Picture taken from region of pontine nuclei. Bar represents 10 μm.

repeat disorders Fragile-X mental retardation and in Friedreich's ataxia), a gain of novel functions of the encoded protein (as seen in SCA1, SCA2, SCA3, SCA6, SCA7, SCA17, Huntington's disease, Kennedy's disease, dentatorural pallidoluysian atrophy, and oculopharyngeal muscular dystrophy), or a putative increase of function of the gene (SCA12). In Myotonic Dystrophy Type 1 (DM1) and type 2 (DM2), the non-coded expanded CTG and CCTG sequences are transcribed, and mutant mRNA containing expanded CUG and CCUG repeats, respectively, plays a transdominant toxic role in DM pathogenesis (Davis et al., 1997; Mankodi et al., 2001). RNA-mediated pathogenesis involving the mutant transcript containing expanded repeats is also believed to play a critical role in several other genetic disorders including SCA8, SCA12, Huntington's disease like 2 (HDL2), and fragile X tremor ataxias syndrome (FXTAS). Our study provides experimental evidences to suggest that the AUUCU RNA repeats from the SCA10 repeat expansion are sufficient to induce neuronal apoptosis, categorizing SCA10 as a new member of RNA pathogenesis disorders.

We provide convincing evidence that SCA10 pathogenesis results from a trans-dominant gain-of-function of AUUCU repeat RNA. First, transcription of the mutant allele produces toxic transcripts that remain as aggregates within the cell. Second, the toxic AUUCU aggregates complex with the RNA-binding protein, hnRNP K. Third, diminished hnRNP K activity, as well as expression of expanded AUUCU repeat, results in accumulation of PKCδ in the mitochondria and caspase-3 mediated activation of apoptosis. Based on these findings, we conclude that the AUUCU repeat expansion sequesters hnRNP K in intracellular aggregates, leading to loss of function of hnRNP K, which causes activation of caspase-3 mediated apoptosis via translocation of PKCδ to mitochondria. Previous reports suggest that the presence of PKCδ in the mitochondria

results in a decreased membrane potential, release of cytochrome C, and activation of caspase-3 (Brodie and Blumberg, 2003; Majumder et al., 2000; Voss et al., 2005), further supporting our conclusion. Since apoptosis is considered to be a major mechanism of cell death in a variety of human neurodegenerative disorders (Jellinger and Stadelmann, 2000), the novel pathway of apoptosis induced by the mutant SCA10 RNA is directly relevant to the neurodegenerative phenotype of SCA10. Thus, our results provide strong evidence that this novel mechanism of trans-dominant RNA gain of function contributes to the pathogenic mechanism of SCA10.

Our study leaves several important questions, however. Among them, the most important question is whether this novel RNA-mediated toxic gain of function actually happens in the brain of SCA10 patients *in vivo*. To date, we have not obtained brain tissues of SCA10 patients because few patients have died since discovery of the SCA10 mutation, and the few that died did not provide autopsy permission. However, data obtained from fibroblasts of patients, transgenic animals, and cell lines expressing the mutant allele have successfully recapitulated the principal pathogenic mechanism of other neurodegenerative diseases, especially those with repeat expansion mutations (Ashizawa, 2006). Thus, our current data are likely to represent the major pathogenic mechanism of SCA10 that takes place in patient's brain.

The detailed SCA10 mechanism has yet to be validated. First, we believe that the AUUCU RNA aggregates are toxic to the cells because they complex with hnRNP K. However, the formation of aggregates is not necessarily a required event for the mutant RNA to exert its toxicity. Binding of the soluble form of the mutant RNA to hnRNP K may be sufficient to cause the loss of function of hnRNP K with a release of PKCδ, and the aggregate formation could be a secondary phenomenon. Second, we hypothesize that

hnRNP K pathologically binds the AUUCU expansion and prevents normal hnRNP K and PKCδ complexes, mimicking overexpression of PKCδ within the cell. Here, we investigate the importance of PKCδ in regard to hnRNP K loss of activity, but hnRNP K is highly ubiquitous within the cell. Loss of availability of hnRNP K could lead to

Figure 2.8. Mechanism for Diverse SCA10 Phenotypes Due to hnRNP K Altered Function

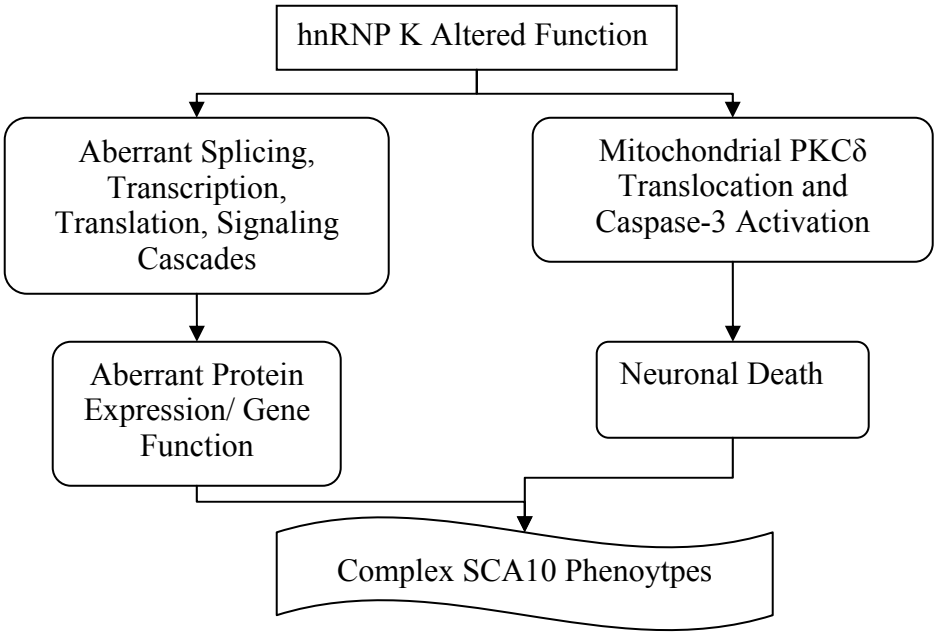

widespread effects within the cell such as alterations in transcription, splicing, and cell signaling, which may account of the phenotypic variability seen in SCA10 (Figure 2.8). However, our results demonstrate that the interruption of the interaction between hnRNP K and PKCδ is important in SCA10. Previous studies have shown that hnRNP K is constitutively bound to PKCδ, but upon binding to nucleic acids, hnRNP K can no longer

interact with PKCδ (Bomsztyk et al., 2004; Voss et al., 2005). We have not obtained the experimental evidence to support that binding of hnRNP K to expanded, but not normal-size, AUUCU repeat RNA leads to release of PKCδ. However, the massive translocation of PKCδ to mitochondria in SCA10 cells, fibroblasts expressing expanded AUUCU repeat, and fibroblasts treated with hnRNP K siRNA argue for this mechanism. Studies have shown multiple apoptotic activators induce PKCδ translocation into the mitochondria, including response to oxidative stress or overexpression (Majumder et al., 2000). Mitochondrial translocation has been shown to act in a feedback regulatory loop with production of ceramide, which results in an alteration in calcium signaling events and mediates the H_2O_2 loss of membrane potential, release of cytochrome c, and activation of caspase-3 (Sumitomo et al., 2002). While it is possible that the expanded AUUCU repeat causes PKCδ translocation via other mechanisms such as oxidative stress, our data showing that overexpression of hnRNP K rescues AUUCU-mediated apoptosis argue against it.

Our present data do not rule out the possibility that additional proteins are complexed to the mutant transcript. Furthermore, hnRNP K is ubiquitous within the cell and has important functions in multiple cellular processes such as transcriptional regulation, cellular proliferation, and cell signaling. It is plausible that a partial loss of function of hnRNP K does not only facilitate the translocation of PKCδ to the mitochondria, but potentially affect various cellular processes regulated by hnRNP K, contributing to the development of complex SCA10 phenotypes.

It is still unknown the exact effects of PKCδ translocation to the mitochondria and how the onset of apoptosis does not lead to immediate and complete neuronal death *in vivo*. It is likely that variable expression patterns of ATXN10 mRNA, hnRNP K protein

and PKCδ protein in different areas of the brain at different times of life prevents early death and results in this intriguing mechanism providing a late age onset.

The toxic interaction of transcribed repeat expansion with RNA binding proteins is a thematic mechanism for some of the microsatellite repeat expansion disorders, such as DM1, DM2, and FXTAS. Additionally, the aberrant cellular processing involving mitochondria is recurrently seen in repeat expansion disorders. The thematic nature already found in the hereditary expansion disorders may justify investigations of a wide range of RNA-binding proteins in relation to a variety of repeat expansions. RNA binding proteins are likely candidates for sequestration by mutant expanded transcripts in other disorders resulting from large expansion of polynucleotide sequences.

EXPERIMENTAL PROCEDURES

Cell Culture

SCA10 fibroblasts were isolated from skin biopsy of members of a Mexican SCA10 family containing approximately 2200 repeats and a Brazilian family containing 800 repeats. Cells were cultured in MEM with Eagle-Earle salt and 2 mM L-glutamine containing 15% fetal bovine serum and antimytotic in 5% CO_2 at 37^{o}C in 75 cm^2 flasks. Rat neuronal PC12 cells were cultured at Ham's F12K medium with 2 mM L-glutamine adjusted to contain 1.5 g/L sodium bicarbonate, 15% horse serum, 2.5% fetal bovine serum in 5% CO_2 at 37^{o}C in 75 cm^2 flasks.

Construction of Plasmids

The cytomegalo virus (CMV) promoter sequences in plasmid pCDNA3.1-hygro-lacZ (Invitrogen) were replaced with the *MfeI* /*BamHI* fragment of the rat prion promoter

sequences (~3.5 kb) using standard cloning strategies. The PrP promoter was cloned to achieve predominantly brain-specific expression of the transgene. A synthetic polylinker sequence was cloned at the *XhoI* site downstream of the *LacZ* and upstream of the BGH poly A sequences. The expanded ATTCT repeat sequences from the SCA10 hybrid cells were PCR amplified with forward primer 5'-CCAAGGATGCAGGTGCCACAGCATCTC-3' and reverse primer: 5'-ATATGCATCCAGCTTCTGATTACATGGACT-3'. The purified PCR product was cloned into the *SwaI* site, present in the polylinker sequences using T4 DNA ligase. The presence of expanded ATTCT sequences in the transgenic plasmid was confirmed by digesting the plasmid DNA with *SfiI* that flank the *SwaI* site. The plasmid encoding the expanded ATTCT repeats were grown in *E. coli* SURE bacteria at 16^{o}C to minimize the deletion of the repeat sequences. The transgenic plasmid DNA containing the *LacZ* and ~800 ATTCT repeats was then digested with *MfeI* and *NaeI* and digested DNA was electrophoresed on agarose gel. The ~10 kb DNA fragment containing the entire transgene was purified from agarose gel using gel extraction kit (Qiagen). The cloned ATTCT repeats under CMV and T7 promoter contain 650 bp of upstream and 500 bp of downstream *ATXN10* sequence in addition to the ATTCT repeats. The control plasmids containing the same *ATXN10* flanking regions and 12 ATTCT repeats were PCR amplified from a normal subject.

Construction of the Transgenic Mouse

The transgene containing expanded ATTCT repeat described above and illustrated in Figure 1B was microinjected into the fertilized eggs derived from pregnant female mice according to standard procedure. The microinjected fertilized eggs were then transplanted into the uterus of pseudo-pregnant surrogate mothers to obtain founder

transgenic mice. The presence of the transgene and the repeat in the transgenic founder mice were confirmed by both Southern blot as well as repeat primed PCR analyses.

Repeat-Primed PCR in Transgenic Mice

Mouse genomic DNA was collected from tail samples using a basic phenol/chloroform precipitation. Repeat-primed PCR was performed as previously described (Matsuura and Ashizawa, 2002).

Isolation and Identification of AUUCU RNA Binding Proteins

The plasmid pcDNA-control as well as pcDNA-(ATTCT)n were first linearized with Bam HI and the linear plasmid was *in vitro* transcribed with T7 RNA polymerase using Riboprobe System T3/T7 (Promega) with biotinylated NTPs. Biotinylated rCTP was mixed with the other rNTPs during transcription to incorporate the biotin-labeled rCTP into the single-stranded (AUUCU)n RNA molecules. After *in vitro* transcription, the template DNA was removed from the (AUUCU)n RNA products by treating with RNAse-free DNAse I and then purified by passing through a Qiagen RNA purification column. The single-stranded and biotin-labeled (AUUCU)n RNA and control RNA molecules were boiled briefly and gradually cooled to room temperature to allow them to adopt higher order nucleic acid structures. The formation of higher order structure was confirmed by analyzing the (AUUCU)n-RNA product on agarose gel. To identify proteins that specifically bind with the (AUUCU)n RNA, nuclear extracts from brain were made from a 2 month old B6 mouse using NE-PER Nuclear and Cytoplasmic Extract Reagent (Pierce) according to vendors specification. The AUUCU-RNA-total protein mixtures were incubated at 4ºC overnight, and unbound proteins were washed by using RNA washing buffer (0.5 % NP-40, 100 mM NaCl, 50 mM Tris-HCl) four times.

The proteins that remain bound to the magnetic beads after extensive washing were extracted by boiling the magnetic beads in 1X SDS-PAGE loading buffer. The extracted proteins were loaded onto a 4-12% acrylamide gel and electrophoresed. The RNA-binding proteins that appear as unique bands on the PAGE were excised, digested with trypsin and then analyzed by MALDI-TOF assay at Biomolecular Resource Facility Mass Spectrometry Core at UTMB and the sequence was identified by searching the rodent protein database.

Antibodies and Western Blots

Mouse monoclonal anti-hnRNP K was obtained from Acris Antibodies GmbH, anti-β-Actin antibodies were purchased from Abcam, and monoclonal anti-PKCδ (G-9) was purchased from Santa-Cruz. Alexa Fluor 488 goat anti-mouse was purchased from Molecular Probes. To prepare the cell extracts, cells were washed with 1 x PBS and collected using a cell lifter (Fisher Scientific) and spun down at 1500 rpm. The cell pellets were lysed for 10 min at 4^{o}C in RIPA buffer (10 mM Tris-HCl pH 8.0, 150 mM NaCl, 1 mM EDTA, 1% Nonidet P-40, 0.5% of deoxycholate, 0.1% SDS) containing freshly added protease inhibitor cocktails (Roche Applied Sciences) and 1 mM of phenylmethylsulfony fluoride (PMSF), sheared through a 27-gauge needle, and centrifuged at 14,000 rpm for 10 min. The resulting supernatants were used for immunoblotting. For western blotting, twenty micrograms of whole cell lysate was electrophoresed in a 10% SDS-polyacrylamide gel and then transferred to nitrocellulose membranes. Blots were washed with immunoblotting buffer (TBST) (20 mM Tris, 150 mM NaCl, and 0.2% Tween 20) and blocked with 5% milk in TBST for 1 hour at room temperature. Membranes were then incubated overnight in TBST at 4°C with diluted primary antibodies. The antibody against hnRNP K was diluted 1:1000 and the anti-β-

actin antibody was diluted 1:2000. After washing with TBST, membranes were then incubated with HRP-conjugated donkey anti-rabbit or sheep anti-mouse immunoglobulin G antibodies (Amersham) in 5% milk in TBST for 1 h at room temperature. After washing, the target proteins were detected using the ECL Western blotting detection kit (Amersham, Piscataway, NJ). Expression levels of β-actin (Abcam, Inc) were used as controls for protein loading.

TUNEL Assay

Cells were grown in chamber slides overnight prior to TUNEL assay. TUNEL assay was performed according to vendor instructions (Roche). Student's t-test was used to calculate statistical significance (n=6).

Caspase-3 Assay

Caspase-3 assay was performed according to instructions supplied by vendor (Calbiochem). P values were calculated using student's t-test (n=3).

Transfection

The rat neuronal PC12 cells were transfected with plasmid DNA or siRNA by Lipofectamine 2000 transfection reagent (Invitrogen) according to the recommendations from the manufacturer. The siRNAs of rat hnRNP K si*GENOME™ SMART*pool reagents were purchased from Dharmacon. si*CONTROL* Non-Targeting siRNA #1 from Dharmacon was used as a negative control for all siRNA experiments. Approximately 100 nmoles of the siRNA pools were applied for the down-regulation of hnRNP K PC12 cells, and different assays were applied 72 hrs after the transfection. Approximately 4ug of plasmid DNA (either short or expanded repeat or hnRNP K) was transfected according

to Lipofectamine instructions in 6-well plates. Fibroblasts were transfected using the human dermal fibroblast nucleofector kit for electroporation (Amaxa). Plasmids expressing either short or expanded repeat were transfected at 3ug according to kit instructions and siRNA (both hnRNP K and Ataxin-10) was transfected at 100pMol according to kit instructions.

Fluorescent *in Situ* Hybridization (*FISH)*

RNA foci were detected using a Cy3-labeled $(AGAAU)_{10}$ RNA riboprobe. Slides were pre-hybridized at 65ºC in ULTRA-Hyb oligo hybridization buffer from Ambion for 1.5 hours. Slides were then hybridized overnight in 250ng $(AGAAU)_{10}$/ 1 ml hybridization solution at 45ºC. Slides were rinsed with PBS three times and then extensively washed 4 times 5 minutes each to remove all non-specific binding probes. Slides were then mounted with DAPI mounting medium.

Perfusion, *FISH,* and Immunodetection of the Transgenic Mouse Brain

Transgenic mice anesthetized with Avertin were perfused through the aorta, first rinsing for 15 minutes with PBS and then 60ml of fresh 4% paraformaldehyde (PFA) in DEPC water. The brain was carefully removed and stored in 4% PFA at 4ºC with gentle agitation overnight. Brain tissue was then placed in 30% sucrose overnight. Mouse brains were fixed in 4% PFA, paraffinized, and sectioned sagittally. RNA foci were stained using a Cy3-labeled $(AGAAU)_{10}$ riboprobe complementary to the transcribed ATTCT repeat. First, paraffin was removed from the brain sections and slides were dehydrated with 70%, 95% and 100% Ethanol in DEPC water, and washed using DEPC PBS. The protocol described above for *FISH* in cell culture was used for *FISH* on sagittal sections following removal of paraffin. Following *FISH,* hnRNP K was detected

by immunohistochemistry. Sections were blocked with DAKO antibody blocking solution (serum-free) and later double stained with anti-hnRNP K 1:1000 in DAKO antibody diluent. Goat anti- mouse 488 was used to identify hnRNP K and slides were visualized using a Hamamatsu Camera Controller using DP controller software in the histopathology core lab at UTMB.

Co-localization of PKCδ and Mitochondria

Fibroblasts were transfected with plasmids pcDNA-$(ATTCT)_{10,}$ pcDNA-$(ATTCT)_{500}$, siRNA hnRNP K or si*Control* through electroporation. Transfections were conducted in chamber slides. 36 hours after repeat transfection and 72 hours after RNAi transfection, the cells were treated with mitotracker deep red 633 (Invitrogen) at a concentration of 250 nM in cell culture medium. Cells were incubated at 37ºC for 30 minutes. After washing the cells three times with PBS, cells were then fixed with 4% PFA for 30 minutes at room temperature. Cells were washed 3 times with PBS and stored in 70% Ethanol for up to 24 hours. Cells were blocked with DAKO antibody blocking solution (serum-free) and later double stained with anti-PKCδ 1:500 in DAKO antibody diluent. Goat anti-mouse 488 was used to identify PKCδ. Fluorescent photomicrographs were taken using a Hamamatsu Camera Controller using DP controller software in the histopathology core lab at UTMB.

Chapter III:

Characterization of the SCA10 Transgenic Mouse

SUMMARY

Spinocerebellar Ataxia type 10 is a member of the growing number of debilitating microsatellite expansion disorders resulting in cerebellar degeneration. SCA10 is caused by an expanded ATTCT repeat in the ninth intron of Ataxin 10, a protein of unknown function. To investigate the mechanism of SCA10, transgenic mice containing five hundred expanded ATTCT repeats were generated. Behavioral, molecular, and histopathological analyses of the mice suggests that the ATTCT repeat is not stably transmitted through generational breeding and that the behavior of the mice, as well as pathogenicity of the repeat, directly correlates to the length of the repeat expansion. The transgenic brains contain aggregations of the transcribed ATTCT repeat, which bind and sequester the RNA binding protein, hnRNP K. Vacuolization in the regions of the brain containing aggregates was indicative of autphagy. The SCA10 transgenics provide a promising model for investigation of the RNA-mediated toxic gain of function mechanism of SCA10.

INTRODUCTION

Expansion of an ATTCT microsatellite repeat in the intron of ataxin 10 (*ATXN10)* results in an autosomal dominant neurodegenerative disorder, Spinocerebellar Ataxia Type 10 (SCA10) (Matsuura et al., 2000). In the wildtype population, the ATTCT

microsatellite is repeated anywhere from 10-29 times; expansion from 800 to 4500 repeats results in SCA10 with middle-range expansions between 200 and 850 repeats causing reduced penetrance (Alonso et al., 2006; Matsuura et al., 2006; Raskin, In press). *ATXN10* contains 12 exons and spans 173 kb, with the ATTCT repeat occurring in the large, ninth intron. The exact function of the ATXN10 protein is currently unknown, though it is thought to be important in protein-protein interaction due to its two armadillo domains (Marz et al., 2004). SCA10 was first described in Mexican patients but was later diagnosed in Brazil and Argentina (Gatto, in press). The SCA10 phenotypes are variable depending upon the population, with families from Spanish ancestry appearing to have worsened symptoms and an additional phenotype of epilepsy (Raskin, In press). Not only do the SCA10 phenotypes differ in relation to the ethnicities, data suggests that the purity of the repeat may also vary between the ethnicities with the complexity of the repeat correlating with the complexity of the phenotypes (Matsuura et al., 2006) and unpublished data). Presenting with ataxia, SCA10 patients progressively worsen with complex phenotypes affecting gait, limb usage, motor coordination, and speech - all of which contribute to a diminished quality of life for the patient and the family.

Loss or gain of function of the ATXN10 protein does not appear to be the mechanism for disease manifestation of SCA10. Wakimiya et al. demonstrated that the expanded form of *ATXN10* is properly transcribed, spliced, and processed within patient derived cell lines (Wakamiya et al., 2006). Additionally, allele-specific RT-PCR analysis of *ATXN10* transcripts and somatic cell hybrid studies suggested that the mutant *ATXN10* transcript accounts for 50% of the transcripts in patient cell lines, refuting the possibility of haploinsufficiency. In the previous chapter, data suggested that the primary pathogenic molecules in SCA10 are the expanded AUUCU transcripts. By forming

atypical aggregates within the cell, the transcripts complex with the RNA binding protein, heterogeneous nuclear ribonucleoprotein kinase (hnRNP K). hnRNP K contains three K homology (KH) domains known to be important in the binding of nucleic acid, as well as a protein binding domain, the K interactive (KI) region (Bomsztyk et al., 2004). Normally, hnRNP K binds constitutively to a protein kinase, protein kinase C δ (PKC δ) (Schullery et al., 1999). However, when hnRNP K is bound to RNA, the PKC δ binding site is no longer accessible (Bomsztyk et al., 2004; Ostrowski et al., 2004). The decreased availability of hnRNP K, due to sequestration of hnRNP K to the AUUCU foci, and the excess PKC δ within the cell, resulting from the release of PKCδ from hnRNP K, is hypothesized to lead to activation of apoptosis via caspase-3. PKC δ is present in mitochondria in fibroblasts from SCA10 patients, where it is thought to activate caspase-3 through disruption of the mitochondrial membrane potential and release of cytochrome C (Garrido et al., 2006; Majumder et al., 2000; Steinberg, 2004). It was demonstrated in the second chapter that expression of expanded AUUCU repeat RNA by transfection of the repeat in cell culture results in activation of caspase-3 mediated apoptosis, as well as translocation of PKCδ to mitochondria. Additionally, inactivation of hnRNP K was shown to induce caspase-3 mediated apoptosis, as well as PKCδ translocation to mitochondria. Both induction of SCA10 cellular phenotypes by expression of expanded repeat and inactivation of hnRNP K further promote the hypothesis that hnRNP K is sequestered by AUUCU repeats, and leads to translocation of PKCδ and activation of caspase-3.

To investigate the molecular effects of expression of expanded AUUCU repeat *in vivo*, we developed transgenic mice with a transgene containing a prion promoter (PrP) to target expression of approximately 500 ATTCT repeats in the non-coding region to brain.

Molecular analysis of transgenic mice revealed that the expanded ATTCT repeat is unstably passed to offspring, with both expansion and contraction occurring in subsequent generations. Motor deficit was demonstrated through behavioral analysis and compared to brain pathology at the histological level. Immunohistochemical analysis as well as fluorescent *in* situ hybridization (*FISH*) on sagittal sections of the transgenic brain tissue demonstrated AUUCU aggregates that colocalize with hnRNP K, further supporting the hnRNP K loss of function hypothesis. Additionally, PKCδ was found to have mitochondrial translocation in regions of the brain where AUUCU foci and hnRNP K colocalized. Perinuclear vacuoles were seen in the regions of the brain with a high proportion of AUUCU aggregates. Further analysis of the vacuolization suggests a possible role for autophagy in the SCA10 transgenics. The data presented here suggests that the expanded ATTCT repeat is sufficient to induce neurodegeneration and SCA10-like phenotypes in transgenic mice. Instability of transmission of repeats provides a rare opportunity to directly correlate behavior of transgenic mice with the length of repeat expansion.

RESULTS

Transgenic Mice Contain Expanded ATTCT Repeats that Contract Through Transmission

To investigate the effects of expanded ATTCT repeat in mice, we developed a transgene containing approximately 500 ATTCT repeats in the non-coding region from SCA10 Mexican patient DNA. The transgene included a prion promoter (PrP), confining expression primarily to brain, a *LacZ* reporter gene, and a BGH poly A signal (Figure

3.1A). The mice were genotyped by PCR using two sets of primers at opposite ends of the LacZ gene. Repeat-primed PCR (RP-PCR), a technique where the 5' primer flanks the repeat expansion, while the 3' primer contains 8 ATTCT repeats and a hanging tail sequence not present in the genome, was utilized to verify expansion of repeat within the transgenic animals (Matsuura and Ashizawa, 2002). The 3' primer can anneal anywhere within the repeat expansion, providing a ladder of various sized repeats when run on a polyacrylamide gel (Figure 1B). The 5' primer was derived from the human genome and does not anneal to the region flanking the *ATXN10* ATTCT repeat and only will amplify the region in the transgene.

Repeat-primed PCR on founder, F1, and F2 generations was utilized to further investigate the repeat stability within the mouse lines. During initial investigation, expansion was seen in the founders, while a stepwise decrease was seen from founder to F1 and F1 to F2 (Figure 1B). The variability in the length of the repeat seen on polyacrylamide gel suggested that the repeat contracted through generational breeding of the transgenic mice. However, further investigation comparing a larger representative number of offspring showed both contraction and expansion in the F1 and F2 transgenic mice (Figure 1C). The repeat was found to contract and expand similarly in mice bred from male and female founders. The female founder tested resulted in 2 contractions, 2 expansions, and 1 stable transmission. The male founder tested resulted in 1 contraction, 1 expansion, 2 stable transmissions, and 1 inconclusive reaction (represented by pie graph, Figure 1D). Thus, it is unlikely that stable transmission depends on sex given the variability found between both paternal and maternal transmission. Variability in both

Figure 3.1. Expanded ATTCT repeats in Transgenic Mice are Unstably Transmitted

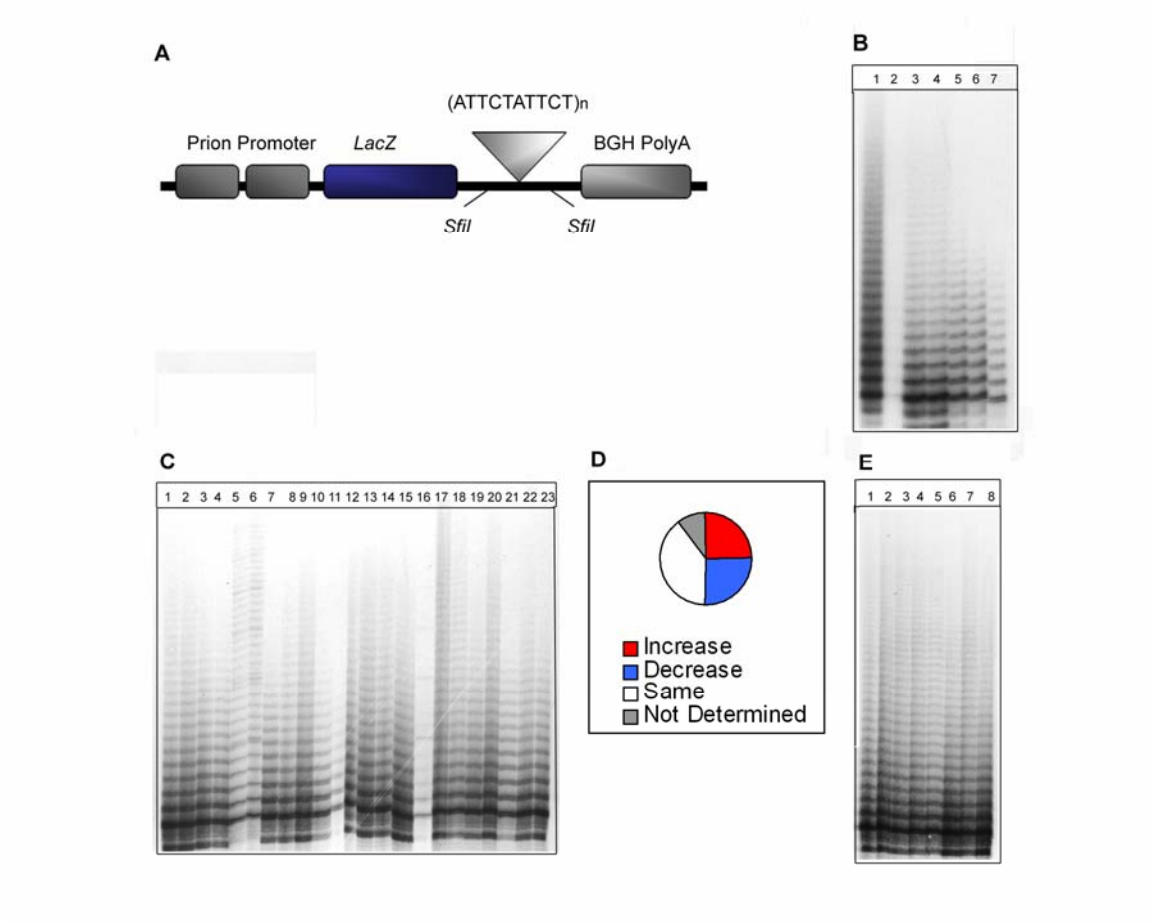

A. The transgene contains a prion promoter, known to drive expression to CNS-derived tissues, a *LacZ* reporter gene, and BGH poly A signal, and approximately 500 ATTCT repeats. B. Initial RP-PCR showing step-wise decline of repeat expansion from Founder to F1 and F1 to F2 in the only 3 founders that bred. Lane 1 – positive control from plasmid DNA, 2 - PCR genotyped wildtype mouse, 3 – Founder 1, 4 – Founder 2, 5 – F1 from founder 1, 6 – F1 from Founder 2, 7 – F2 from Founder 2. C. Further evaluation of repeat stability in DNA from mouse tail. Lane 1 – Founder 1, Lane 2-6 – F1 from founder 2, Lane 7-11 – F2 from founder 2, Lane 12 – Founder 3, Lane 13-17 – F1 from founder 3, Lane 18-23, F2 from Founder 3. D. Analysis of repeat stability in various tissues. Lane 1 – cortex, Lane 2 –cerebellum, Lane 3 – heart, Lane 4 – Liver, Lane 5 – Muscle, Lane 6 – Skin, Lane 7 – Lung, Lane 8 – Tail.

sexes in mice is in contrast to human patients where instability in sperm has been shown to result in either contraction or expansion of the repeat, resulting in anticipation in expanded, paternally-transmitted alleles (Matsuura et al., 2004). While the repeats expressed in the contracted F1 and F2 transgene are shorter than the founders, they are still are expanded beyond the normal allele size. Thus, all F1 tested contain abnormal, expanded ATTCT repeats. The F2 generation contains some large, expanded repeats and some repeats present in the normal range. To further verify repeat stability within different tissue samples, we performed RP-PCR on DNA extracted from F2 mouse tissues. DNA from tail, brain, heart, lung, muscle, liver, and skin all showed relatively the same size repeat expansion by RP-PCR (Figure 3.1E). While RP-PCR has not been used previously for detection of expansion size, difficulties in producing a Southern blot of the transgene, due to a lack of restriction sites within the transgene, prompted investigation with RP-PCR. These findings suggest that the repeat passes unstably, with either contraction or expansion, from generation to generation in mice, regardless of gender, while somatic instability is relatively limited.

The Transgene is Expressed Primarily in Brain

Previous reports suggest that Prion promoter is primarily expressed in CNS-derived tissues (Fischer et al., 1996). To verify that the expression of the PrP-driven transgene is primarily expressed within the brain, we evaluated the expression of the transgene throughout organs of the transgenic mice by quantitative RT-PCR. Primers were designed in the *LacZ* gene region for identification of the transgene. Various regions of brain were tested with cortex and cerebellum showing the highest level of expression (Figure 3.2A). Some expression was also seen in the non-CNS derived tissues with the highest levels present in the liver.

Figure 3.2: The Prion Promoter is Expressed Extensively Throughout the Brain

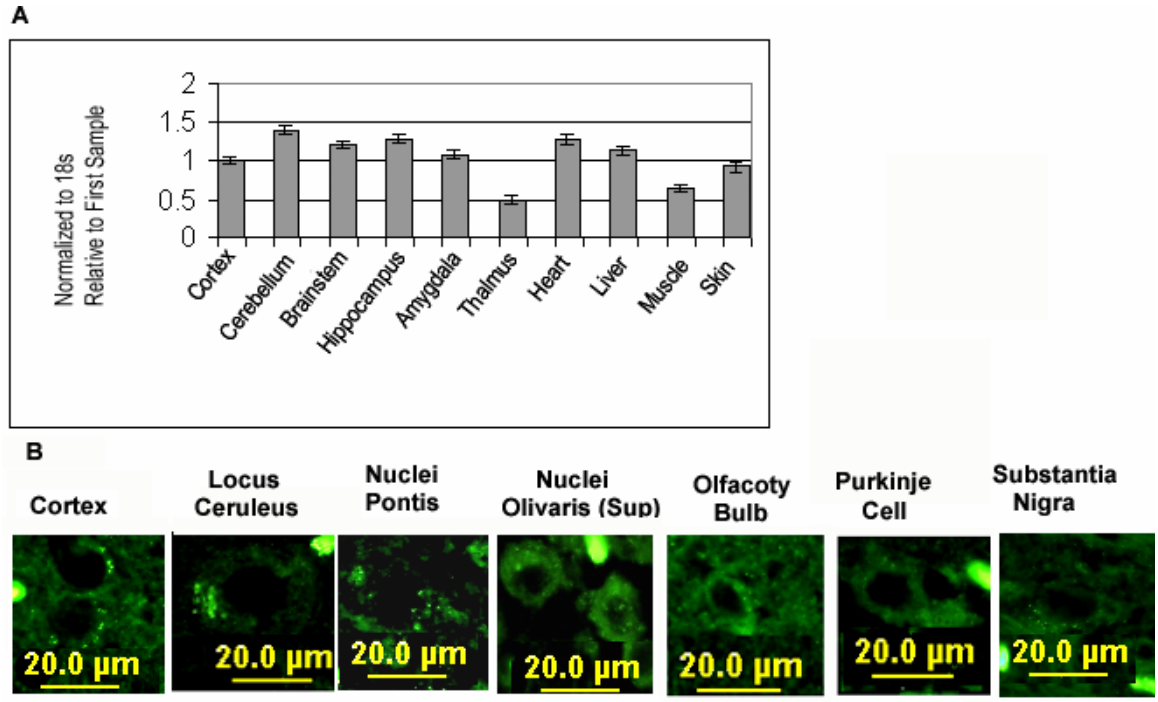

A. Quantitative RT-PCR shows presence of transcript throughout the brain with expression in tissues not CNS derived. Samples were normalized to 18s and were relative to the first sample, cortex. Wildtype mice show no expression, less than 0.0001, of the LacZ transgene (not shown). B. Expression of the transcript as immunostained with anti-β-galactosidase. The β-galactosidase antibody showed both punctuate staining (as in cortex, locus ceruleus, and nuclei pontis, substantia nigra) and broad cytolasmic staining (nuclei olivaris, olfactory bulb, and Purkinje cells). Expression was semi-quantitatively analyzed in Table 1.

Table 3.1. Comparison of Ataxin-10 Expression to Transgenic *LacZ* Expression

Regions of Brain	Human	Mouse	SCA10 Transgenic
	ATXN10	*ATXN10*	*LacZ*
Olfactory Bulb	ND	++	++
Cerebral Cortex	0/+	0/+	+++
Striatum	0	0/+	ND
Locus Ceruleus	+	+	+++
Substantia Nigra	0	0	++
Midbrain Raphe	+/++	++	ND
Nuclei Pontis	+/+++	++/+++	+++
Nuclei Cuneatus	+++	ND	+++
Nuclei Vestibularis	++	++	+
Nuclei Olivaris	++	++	+++
Nuclei Hypoglossus	+/++	ND	+++
Purkinje Cells	+/++	+/+++	+/++
Deep Cerebellar Nuclei	ND	+++	++
Spinal Motor Neurons	+	+	ND
0 - no observable staining + - +++, semi-quantitative staining ND- not determined			

(Marz et al., 2004). derived from mouse on the transgenic brains. Gray shows similar levels of expression.

LacZ Expression is Present in the Transgenic Brain

To verify regions of the transgenic brain affected by the expression of the transgene, we performed immunohistochemistry with monoclonal β-galactosidase derived from the mouse on the transgenic brains. Wildtype littermates were used as a negative control, resulting in virtually no background from the β-galactosidase antibody. Expression is expected to verify the results found in quantitative RT-PCR at the cellular level. Under fluorescent microscopy, β-galactosidase was visualized and compared to

previously reported PrP expression (Boy et al., 2006). Extensive expression is seen in the cerebral cortex, especially the frontal lobe, the granule cells of the cerebellum, granule cells and pyramidal cells of the hippocampus, the pontine nuclei, locus ceruleus, and substantia nigra (Figure 3.2B). The region of expression of *LacZ* and the previously reported expression of Ataxin-10 by Marz et al. can be compared to determine the suitability of the SCA10 transgenic mice for replicating SCA10 (Marz et al., 2004) (Table 3.1).

Behavioral Analysis of Transgenic Mice Suggests Primary Motor Deficit:

Physically, the transgenic mice appear fairly normal with the exception of exhibiting abnormal grooming behavior determined by patchy hair growth on the back and urine stained fur, as well as claw withdrawal reflex (Figure 3.3A). Typically, when mice are held by the tail, the reflex is for the hind legs to sprawl. However, the transgenic mice exhibited claw withdrawal reflex, drawing in the hind legs. Mice exhibited normal postural reflex when the cage was rapidly moved back and forth or up and down. The mice had a normal righting reflex, ear blink and eye twitch. However, the transgenics displayed abnormal whisker orienting reflex (Figure 3.3B). When the whiskers of the mice are lightly touched with a cotton swab, the normal response of the mouse is to stop moving the whiskers or to orient toward the side of the stimulus. The wildtype littermates performed normally on the whisker orienting reflex. However, transgenic mice did not stop whisker movement or orient toward the stimulus ($n=7$, $p<0.001$).

Figure 3.3. Behavioral Analysis Suggests Mice Expressing Expanded AUUCU Repeats are Uncoordinated.

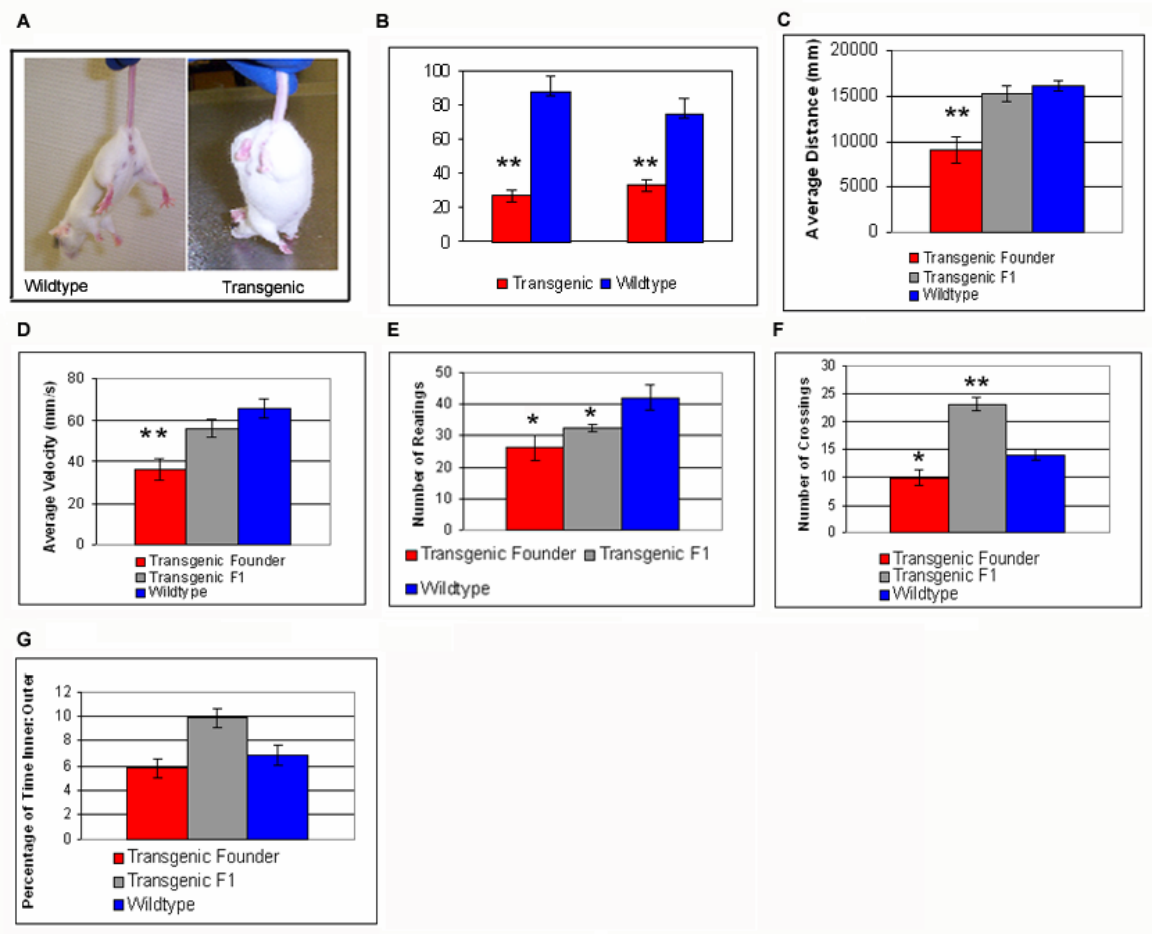

A. Transgenic mice display the claw clasping reflex. B. Percentage of reactions to whisker flick neurological test. C. The average distance (mm) traveled during open field analysis. D. When placed in an open field apparatus for five minutes, founder mice travel at a significantly slower average velocity (mm/s) than wildtype littermates and F1 transgenic mice. A stepwise velocity difference is indicated by the three groups of mice with founders traveling slowest, then F1, and wildtype traveling fastest. E. The number of rearing as analyzed by software as elongation ratio. F. The number of crossings, from the outer to the inner, for founder, F1, and transgenic. G. The percentage of time spent in inner vs. outer arena. Wildtype and transgenic founders behave indistinguishably from each other with F1 appearing to spend more time in the inner arena, but no significant difference is found.

Abnormal whisker orienting reflexes have been implicated as deficit in the primary motor cortex (Crawley, 2000).

To evaluate the behavior of the SCA10 transgenic mice, we performed a battery of behavior analyses formulated to target neurological deficit with focus on primary motor deficit. The founder mice at approximately 6 months of age were placed in a clear, Plexiglas open field apparatus, where they were videotaped and computer analyzed. Horizontal and vertical movement, along with total distance, speed traveled, rearings, crossings, and percentage of inner: outer arena time were measured. The founder mice traveled a significantly less distance ($n=5$, $p=0.01$) at a significantly slower speed ($n=5$, $p=0.01$) than their wildtype litter mates (Figure 3.3C and 3.3D, respectively), while the F1 transgenics did not perform significantly differently in velocity or distance (Figure 3.3C and 3.3D). The transgenic founders performed the worst at velocity and distance, with F1 mice performing intermediately between transgenic founders and wildtype mice. The transgenics also performed significantly different in rearings, with founders rearing the least ($n=5$, $p<0.05$), F1 intermediately ($n=5$, $p<0.05$), and wildtype rearing the most (Figure 3.3E). As for crossings, founders crossed the center of the open field apparatus significantly less than wildtype mice ($n=5$, $p<0.05$), while F1 crossed significantly more ($n=5$, $p=0.001$) (Figure 3.3F). No significant differences were seen in the amount of time spent in the center versus the outside of the arena (Figure 3.3G). These findings suggest that the SCA10 transgenics have impaired motor and exploratory behaviors relative to the size of the repeat expansion.

Figure 3.4. Transgenic Mice Demonstrate Decreased Learning Abilities and Ataxia

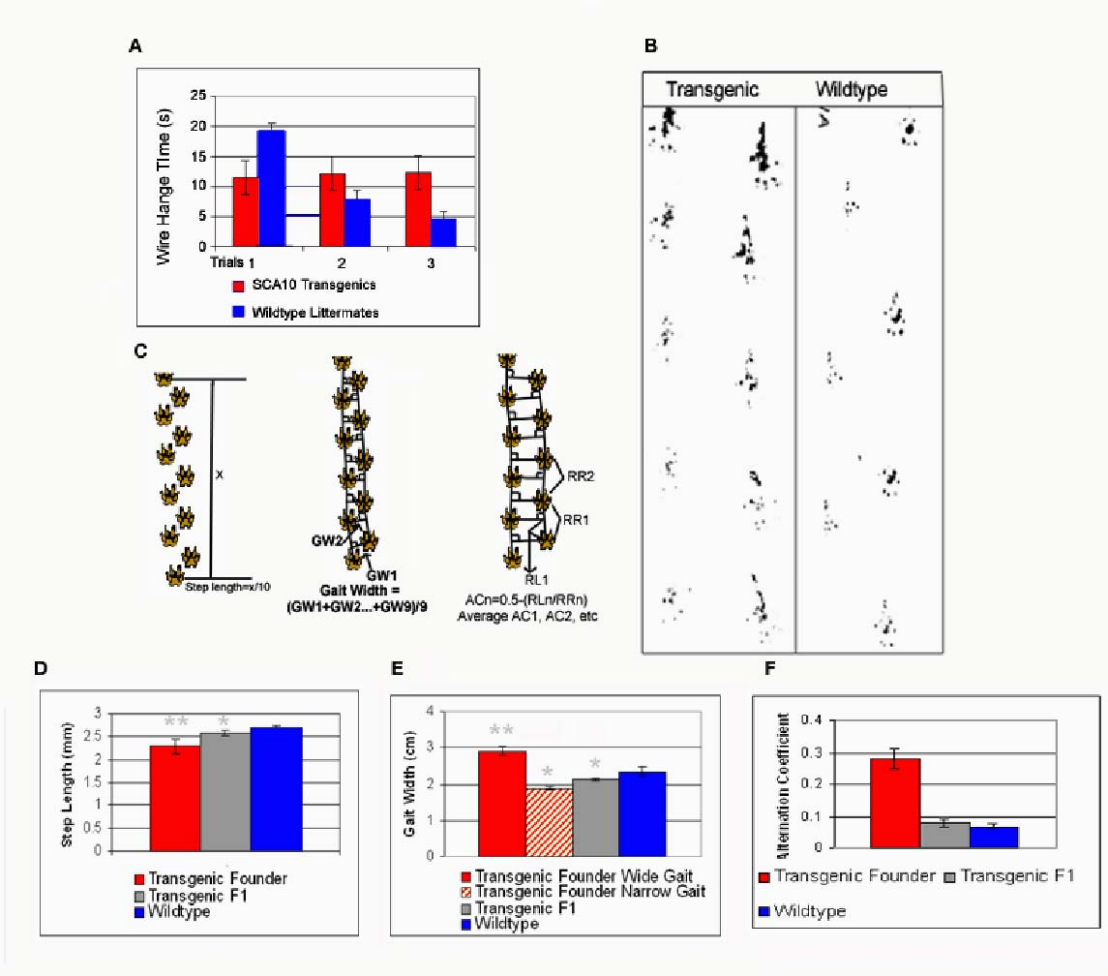

A. Amount of time in seconds mice hang on to a wire rod. Stepwise decrease in wildtype mice suggests learning, while transgenics (F1 and founders) hang relatively the same time each trial. B. Footprints taken from wildtype and transgenic mice. C. Diagrams representing how step length, gait width, and alternation coefficient were calculated. D. Step length (cm) measured from footprint analysis on founder, F1, and wildtype littermates over a series of ten steps and two trials. E. Gait width measured from footprint analysis over a series of 10 steps and two trials. Two groups occur in the founders with 2 mice significantly narrower than wildtype littermates and 2 mice significantly wider than wildtype littermates. F1 mice consistently had shorter gait width. F. Measure of alternation from footprint analysis of 10 steps and two trials. No significant difference was seen between the three groups, but one founder shows a distinct difference from the rest of the groups.

Additionally, strength and motor abilities of the transgenics were investigated with a wire rod. The rod was inverted and held approximately 40cm above the home cages. The mice performed three trials on two consecutive days with the amount of time the mice held on to the wire rod recorded. The transgenics held on to the wire rod significantly less time than their wildtype littermates ($n=7$, $p<0.05$) during the first trial on both days of testing (Figure 3.4A). However, on the second and third trial both days, the wildtype and transgenic held on for approximately the same time, with the wildtype mice holding on significantly shorter ($n=7$, $p<0.05$) on the second versus the first trial and significantly less between the third and second trial ($n=7$, $p<0.01$). These data show learning for the wildtype littermates, while the transgenic mice held on relatively the same amount of time for each trial. Taken with the whisker flick reflex, the battery of neurological examinations suggests that the SCA10 transgenic mice may exhibit a primary motor deficit as well as a learning deficit.

To investigate the possibility of additional motor deficit, the hind limbs of the mice were painted with a non-toxic ink and encouraged to walk through a square, wooden apparatus lined with Whatman paper. The front of the apparatus was closed after the mice were placed on the paper, and the mice were permitted one minute to exit the back of the apparatus. Mice that required more than one minute were re-tested. Footprint analysis has commonly been used as a behavioral tool in mice with neurodegenerative effects, especially those anticipated to have a gait ataxia (SCA1,

Figure 3.5. AUUCU Transcript forms Foci in Aged, Transgenic Brain

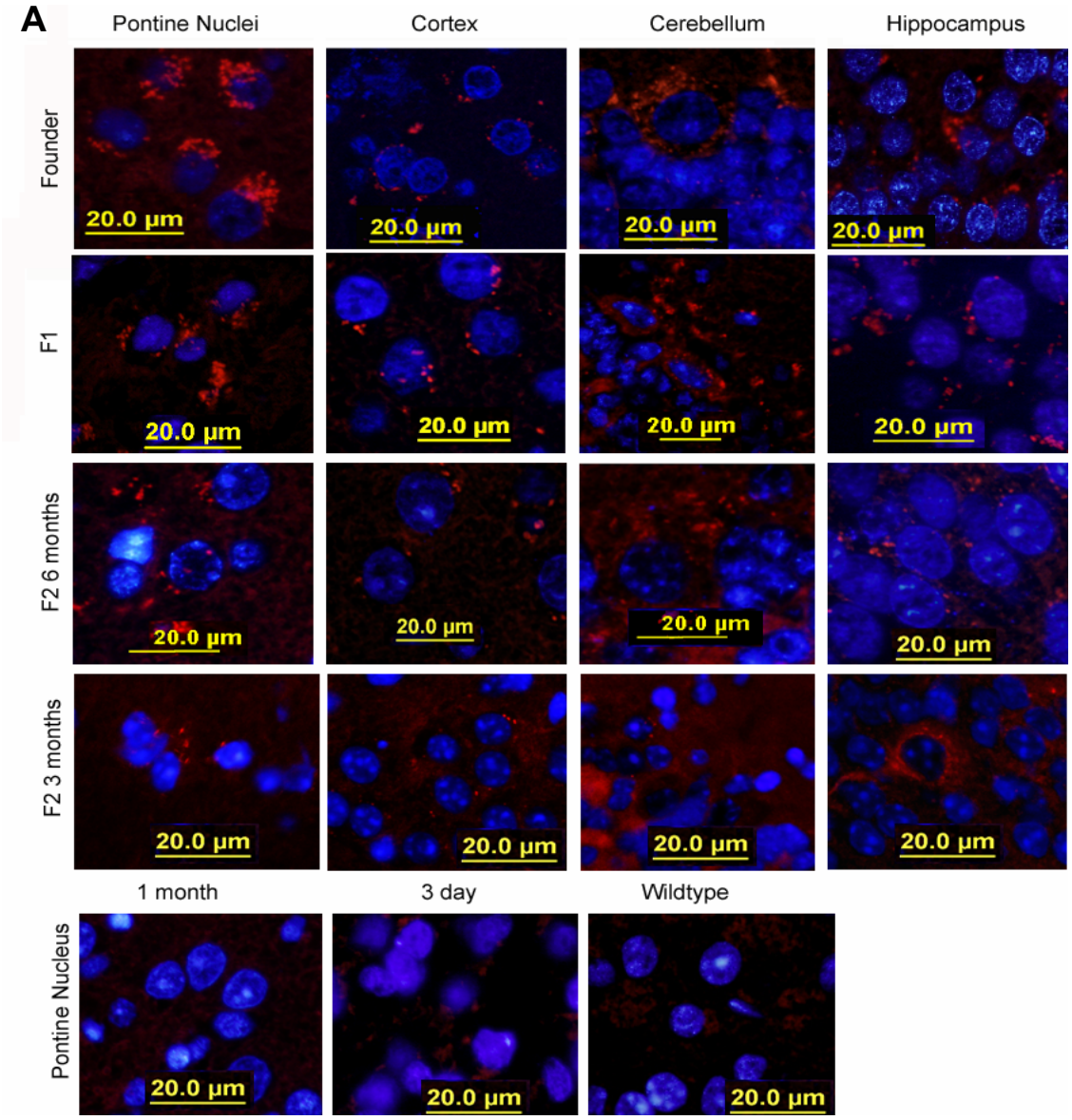

A. AUUCU aggregates are seen in cerebellum, cortex, pontine nuclei, and hippocampus. Aggregates are less pronounced in younger mice, most obviously seen in the pontine nucleus. Aggregates were seen in 9 month and 3 month F2 transgenic brains, but were not visible in 1 month and 3 day transgenic brain sections. Representative sections of pontine nucleus from 1 month, 3 day, and wildtype mice show no aggregates.

SCA8). Given the ataxic nature of SCA10 patients, we were interested to learn if the mice also suffered from an ataxia-like phenotype. Various statistical analyses were conducted using the footprints: step length, gait width, and alternation coefficient. Step length and gait width measure the average length and width of ten steps and are averaged over two trials (Figure 3.4C). Alternation coefficient also is averaged over a length of ten steps and two trials and measures the evenness of the steps: the distance of the two corresponding steps on the right paw should be directly bisected by the left paw (Figure 3.4C).

Both the transgenic founders (n=4, p=0.01) and F1 mice (n=4, p=<0.05) had a significantly shorter step length than wildtype littermates (Figure 3.4D). In measuring gait width, two groups emerged in the founding population with 2 mice having a significantly wider gait width (n=2, p=0.01), and the other 2 mice tested having a significantly narrow gait width (n=2, p<0.05) (Figure 3.4E). F1 mice consistently had a significantly narrower gait width (n=4, p=0.05) than wildtype littermates, regardless of which founder mouse – either wide-stepping or narrow stepping – it was bred. No significant difference between the three groups was seen in alternation coefficient (Figure 3.4F).

Transgenic Mouse Brains Contain AUUCU Aggregates

The expanded ATTCT repeat within the *ATXN10* gene of SCA10 patients has been shown to be normally transcribed and spliced, forming a normal, but expanded, AUUCU transcript. Previously, we have shown the presence of expanded RNA

transcripts as aggregations of AUUCU within SCA10 fibroblasts and PC12 cells transfected with expanded repeat. To investigate the presence of AUUCU aggregations within the transgenic mouse brain, transgenic brains of founder, F1 and F2 mice were sagittally sectioned. The sections were subjected to fluorescent *in situ* hybridization (*FISH*) with a Cy3-$(AGAAU)_{10}$ riboprobe. Extensive aggregations of the AUUCU repeats were seen in brains from founder and F1 mice, with few aggregates seen in F2 transgenic mice (Figure 3.5). More aggregates were seen in six month old F2 mice than were seen in three month old F2 mice (Figure 3.5). No aggregates were seen in the 1 month and 3 day old F2 mice. The variability between AUUCU aggregates in founder, F1 and F2 is likely to represent an increase in AUUCU foci with age. When aggregates were present, they were located in frontal cortex, pontine nuclei, locus ceruleus, nuclei hypoglossus, and hippocampus. Similar aggregations were not present in wildtype mice, with minimal background staining present. *FISH* sections also were subjected to immunohistochemistry with a monoclonal antibody to β–galactosidase. Aggregations were found to be present in the regions of the brain where β–galactosidase staining occurs, representing PrP expression (shown in Figure 3.6). β–galactosidase staining was found to colocalize with the AUUCU foci, suggesting that AUUCU is not spliced from the transcript.

AUUCU Aggregates in the Transgenic Brain Colocalize with Heterogeneous Nuclear Ribonucleoprotein Kinase

In the previous chapter, hnRNP K was not only pulled down by *in vitro* bead-

Figure 3.6. β-Galactosidase Colocalizes with Expanded AUUCU Aggregates

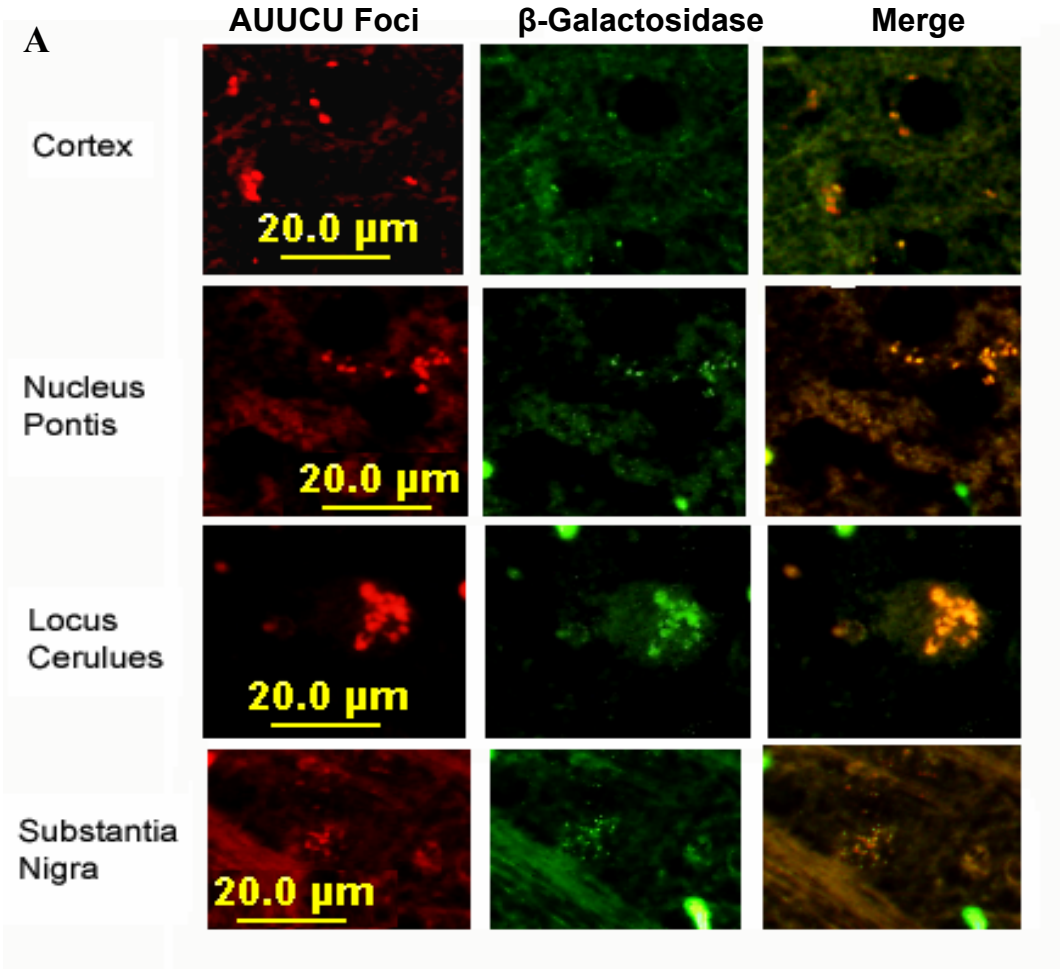

A. Immunostaining of β-Galactosidase and *FISH* demonstrates punctuate, colocalization with AUUCU aggregates. Colocalization is seen everywhere aggregates occur. Representative samples are shown from cortex, nuclei pontis, locus ceruleus, and substantia nigra. No β-Galactosidase staining was seen in wildtype mice (data not shown).

binding experiments, but hnRNP K also colocalized with PC12 cells transfected with expanded repeat. To investigate the colocalization of hnRNP K with AUUCU aggregates in the transgenic brain, we performed *FISH* using a Cy3-$(AGAAU)_{10}$ riboprobe in conjunction with immunohistochemistry with anti-hnRNP K. hnRNP K was found to distinctly colocalize with AUUCU foci in transgenic brains, with colocalization occurring virtually everywhere foci were present in founder, F1, and F2 sections (Figure 3.7). No AUUCU aggregates were seen in wildtype littermates, thus no colocalization occurred. These results suggest that hnRNP K is sequestered to the AUUCU aggregates in transgenic brain, as was previously seen in cell culture.

PKCδ is Localized to Mitochondria in Transgenic Mice

To investigate the effects of hnRNP K sequestration by AUUCU foci, we evaluated the localization of PKCδ in the mitochondria. Previously, studies have shown that PKCδ and hnRNP K can be coimmunoprecipitated, and are likely to exist as a complex within the cell (Schullery et al., 1999) We hypothesize that sequestration of hnRNP K will result in an abnormal amount of free PKCδ within the cell, mimicking an overexpression of PKCδ. Overexpression of PKCδ previously has been shown to induce caspase-3 mediated apoptosis due to a tanslocation to the mitochondria, reduced membrane potential and release of cytochrome C (Garrido et al., 2006; Majumder et al., 2001; Steinberg, 2004; Voss et al., 2005). In the previous chapter, our hypothesis was supported by the abnormal presence of PKCδ in the mitochondria in SCA10 fibroblasts and little PKCδ in the mitochondria within normal fibroblasts. PKCδ translocation to

Figure 3.7. hnRNP K is Sequestered to the AUUCU Foci

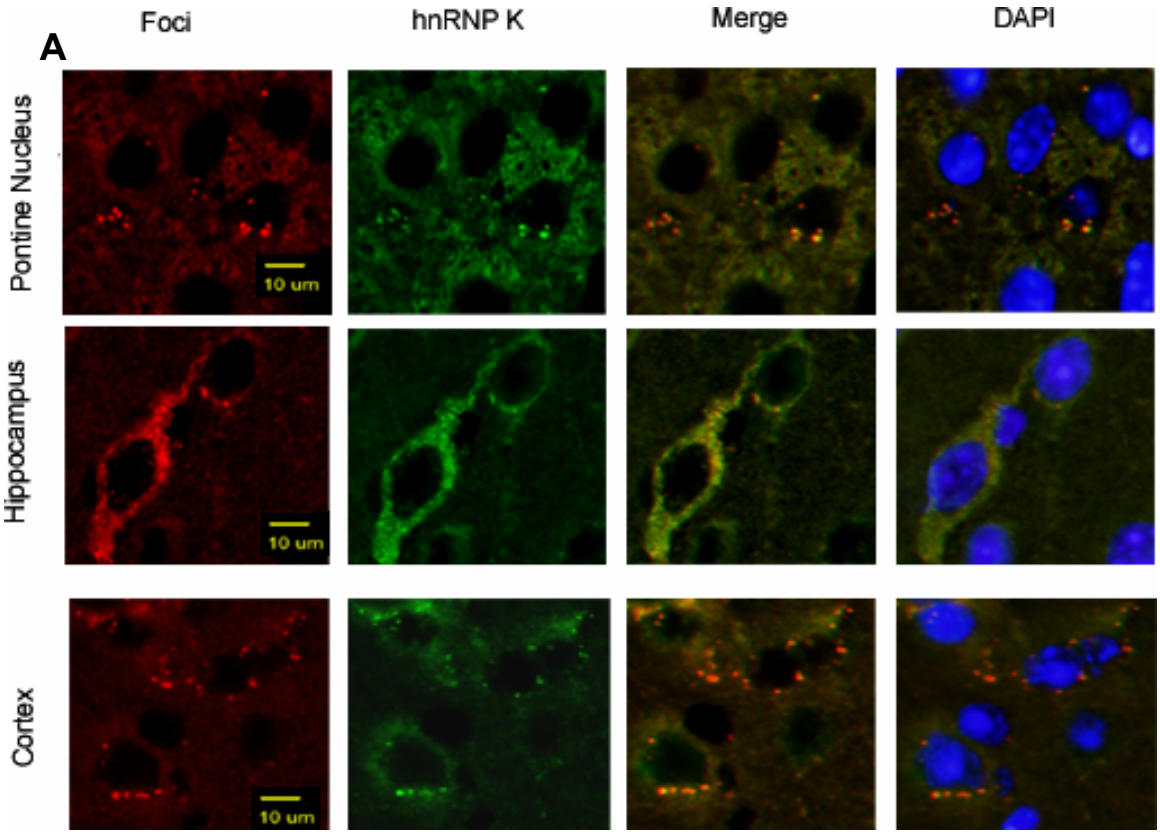

A. *FISH* using a Cy3-labed AGAAU riboprobe and immunohistochemistry to hnRNP K on sagitally sectioned transgenic brains. These sections were taken from 3 month F1 mice. hnRNP K and AUUCU foci colocalize virtually everywhere foci occur, but only pontine nucleus, hippocampus, and cortex shown. Wildtype mice not shown due to lack of foci.

mitochondria was inducible in normal fibroblasts through expression of expanded AUUCU repeat or inactivation of hnRNP K. Based on these results, the presence of PKCδ within the mitochondria of transgenic brains, specifically in regions expressing the transgene, was predicted. First, we performed immunohistochemistry on PKCδ and identified mitochondria using cytochrome oxidase complex I subunit IVa, known to be a mitochondrial marker. PKCδ expression in wildtype brains was compared to expression in transgenic brains. Significant colocalization of PKCδ and mitochondria was seen in transgenic mice in the pontine nuclei and the frontal cortex, regions where significant AUUCU aggregates were found to colocalize with hnRNP K (Figure 3.8A). Relatively no overlap between PKCδ and mitochondria was seen in widltype mice (Figure 3.8A). These findings suggest the transgenic brains successfully recapitulate the PKCδ translocation to mitochondria previously seen in SCA10 fibroblasts.

AUUCU Aggregates are Present within Mitochondria in Transgenic Mice

In the previous chapter, SCA10 fibroblasts contained AUUCU aggregations mostly nuclearly, with some perinuclear and cytoplasmic aggregations. However, upon analysis of the AUUCU aggregates in the transgenic brain, we noticed punctate staining mostly surrounding the nucleus. The distinct nature of the staining prompted the investigation of the exact localization of the RNA transcript containing the repeat expansion. *FISH* and immunohistochemistry to COXI complex IVa, a mitochondrial marker, suggests that the foci are present primarily within the mitochondria in most areas

Figure 3.8. Both PKCδ and AUUCU Foci Localize to Mitochondria in Transgenic Brain

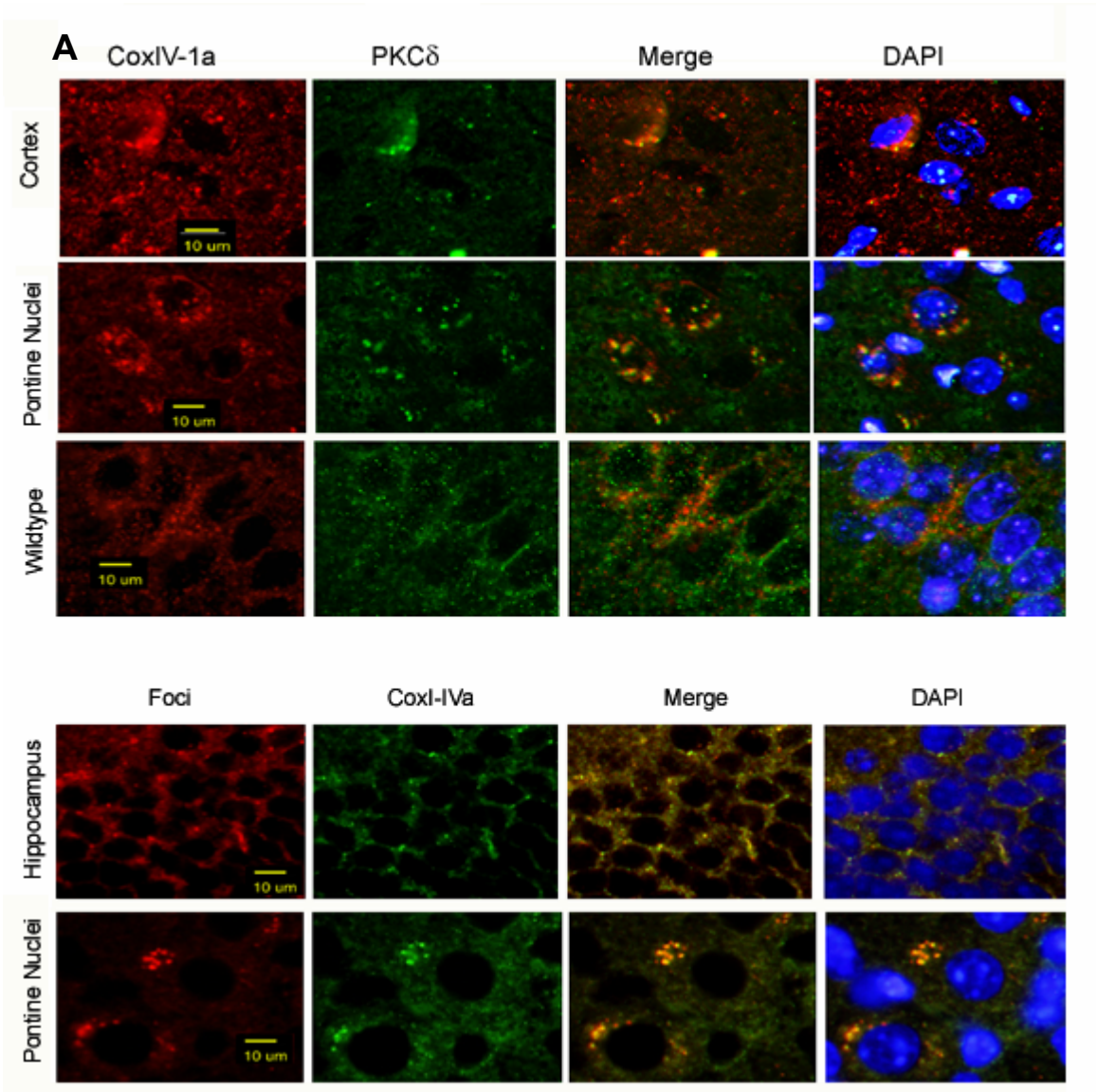

A. Immunohistochemistry of PKCδ and mitochondria showing colocalization in transgenic brain. Wildtype brains did not show colocalization of PKCδ to mitochondria. B. *FISH* of AUUCU foci and immunohistochemistry of mitochondria. AUUCU aggregates are present within mitochondria in transgenic brain.

of the transgenic brain. Extensive colocalization of COXI and the AUUCU aggregates is seen in the frontal cortex, pontine nucleus, and hippocampus (Figure 3.8B).

Transgenic Brains Contain Frontal Cortex Vacuolization

Basic hematoxylin and eosin (H&E) staining was performed on the sagittally sectioned brains to evaluate brain structures. In the frontal pole, the transgenic brains contained neurons that appeared to contain large vacuoles that pushed the nucleus and cytoplasm to the boundary of the cell (Figure 3.9). Some cellular shrinking was seen in the wildtype brain processed concurrently, but was relatively insignificant compared to the vacuolization seen in the transgenic. To investigate the contents of the vacuoles, we performed periodic acid-Schiff (PAS) staining. Periodic acid oxidizes glycols to aldehydes, while the subsequent exposure to Schiff releases a pararosaniline adduct and stains glycols bright pink to red. The PAS staining revealed that the vacuoles indeed contained glycogen. PAS positively stained vacuoles were present in all regions of the brain where vacuolization was seen (Figure 3.9B). Wildtype littermates were used as a control. The PAS staining present in the transgenic brains was darker and generally occurred within the vacuoles (Figure 3.9B). PAS has been used widely for glycogen storage diseases, and recently has been implicated as a precursory indicator of autophagy.

Figure 3.9. Vacuolization Positive for Periodic Acid Schiff Present in Transgenic Brains

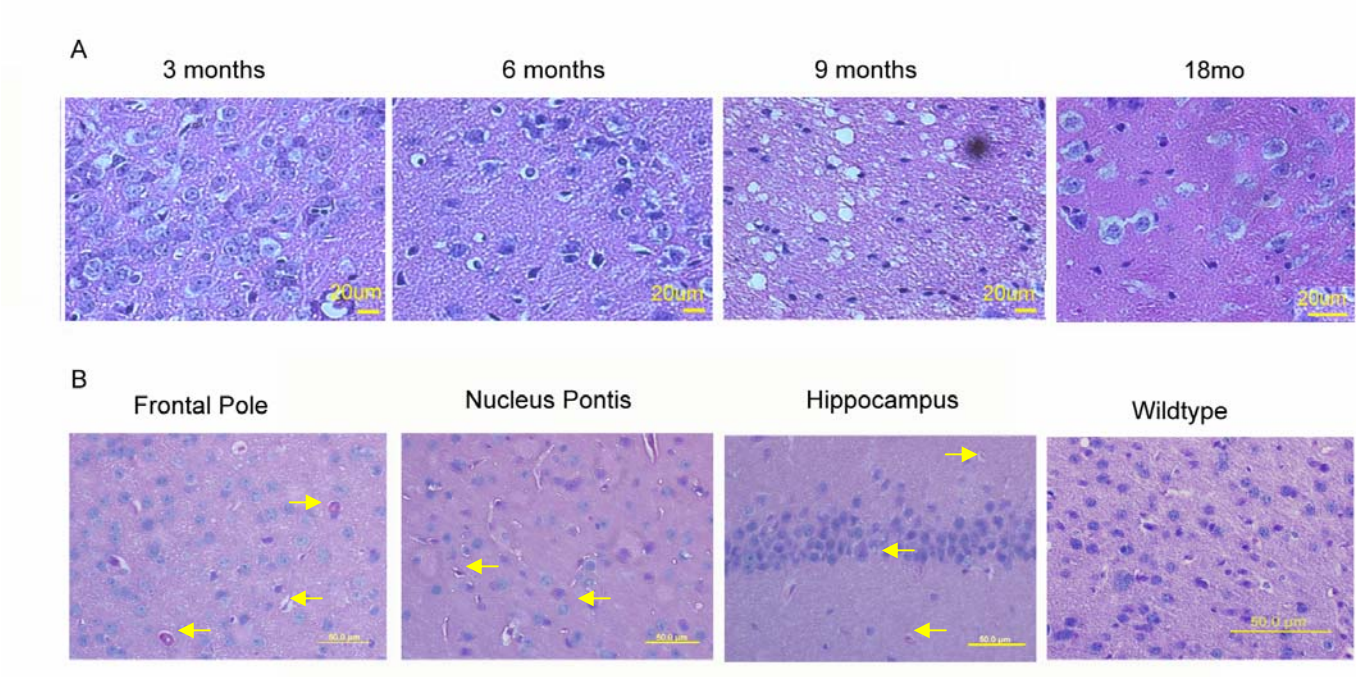

A. Hematoxylin and Eosin of sagitally sectioned transgenic brains showing extensive vacuolization within the frontal pole, which increases with age. B. 3 month old transgenic brains contain vacuoles which stain positive for periodic acid Schiff (pink-maroon) in various regions of the brain. Wildtype brains were not remarkably positive for PAS staining, nor did they show extensive vacuolization as seen in the transgenic brains.

DISCUSSION

Since the first gene transfer to mice was successfully executed in 1980, mechanistic studies of genetic diseases have been considered virtually null and void without a successfully engineered genetic mouse model. While *in vivo* cell culture is useful, it cannot provide the natural environment present within the mouse with multiple interacting tissues and extracellular stimuli. Transgenic mice are routinely used in repeat expansion disorders to investigate behavioral and histopathological changes induced primarily from an endogenous expanded repeat. In most repeat expansion disorders, repeat stability varies between different tissues within various aged mice. In one model of DM1 transgenic mice, 162 CUG repeats were shown to vastly expand in 20-month old mice, in various tissues, most markedly with expansion up to 650 repeats in kidney (Fortune et al., 2000). FRDA transgenic mice also showed age and tissue-dependent instability, specifically within the cerebellum, with instability beginning around 2 months (Al-Mahdawi et al., 2004; Clark et al., 2007). In one Huntington Disease mouse model, a frameshift mutation prevented the transcript containing 44 CAG repeats from being translated and resulted in wildtype phenotype and a remarkably stable repeat (Goldberg et al., 1996), contrary to instability seen in primary cell culture of fibroblasts from other HD transgenics (Manley et al., 1999). The findings of wildtype phenotype in the untranslated HD transgenic not only suggested that the HD mutation was not due to an RNA gain of function, the stability of the repeats also suggested that surrounding genomic sequences could be important in the mechanism of repeat instability (Goldberg et al., 1996).

In humans, long, normal range repeat expansions are generally considered hypermutable, with a potential for expansion (Duenas et al., 2006; Gatchel and Zoghbi, 2005). SCA10 transgenic mice demonstrated both contraction and expansion of ATTCT repeat with each generation of breeding, showing instability within transmission as is often seen in transgenics as well as in the human disorder. The absence of repeat variability within the SCA10 transgenic tissues suggests that the instability may occur within the germ line. However, the male and female founder mice both had contracted and expanding offspring suggesting that, unlike in human SCA10, the repeat is equally unstable in male and female transgenic mice.

Shrinkage of the transgenic ATTCT repeat provides a unique opportunity for comparison of histopathology and behavior based solely on the size of ATTCT repeat expansion. According to quantitative RT-PCR results and previous reports, the transgene is expressed primarily in CNS-derived tissues. Thus, behavioral analyses and histochemistry was limited to CNS-derived tissues. Extensive expression of β-galactosidase in frontal cortex, hippocampus, and pontine nucleus suggested that behavior of the transgenic mice should be significantly distinguishable from wildtype if the repeat is toxic. Based upon the open field analysis and the footprint analysis, it can be concluded that the founder, F1, and wildtype mice behave as 3 distinguishable groups in most measurements. These findings suggest that behavior directly correlates to length of repeat, with founder mice showing the most drastically altered behavior and F1 mice generally showing intermediate behavior to founder and wildtype mice. In the wire hang experiment, the founder and F1 mice were grouped in comparison to wildtype mice,

revealing significant learning differences between transgenic and wildtype animals. While a significant difference in behavior was seen in the transgenic mice, it should be noted that the transgenic mice express approximately 500 repeats, and reduced penetrance has been attributed to human patients in the 280-850 range (Matsuura et al., 2006; Raskin, In press). It is possible that reduced penetrance may be present within the 500 ATTCT repeat range in mice, and skew statistical data.

AUUCU aggregates were shown in the previous chapter to be the major toxic factor resulting in caspase-3 mediated apoptosis in cell culture. To investigate the toxicitiy of the AUUCU aggregates *in vivo*, *FISH* was performed on sagittally sectioned mouse brain. Extensive aggregation of AUUCU repeats was seen in the founder and F1 transgenic mice, while aggregates were seen in three month old-F2 transgenic mice and virtually no staining was seen in 1 month and 3 day old F2 transgenic mice or wildtype littermates. Based upon our previous findings that AUUCU sequesters hnRNP K, immunohistochemistry with anti-hnRNP K antibody was performed. Mouse brain contained distinct colocalization between AUUCU aggregates and hnRNP K, further validating the tissue culture findings, and the sequestration of hnRNP K hypothesis. In the last chapter, we investigated the expression of PKCδ, specifically the translocation to mitochondria. Once more, PKCδ was found in the mitochondria of the transgenic brains in regions where extensive expression of aggregates and sequestration of hnRNP K occurred. Some regions which contained aggregates showed modest translocation of PKCδ and mitochondria, despite extensive aggregates and hnRNP K. Our hypothesis suggests that when hnRNP K is sequestered by AUUCU aggregates, abnormal amounts

of PKCδ are left free within the cell. It is likely that a gradient may occur where regions with very high levels of expression of hnRNP K will have diminished effects compared to regions with lower levels of hnRNP K, where sequestration would be more devastating to the cell.

Histological examination of transgenic mice with H&E revealed extensive vacuolization in the frontal cortex of the transgenic brain as well as in the pons and the brainstem. Vacuolization occurred in the regions where extensive AUUCU aggregations were seen in the adjacent sagittal section, suggesting the aggregates result in vacuolization. The vacuoles stained positive for periodic acid Schiff, implicating a possible role for autophagy that deems worthy of further investigation. The mechanism tested thus far directly results in caspase-3 mediated apoptosis. A resounding debate currently exists between apoptosis mechanisms in late-onset neurodegenerative disorders and the possible role of autophagy. Given the translocation of PKCδ to the mitochondria, and the supposed release of cytochrome-C and activation of caspase-3, why doesn't every neuron expressing expanded AUUCU repeat automatically undergo cell-mediated apoptosis? Many believe that autophagy plays a protective role in repeat expansion disorders until later in life when the negative affects of the aggregates become so extensive that the cell can no longer function. The SCA10 transgenic model, though not fully investigated for autophagy, provides an intriguing model for an autophagy/apoptosis relationship.

While the sequestration of hnRNP K provides a direct mechanism for activation of caspase-3, many other mechanisms resulting in SCA10-like phenotypes are plausible.

It is probable that the expanded AUUCU repeat not only sequesters hnRNP K, but also sequesters other RNA binding proteins. Additionally, hnRNP K is a highly interactive protein known to be ubiquitously expressed and have a multifaceted role within the cell. The sequestration of hnRNP K is likely to result in a cascade of effects. hnRNP K has previously been shown to bind and activate the TATA-binding protein, interact with the Src-homology domain and PI3-K, and also interact with p53. Given its versatile role within the cell, it would be presumptuous to classify the sequestration of hnRNP K and the translocation of PKCδ to mitochondria as the only viable mechanism leading to SCA10. Other proteins sequestered to the repeat, along with other pathological functions resulting from the sequestration of hnRNP K, are needed to establish the mechanism of SCA10.

MATERIALS AND METHODS

Construction of the Transgenic Mouse

The ATTCT repeat sequences were PCR amplified from SCA10 hybrid cells derived from Mexican SCA10 patients. PCR amplification was done using the forward primer 5'-CCAAGGATGCAGGTGCCACAGCATCTC-3' and the reverse primer 5'-ATATGCATCCAGCTTCTGATTACATGGACT-3'. The PCR product, and subsequently derived transgene, contains 650 bp upstream to expanded ATTCT repeat and 500 bp downstream of the repeat. The PCR product was gel-purified using a Qiagen gel purification kit and cloned into the *SwaI* site of pcDNA 3.1-hygro-*LacZ*. The cytomegalo virus (CMV) promoter sequences in pcDNA 3.1-hygro-*LacZ* were removed

prior to insertion of the expanded ATTCT repeat and replaced with the *Mfe*/*BamhI* fragment of the rat prion promoter sequences (~3.5kb) using standard cloning strategies. A synthetic polylinker sequence also was cloned into the *XhoI* site downstream of *LacZ* and upstream of the BGH polyA sequences prior to insertion of the expanded ATTCT repeat. The synthetic polylinker sequence provided the *SwaI* site the repeat was subsequently cloned into, using T4 DNA Ligase. Expanded ATTCT repeat was confirmed by digestion of the plasmid with *SfiI*, flanking the *SwaI* site. The plasmid encoding the expanded ATTCT repeats were transfected into *E. coli* SURE bacteria at 16°C to provide slower growth rates and minimize deletion of repeat sequences. Digestion of the transgenic plasmid with *MfeI* and *NaeI* was the electrophoretically separated on an agarose gel. The ~10 kb fragment was purified from the agarose gel using the Qiagen gel extraction kit. Control plasmids containing the same flanking regions and normal ATTCT repeats were derived from normal human DNA.

Fertilized eggs derived from pregnant female mice were microinjected with the transgene containing expanded AUUCU repeats. The microinjected eggs were transplanted into the uterus of pseudo-pregnant surrogate mothers to obtain founder mice. Both Southern blot and repeat primer PCR were used to confirm the presence of the transgene in the new SCA10 transgenic line.

PCR Genotyping

PCR genotyping was performed using two sets of primers, both present in the region of the *LacZ* gene. The first set of primers amplified the 5' end of the LacZ gene with the forward primer 5'-GATTGGCCTGAACTGCCAGCT-3' and reverse primer 5'-

GTCGATATTCAGCCATGTGCC-3'. The second set of primers amplified the 3' end of the LacZ gene with forward primer 5'-ATGGTGCTGCGTTGGAGTGAC-3' and reverse primer 3'-GACATGCAGAGGATGATGCTC-5'. PCR products were run on a 0.8% agarose gel and eletrophoresed for 45 minutes at 120V.

Repeat-primed PCR

Genomic DNA was extracted from mouse tail and other mouse tissues using either the Qiagen DNeasy Blood and Tissue Extraction kit or by a basic phenol:chloroform precipitation. RP-PCR was performed on 140ng genomic DNA using the forward primer 5'-GAAGACAAATAGAAACAGATGGCAGA-3' and the reverse primer 5'--3'. The protocol was slightly modified from Matsuura et al., with Gamma-33P-ATP (Matsuura and Ashizawa, 2002). The forward primer was labeled using polynucleotide kinase and column purified. Approximately 140ng of DNA was used in the 20µl PCR reaction, with 7.5 ul HotStart master mix Taq, 2 µl of labeled 5' primer, 0.8 µl unlabeled 5' primer (10uM), and 1 µl 3' primer (10mM). Thirty cycles were completed with an initial denaturation at 95˚C for 15 minutes, followed by denaturation for 30 seconds and 94˚C, annealing at 60˚C for 30 seconds, and amplification at 72˚C for 2 minutes, with a final elongation at 72˚C for 10 minutes. RP-PCR products were electrophoresed on 6% polyacrylamide gel made from National Diagnostics ready-made gel solutions for approximately 4 hours.

Quantitative RT-PCR

Quantitative RT-PCR was performed by the RT-PCR core lab at the University of Texas Medical Branch. Primers were designed in the *LacZ* gene region. RNA was extracted from mouse brain and tissues after perfusion with ice cold 1% phosphate-buffered saline and tissues were immediately placed in RNA later and stored at -80°C. Further extraction was performed following the protocol in the Qiagen RNeasy Protect kit with tissue disruption performed using a sterile, RNAse free Eppendorf-sized pestle. Homogenization subsequently was performed with syringe and a 20 gauge needle.

Perfusion and Mouse Brain Sectioning

Transgenic mice were anesthetized with Avertin and perfused through the aorta. Pefusion occurred with ice cold phosphate buffered saline (PBS) for 15 minutes PBS and then 60ml of fresh 4% paraformaldehyde (PFA) in DEPC water. The brain was carefully removed and stored in 4% PFA at 4ºC with gentle agitation overnight. Brain tissue was then placed in 30% sucrose overnight. Mouse brains were then stored in 70% ethanol until all brains could be processed and sectioned simultaneously. Mouse brains were fixed in paraffin and sectioned sagittally at 5 um. Sagittal sectioning was performed by the Research Pathology Core lab.

Fluorescent *in situ* Hybridization

RNA foci were stained using a Cy3-labeled $(AGAAU)_{10}$ riboprobe complementary to the transcribed ATTCT repeat. First, paraffin was removed from the brain sections by 10 minutes in xylene, 10 minutes in xylene:ethanol, and slides were

rehydrated 10 minutes in 100% ethanol, 10 minutes 70% ethanol, and 10 minutes DEPC water. Better probe penetration was accomplished by immersing slides in 200 mM HCL in DEPC water for 10 minutes. Slides were rinsed with DEPC water. The protocol previously described in Chapter 2 for *FISH* in cell culture was modified for *FISH* on sagittal sections following removal of paraffin, with the exception of the slides being hybridized at a temperature of 45˚C.

Immunohistochemistry

hnRNP K antibody was obtained from Acris antibodies and was monoclonal from mouse. B-galactosidase monoclonal antibody from mouse was obtained from Abcam and was tested for specificity in wildtype mice. Both PKCδ (G-9) monoclonal antibody derived from mouse and PKCδ(C-20) polyclonal antibody derived from rabbit were obtained from SantaCruz biotechnology. COX I-complex Iva was obtained from Invitrogen Molecular Probes. Fluorescent secondary antibodies were also obtained from Invitrogen molecular probes, including goat anti-mouse 488, 568, and 633, and goat anti-rabbit 488, 568, and 633.

Both wildtype and transgenic slides were concurrently processed first by blocking with 1x antibody dilution buffer (ADB) (10% goat serum and 0.3% triton-X 100 in 1x PBS) overnight. Primary antibody was diluted (either hnRNP K, PKCδ, COXI-Iva, or β-galactosidase) 1:500 in ADB. Unbound primary antibody was removed by washing for 10 minutes 3 times. Either goat anti-mouse or goat anti rabbit secondary antibody from Molecular Probes was used to visualize the localization of primary antibody. Antibodies

were visualized using either a Hamamatsu Camera Controller using DP controller software in the histopathology core lab at UTMB or Zeiss confocal microscopy at Baylor College of Medicine.

Open Field Analysis

Open field was performed at 6 months of age for all animals tested in the behavioral core facility of the animal resource center at University of Texas Medical Branch. Four mice were simultaneously videotaped in 40cm square Plexiglas boxes. Videotape surveillance was analyzed using TopScan EZ software available from Clever Systems, Inc. Data regarding total distance, velocity, rearing, and percentage of time in inner arena versus outer arena was calculated and compared using a student's t-test.

Wire Rod Hang

Mice were placed on a metal rack approximately 2mm in diameter. The rack was inverted approximately 40cm above the home cage. The amount of time the mouse was able to hold on to the wire rack was recorded. Three trials were completed on two consecutive days with at least thirty minutes between each trial.

Footprint Analysis

The hind paws of mice were painted with non-toxic ink. The mice were permitted to walk through a narrow, wooden tunnel 6 cm wide and 39 cm long. Two trials were completed with each mouse. Step length was measured by obtaining the length for the mouse to take ten steps and divided by ten to obtain an average and then averaged over

two trials. Gait width was measured by drawing a line from the center of the first step to the center of the second step on both the left and right side. A line with a 90º angle with respect to the line between the two steps was drawn from the left step to the right step. The length of the line (GW1) between the left and right steps was averaged over ten steps to obtain average gait width. Alternation coefficient was measured first by obtaining RR1, the length between each individual step on one side. Then, RL2, the length between the step on one side and the step on the other side as measured by the 90º line created in calculation of GW1. Alternation is finally calculated by:

$$\frac{0.5\text{-}RLn}{RRn} = ACn$$

for each step. The absolute value of the alternation coefficient is taken and then averaged (RR1 – RR5) on for the right side. The same process is undergone on the left side.

Periodic Acid-Schiff staining

The brain sections were deparaffinized and rehydrated as described in the *FISH* section. Slides were stained using the Sigma-Aldrich Periodic Acid Schiff kit.

Chapter IV:

Rescue of the Cellular SCA10 Phenotype

SUMMARY

Compelling data in the Chapter II and Chapter III demonstrated that the ATTCT repeat is transcribed into AUUCU, which forms cellular aggregates that sequester the protein hnRNP K. This chapter investigates intervention into the toxic relationship between hnRNP K and the AUUCU foci. In rescue-targeted experiments, we attack either the AUUCU foci, or the low levels of hnRNP K. Targeted inactivation of *ATXN10* and overexpression of hnRNP K are shown to rescue the SCA10 cellular phenotype in SCA10 fibroblasts, suggesting viable treatment options for SCA10 may exist. Further investigation into the mechanism provides viable options for intervention into the relationship between the expanded RNA repeat and hnRNP K.

INTRODUCTION

The mechanistic data presented thus far suggest that SCA10 is an RNA-pathogenic disorder. The expanded ATTCT repeat is transcribed into a pathologic, expanded AUUCU repeat. Due to previous reports that the mutant transcript is properly processed and spliced, we investigated the fate of the RNA expansion within the cell (Wakamiya et al., 2006). Detection of the expanded RNA repeat as insoluble aggregates by fluorescent *in situ* hybridization suggested that the transcribed repeat is impoperly degraded. Subsequent detection of hnRNP K as an AUUCU-RNA binding protein implicated that hnRNP K may be sequestered by the abormal RNA repeat expansion.

Co-localization of hnRNP K and the AUUCU foci suggests that hnRNP K is indeed sequestered by the transcribed ATTCT repeat. Subsequently, inactivation of hnRNP K, or over-expression of expanded repeat was found to induce cell death via caspase-3 mediated apoptosis. A mechanism linking hnRNP K to caspase-3 activation was investigated and found to involve protien kinase C δ. PKCδ is highly localized in the mitochodria of SCA10 fibroblasts, while normal fibroblasts have virtually no mitochondrial expression. The translocation of PKCδ to mitochondria was inducible with transfection of expanded ATTCT repeat or inactivation of hnRNP K. These findings suggest that PKCδ plays a role in SCA10 RNA-mediated pathogenesis and in activation of caspase-3 due to inactivation of hnRNP K.

In this chapter, we explore the possibility for rescue of the SCA10 cellular phenotypes. Investigating the hnRNP K sequestration hypothesis, rescue can be approached from two directions: the removal of transcript, or the saturation of the repeat with excess hnRNP K. Activation levels of caspase-3 as well as the localization of PKCδ are used to measure the amount of rescue in cell culture, both in human neuroblastoma cells and in SCA10 fibroblasts. Decreased activation of caspase-3 and rescue of PKCδ localization to mitochondria suggests that the effects due to the AUUCU repeat are salvageable and may be viable for further development of treatment options.

RESULTS

Inactivation of Ataxin 10 Transcript Rescues Caspase-3 Mediated Apoptosis

Based upon the hnRNP K sequestration hypothesis, the toxic AUUCU transcript binds and sequesters hnRNP K, preventing hnRNP K from performing important cellular

functions. To correct for this mechanism, two approaches may be employed. First, by inactivating the transcription of *ATXN10*, novel AUUCU aggregate formation is prevented. In fibroblasts derived from SCA10 patients, PKCδ is localized in mitochondria, as seen by immunohistochemistry with a mitochondrial marker and anti-PKCδ (presented in Chapter II). To test whether the AUUCU RNA-mediated translocation of PKCδ to the mitochondria can be minimized by inactivation of the SCA10 transcript, we targeted *ATXN10* transcripts in SCA10 fibroblasts with *ATXN10* siRNA and studied the cellular localization of PKCδ (Figure 4.1). The result was a restoration of normal subcellular localization of PKCδ with a decreased amount of PKCδ in mitochondria in the siRNA-treated SCA10 cells. As expected, control siRNA treatment had no significant effects on the distribution or amount of PKCδ in SCA10 cells (data not shown). We conclude that by interfering with the formation of hnRNP K-AUUCU complexes, hnRNP K can re-establish normal function within the cell, alleviating the pathogenic mechanisms leading to apoptosis. These findings support our hypothesis that the toxic AUUCU transcript is sufficient to activate mitochondrial translocation of PKCδ.

Overexpression of hnRNP K Rescues Caspase-3 Mediated Apoptosis

To approach the rescue of SCA10 based on the sequestration of hnRNP K, a second method can be employed. Instead of inactivating the transcript, it is possible that overexpression of hnRNP K could saturate the pathological binding between the AUUCU transcripts and hnRNP K, and appropriate levels could be utilized to provide the proper

Figure 4.1. PKCδ Leaves Mitochondria in Response to Decreased ATXN10 Transcript

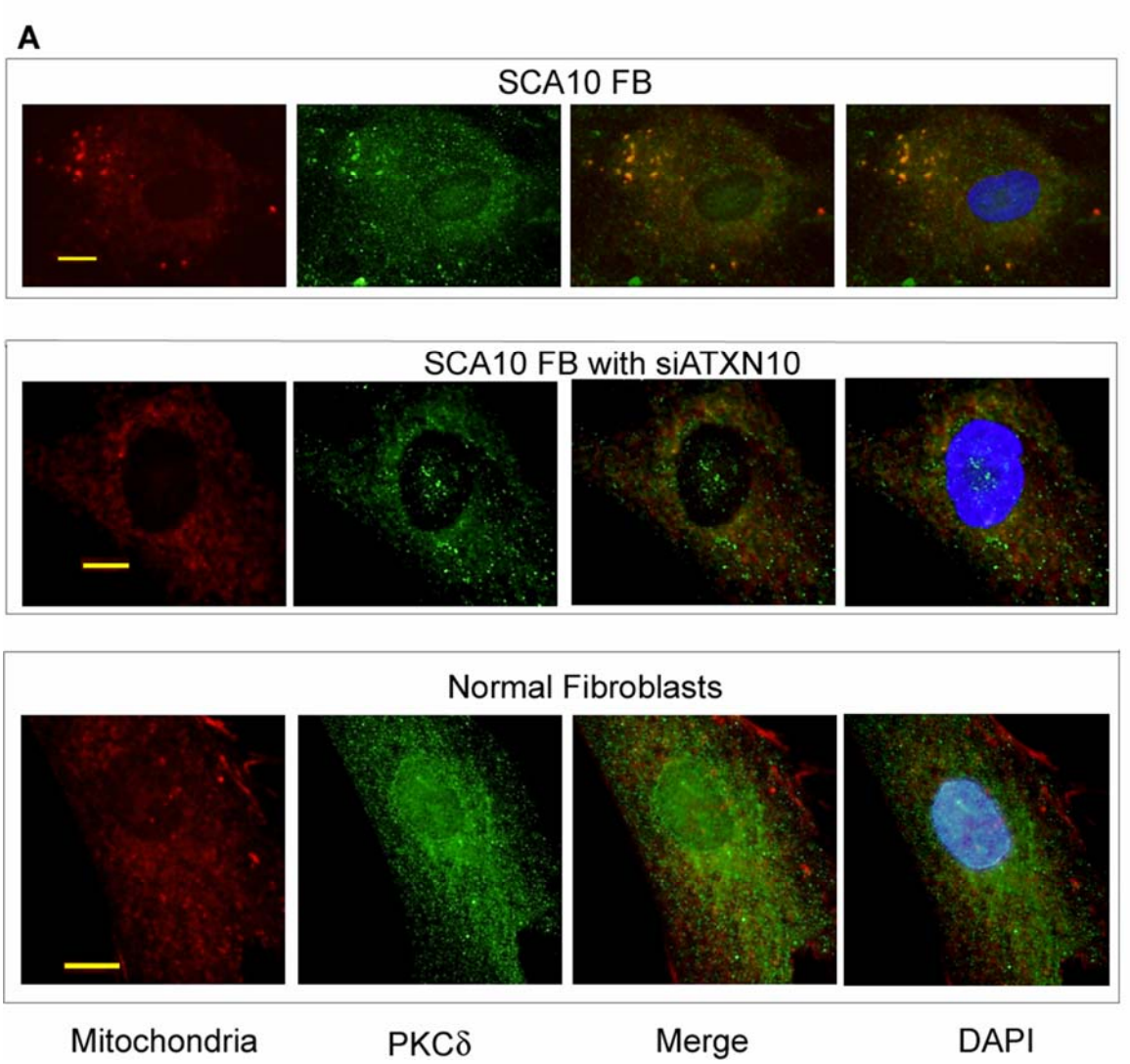

A. The first row shows immunodetection of PKC δ (green) in SCA10 fibroblasts before treatment of ATXN-10 siRNA and mitotracker staining (deep red) showing localization of PKC δ in mitochondria. The second row shows SCA10 fibroblasts stained for PKCδ (green) and for mitochondria (deep red) 72 hours after treatment with ATXN-10 siRNA. Decreased localization of PKC δ is seen in mitochondria with increased expression seen in the nucleus. The third row displays normal, age-matched fibroblasts for a comparison with ATXN-10 treated SCA10 fibroblasts with PKC δ (green) and mitochondria (red).

amounts of hnRNP K for cellular function. cDNA for hnRNP K was cloned into pCMV/myc/nuc expressing neomycin resistance, enabling easy selection of cells transfected with expanded AUUCU repeat containing approximately 500 repeats (Chapter II, Figure 2.1). In addition to PC12 cells overexpressing hnRNP K, PC12 cells without prior transfection were also transfected with expanded ATTCT repeat or normal-length ATTCT repeat (12 ATTCT repeats). Levels of activated caspase-3 were measured. The PC12 cells overexpressing hnRNP K before transfection with expanded repeat, compared to PC12 cells without the hnRNP K transcript, showed a significant decrease in activation of caspase-3 (Figure 4.2A; $n=3$, $p<0.01$). PC12 cells transfected with short ATTCT repeat showed relatively low levels of caspase-3 activation. These results suggest that providing the appropriate levels of hnRNP K to SCA10 cells rescues the cells from apoptosis induced by expanded SCA10 repeat.

Overexpression of GFP-labeled hnRNP K reduces Mitochondrial Translocation of PKCδ

Based upon the finding that overexpression of hnRNP K prior to transfection of expanded repeat results in significantly less activation of caspase-3, we investigated the localization of PKCδ. In normal fibroblasts, PKCδ was expressed primarily in the cytoplasm, with some expression found in the nucleus. However, in SCA10 fibroblasts, PKCδ expression extensively localized in respirating mitochondria, as seen by mitotracker. In order to determine if normal PKCδ localization can be restored by proper hnRNP K levels, SCA10 fibroblasts were transfected with hnRNP K. For this

Figure 4.2. hnRNP K Overexpression Rescues SCA10 Cellular Phenotypes

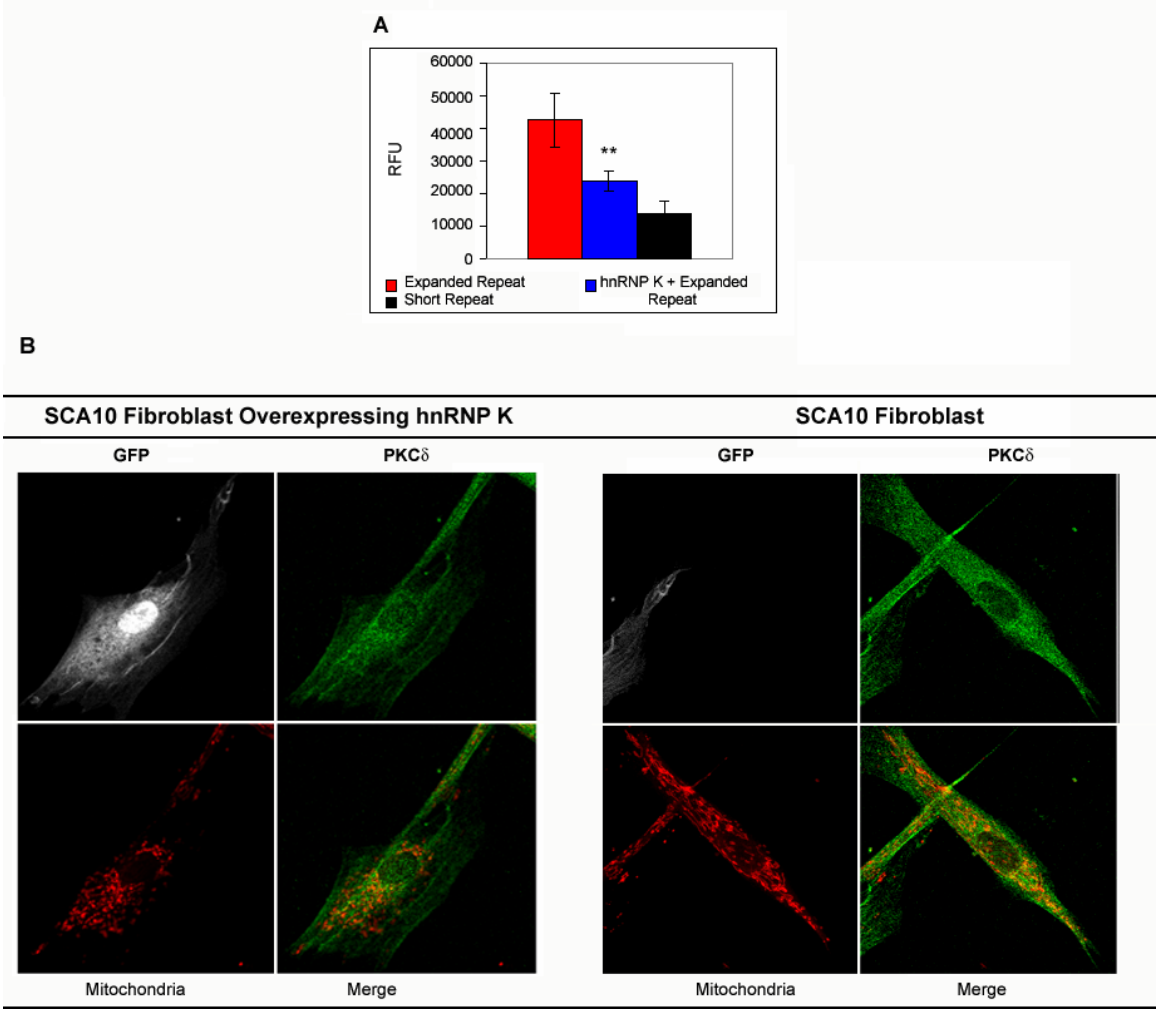

A. Caspase-3 assay measuring relative fluorescent units (RFU) of PC12 cells stably transfected with hnRNP K prior to expanded ATTCT repeat transfection as compared to PC12 cells transfected with short ATTCT repeat and expanded ATTCT repeat. hnRNP K overexpression shows significant rescue of caspase-3 activation. B. Overexpression of GFP-labeled hnRNP K in SCA10 Fibroblasts results in decreased PKCδ localization in mitochondria. Panel on the left is SCA10 fibroblasts transfected with GFP-hnRNP K. Panel on right represents SCA10 fibroblasts not transfected with hnRNP K. PKCδ is represented by green and mitochondria by red for simplification

experiment hnRNP K was conjugately labeled with GFP, to determine which cells were properly transfected with hnRNP K. GFP-labeled cells were compared to cells unlabeled with GFP. Using confocal microscopy and an antibody to PKCδ and mitotracker, PKCδ and mitochondria were found to have significant colocalization in fibroblasts derived from SCA10 patients. However, in the cells transfected with GFP-hnRNP K, decreased levels of PKCδ and mitochondrial colocalization was seen (Figure 4.2B). No change in PKCδ localization was seen in SCA10 fibroblasts without GFP labeling compared to SCA10 Fibroblasts without treatment of siRNA. These findings suggest that saturation of the repeat with hnRNP K results in removal of PKCδ from mitochondria.

Overexpression of KH Domain III Results in Reduced Caspase-3 Activation

Debate surrounds the role of the three KH domains of hnRNP K in RNA binding. Initially, several papers agreed that the third KH domain was essential for binding poly-C RNA and single stranded nucleic acids (Dejgaard and Leffers, 1996; Ito et al., 1994). One study suggests that a small (six or seven nucletide), C-rich box is the only one domain involved (Paziewska et al., 2004). Other studies have identified interactions involving all three KH domains in binding RNA (Siomi et al., 1994; Thisted et al., 2001). Most efforts have been placed in analyzing the third KH domain with regard to nucleic acid binding, formulating crystal structures showing the binding of KH domain III to single standed nucleic acids (Backe et al., 2005). Based upon these previous reports and the finding that overexpression of hnRNP K not only decreased activation of caspase-3, but also translocation of PCKδ to mitochondria, defining the role of the KH domains with

the expanded AUUCU RNA repeat became important. To investigate the role of the KH domains, PCR amplification of mulitple combinations of the domains was utilized to develop transgenes for transfection into human neuroblastoma cell lines (SY5Y). We developed in-frame clones including all three KH domains and the KI region (KHd 1,2,3), containing KH domain 1 and 2 (KHd 1,2), KH domain 2 and 3 (including the KI region) (KHd 2,3), and KH domain 3 (KHd 3) (Figure 3A). To serve as a control, the CMV vector utilized to express the KH domains was transfected without any KH domains. Transfection of these linearized clones into SY5Y cells was selected for with neomycin to produce a stable neuroblastoma cell line expressing regions of hnRNP K possibly important for binding expanded AUUCU repeat. Upon transfection of the stable cell lines with expanded AUUCU repeat, activation of caspase-3 was measured using a caspase-3 activation assay. Caspase-3 levels were normalized to levels of the control CMV vector and normalized to protein levels with a BCA protein assay. KH domain 2 and 3, along with KH domain 3 were found to decrease activation of Capase-3 (Figure 4.3B). KH domain 1,2,3 did not rescue any more or less than the control, while KHd 1,2 showed more activation of caspase-3. While these results are not statistically significant after 5 trials, it should be noted that only approximately 30% of the SY5Y cells are efficiently transfected with repeat expansion. Thus, any rescue present is the result of less than half the population of cells being transfected. The reduced activation of caspase-3 in the transgenes containing the third KH domain suggests that further analysis should investigate the exact region of hnRNP K bound to the AUUCU expansion to develop small peptide intervention.

Figure 4.3. KH Domain 3 Rescues Activation of Caspase-3 Via the Expanded ATTCT Repeat

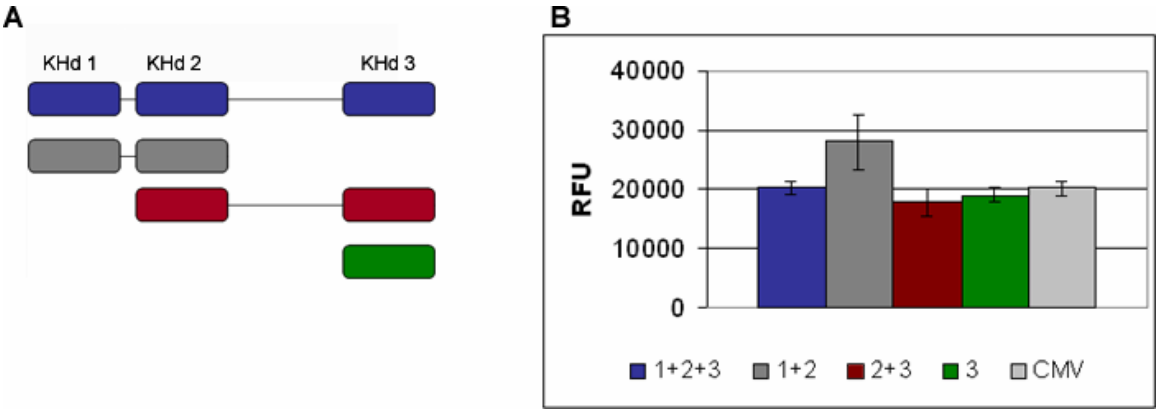

A. Schematic drawing of the various KH domain constructs tested. B. Caspase-3 activation assay measured in relative fluorescent units (RFU). RFU was normalized to BCA and to the control CMV vector not containing KH domains.

DISCUSSION

Translational research has become a buzz word in the past decade. Scientists are increasingly aware of the drive for "bench to bedside" developments. In order to participate in translational research, a complete understanding of the mechanism of the disease is useful. While the toxic AUUCU aggregates are known to sequester hnRNP K and result in PKCδ translocation to mitochondria and activation of caspase-3, it was not understood how cells could survive this direct pathway to apoptosis. Before attempting to rescue the SCA10 cellular phenotype, it was essential to increase understanding of the SCA10 mechanism. Additionally, by attempting to rescue the SCA10 phenotype, the mechanism is more fully understood. If PKCδ can be expelled from the mitochondria of

SCA10 fibroblasts, it is likely that the targeted mechanism is important for SCA10 disease progression, and possibly reversible.

In further support of the hnRNP K sequestration hypothesis, we attempted to rescue the SCA10 cellular phenotype by employing two experiments to either decrease the presence of toxic transcript or increase the availability of hnRNP K. When PC12 cells were stably transfected with full-length hnRNP K prior to transfection of expanded repeat, caspase-3 activation was significantly reduced. Additionally, overexpression of hnRNP K in SCA10 fibroblasts resulted in decreased localization of PKCδ in mitochondria. PKCδ was also expelled from mitochondria via inactivation of the *ATXN10* transcript. Further investigation of the KH domains in hnRNP K revealed two constructs, both containing KH domain 3, that reduced activation of caspase-3 in human neuroblastoma cells pre-transfected with KH domains before transfection with expanded ATTCT repeat. The rescue of caspase-3 activation by providing hnRNP K KH domain 3 provides a possibility for development of therapeutic strategies. One method projected to be important for neurodegenerative disorders involves the development of sequence specific binding of RNA binding proteins (Auweter et al., 2006). Construction of a peptide that would inhibit the binding of hnRNP K to the AUUCU repeat by saturation of the repeat might alleviate sequestration of hnRNP K and subsequent activation of caspase-3.

MATERIALS AND METHODS

Transfection of SCA10 Fibroblasts

Primary fibroblasts derived from SCA10 patients were transfected using the human dermal fibroblast nucleofector kit for electroporation (Amaxa). Plasmid expressing GFP-labeled hnRNP K was transfected at 3ug according to kit instructions.

Small interfering RNA (Ataxin-10) was transfected at 100pMol according to kit instructions.

Transfection of PC12 Cells

PC12 cells were chemically transfected with Lipofectamine 2000 with full hnRNP K and KH domain constructs according to kit instructions. When transfected with hnRNP K or with KH domain transgenes, cells were selected with neomycin 24 hours following transfection. After approximately 7 days of selection, when cells reached confluent growth of approximately 90%, cells were transfected with the expanded ATTCT transgene from Chapter II, Figure 1 with Lipofectamine 2000 according to kit instructions.

Caspase-3 Assay

PC12 cells from the transfection experiments were collected manually by pipetting and centrifuged to obtain approximately 1 x 10^6 cells. The caspase-3 assay was completed according to kit instructions (Calbiochem).

BCA Protein Assay

The BCA protein assay was performed to normalize protein quantities in the caspase-3 assay. Protocol for the BCA assay from Pierce was performed following the Microplate Procedure.

PKCδ and Mitochondrial Localization

Immunohistochemistry of PKCδ and visualization of respirating mitochondria was performed as described in Chapter II. Mitochondria were immunolabeled at 633nm and PKCδ was immunolabeled at 568nm. hnRNP K was GFP-labeled and visualized at 488nm. Once a GFP-labeled cell was identified, a picture was taken of GFP (green),

PKCδ (orange), and mitochondria (blue). To simplify matters for comparison to non-transfected cells, the GFP image was removed and mitochondria were represented by red and PKCδ was represented by green, showing colocalization as yellow. Cells were visualized using a Zeiss confocal microscope at the Optical Imaging Core Lab at University of Texas Medical Branch.

KH domain Constructs

The KH domain constructs were PCR amplified from cDNA clone from ATCC (ATCC number 3583037). Full length hnRNP K was amplified with forward primer, 5'-TCCATTTAATTCAAGAAA-3' and reverse primer 3'-AGATTCACTAAATTTATT-5'. KH domain 1,2,3 was PCR amplified using forward primer KHD1F 5'-CGCCTGCAGAAGATATGGAAGAG-3' and reverse primer KHD3R 3'-TGCGTTCTGTATCTGGTCCTGTGT-5'. KH domain 1,2 was PCR amplified using KHD1F and KHD2R 3'-TCCTCCAATAAGAACAAC-5'. KH domain 2,3 was PCR amplified using KHD 2F 5'-GATTGCGAGTTGAGACTGTTG-3' and KHD3R. KH domain 3 was PCR amplified with KHD3F 5'-ATTATCACTACACAAGTA-3' and KHD3R. The PCR products were amplified using Platinum *Pfx* available from Invitrogen. Initial denaturation occurred at 94˚C for 5 minutes, followed by 30 cycles of denaturation at 94˚C for 30 seconds, annealing at 60˚C for 30 seconds, and amplification at 72˚C for 1 minute with a final extension of 72C for 10 minutes. Reaction conditions included 200ng DNA, 1.5ul of 50mM Mg, 1 ul of 10mM dNTP, 1 ul of 10mM primer, 2.5 units of Taq, 3 ul of buffer, and DEPC water for a 30ul reaction (Sigma: Red-JumpStart Taq). The PCR products were purified using QIAquick PCR purification kit (Qiagen). Purified products were blunt-end ligated into the *HincII* restriction site of pCMV/myc/nuc with T4 DNA ligase on ice, overnight. Ligated reactions were

transfected into DH5α competent cells. Clones were verified by restriction digestion, and positive clones were sequenced to verify in-frame insertion.

Chapter V:

Defining the Mechanism for Late Onset of SCA10

SUMMARY

Debate surrounds neurodegenerative mechanisms resulting in apoptosis. If the toxic AUUCU aggregates bring about the activation of caspase-3, it seems unlikely that apoptosis does not occur at an early stage, resulting in an embryonic lethal disorder. However, SCA10 is an adult onset disorder, usually occurring during the third or fourth decade. Defining the SCA10 mechanism by further evaluating the interaction between levels of hnRNP K protein in the brain as well as the *ATXN10* transcript is needed to fully understand the mechanism and how late-onset occurs. In this chapter, correlative data is presented on the expression of hnRNP K, the presence of AUUCU aggregates, and the *ATXN10* transcript. Decreased expression of hnRNP K throughout life, in addition to variable hnRNP K expression in brain, may provide some explanation for the late onset of SCA10.

INTRODUCTION

Spinocerebellar ataxia type 10 is an adult-onset neurodegenerative disorder. Patient symptoms generally begin in the third or fourth decade with a progressive decline following the onset of the disorder (Raji, 2002). Additionally, an inverse correlation exists with larger repeat expansions correlating to an earlier onset of phenotype (Matsuura et al., 2000). Anticipation is variably present within the families, especially the families with repeat expansion passed paternally (Matsuura et al., 2004). Instability

within the spermline is suggested to lead to either increased or decreased repeat expansion when passed paternally, with increased repeat expansion resulting in anticipation in subsequent generations. Currently, the mechanism for late onset of SCA10, or how increased repeat length can lead to earlier manifestation of phenotypes, is not understood.

While SCA10 is likely due to the toxic RNA species present within the patient brains, sequestration of proteins is shown to be sufficient for the development of SCA10 phenotypes. The sequestration of hnRNP K by the expanded AUUCU RNA may be the instigating role in the cleavage of caspase-3 which results in cellular death of neurons. However, the late onset phenotype of SCA10 poses an intriguing problem in the mechanistic details. Ataxin 10 is highly expressed throughout embryonic development and early in life. Logically, the time of greatest expression should result in the largest number of AUUCU aggregates, the largest sequestration of hnRNP K, and highest pathogenesis. Yet, the exact opposite occurs. To investigate a mechanistic explanation for the late onset of SCA10, expression levels of hnRNP K and transcript levels of ATXN10 were evaluated. We hypothesized that lower levels of hnRNP K within the cell would result in pathogenesis due to a decreased availability of hnRNP K (Figure 5.1). In this chapter, we present data suggesting that decreased levels of hnRNP K in brain tissue plays a key role in the progression of SCA10.

RESULTS

Expression of hnRNP K Decreases Throughout Life

The late onset phenotype of SCA10 leaves an unanswered question in the mechanism described thus far. Ataxin 10 is known to be embryonically important due to

the finding that homozygous *ATXN10*-knull mice are not viable (Wakamiya et al., 2006). Thus, mutated *ATXN10* from SCA10 patients is transcribed early in life, and likely to

Figure 5.1. Schematic for Cellular Effects of Low hnRNP K Expression Levels.

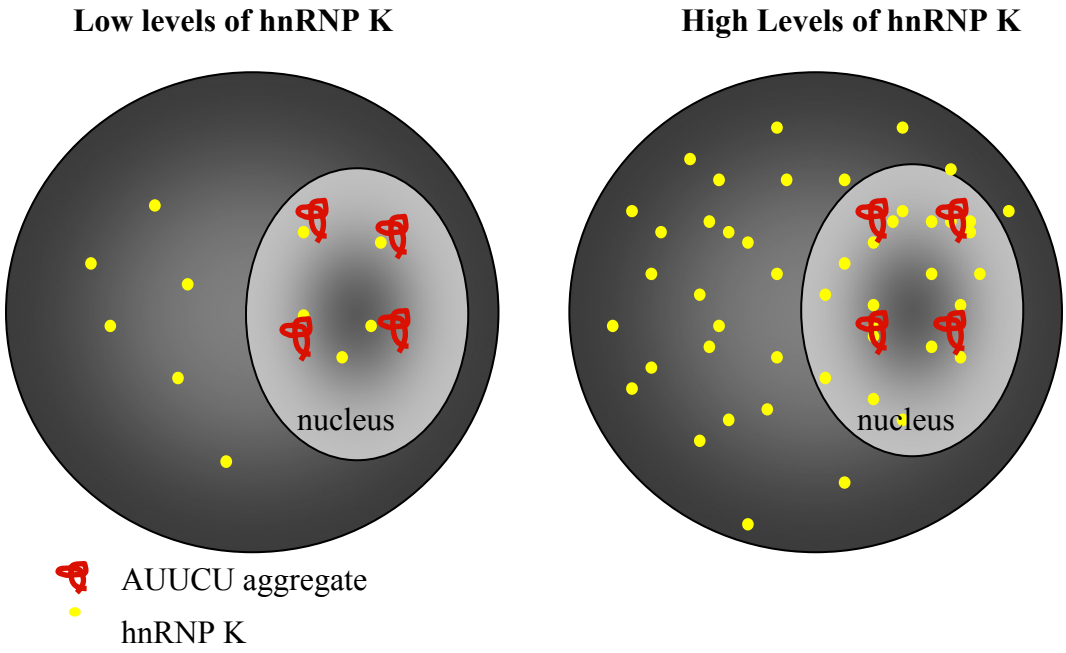

The AUUCU aggregate is expected to have a saturation level of hnRNP K, such that cells expressing high levels of hnRNP K would still have enough hnRNP K to perform cellular functions.

produce toxic, AUUCU aggregates. However, SCA10 phenotype does not develop until around the third or fourth decade in most instances.

To investigate the logistics for the late-onset phenomenon, expression of hnRNP K was measured. A developmental Western blot from 1 day to 1 year of total protein extracted from whole rat brain was used to analyze hnRNP K protein levels throughout

life. As expected, the levels of hnRNP K are high post-natally and through early stages of life and start a gradual decrease around 3 weeks, reaching the lowest levels by 3 months (Figure 5.2A). Levels have decreased more than three hundred times by 12 months, when compared to 1 day (Figure 5.2C). A decrease in the level of hnRNP K throughout life provides a plausible mechanism for late onset of SCA10, based upon the mechanism presented in the hnRNP K sequestration hypothesis.

hnRNP K is Widely Expressed Throughout the Brain

In addition to a decrease in hnRNP K with age, hnRNP K expression throughout brain structures may vary. As shown in Table 1 of Chapter III, Ataxin 10 expression varies significantly in the brain. If high levels of AUUCU transcript were present in one region of the brain, but relatively low levels of hnRNP K were expressed in the same area, the aggregates may sequester the critical level of hnRNP K to result in cellular dysfunction. To investigate this possibility, hnRNP K expression throughout brain was analyzed and compared to ATXN10 expression. hnRNP K was found to be highly expressed in brain with very few areas showing low levels of expression (Table 5.2). Extremely high expression of hnRNP K occurs in the Purkinje and granule cells of the cerebellum; the granule cells of the hippocampus in the dentate gyrus and CA1, CA2, and CA3. High levels of expression are seen in neurons of the cortex, midbrain, and pons (Figure 5.2B). At high levels of magnification of the cerebellum, some cells are seen in the granular layer which show relatively no fluorescence and represent the lowest levels of expression of hnRNP K found in the brain (Figure 5.2B, arrow). Since the primary degeneration seen in SCA10 patients by MRI is cerebellar (Rasmussen et al., 2001; Teive et al., 2004), focusing on expression patterns in cerebellum is likely to be important.

Low to mid levels of expression of Ataxin 10 are reported in the Purkinje cells, but high levels of hnRNP K are seen within Purkinje cells, probably ruling out primary pathogenesis in the Purkinje cells. Deep cerebellar nuclei expression of ATXN10 was not determined by Marz et al., thus comparison of hnRNP K proves difficult (Marz et al., 2004). Possibly, ATXN10 and hnRNP K reach critical levels in the cerebellum where some low hnRNP K expression occurs, such that an appropriate amount of hnRNP K is sequestered and can no longer perform its required function within the cell. A high level of ATXN10 expression is seen in the pontine nuclei, while a mid-high level of expression of hnRNP K is seen. The lower hnRNP K: higher ATXN10 relationship could be important in sequestration, especially since the pontine nuclei plays a key role in most cerebellar pathways. Upon creation of a monoclonal ATXN10 antibody, further investigation should focus on the levels of ATXN10 and hnRNP K in aged brain specimens.

Ataxin 10 Transcript Decreases Throughout Life

Approaching the late-onset hypothesis from an alternative direction, it is possible that an increase in the transcript levels of Ataxin 10 could result in an increase in the cellular aggregates within the brain of SCA10 patients. A decrease in hnRNP K, as well as an increase in *Atxn10* transcript, would provide twice the effect, perhaps explaining the drastic decline in quality of life upon initial SCA10 symptoms. To investigate the levels of ATXN10 transcript, real-time RT-PCR was performed on total RNA taken from whole

Figure 5.2. hnRNP K is Widely Expressed Throughout the Brain and Decreases with Age

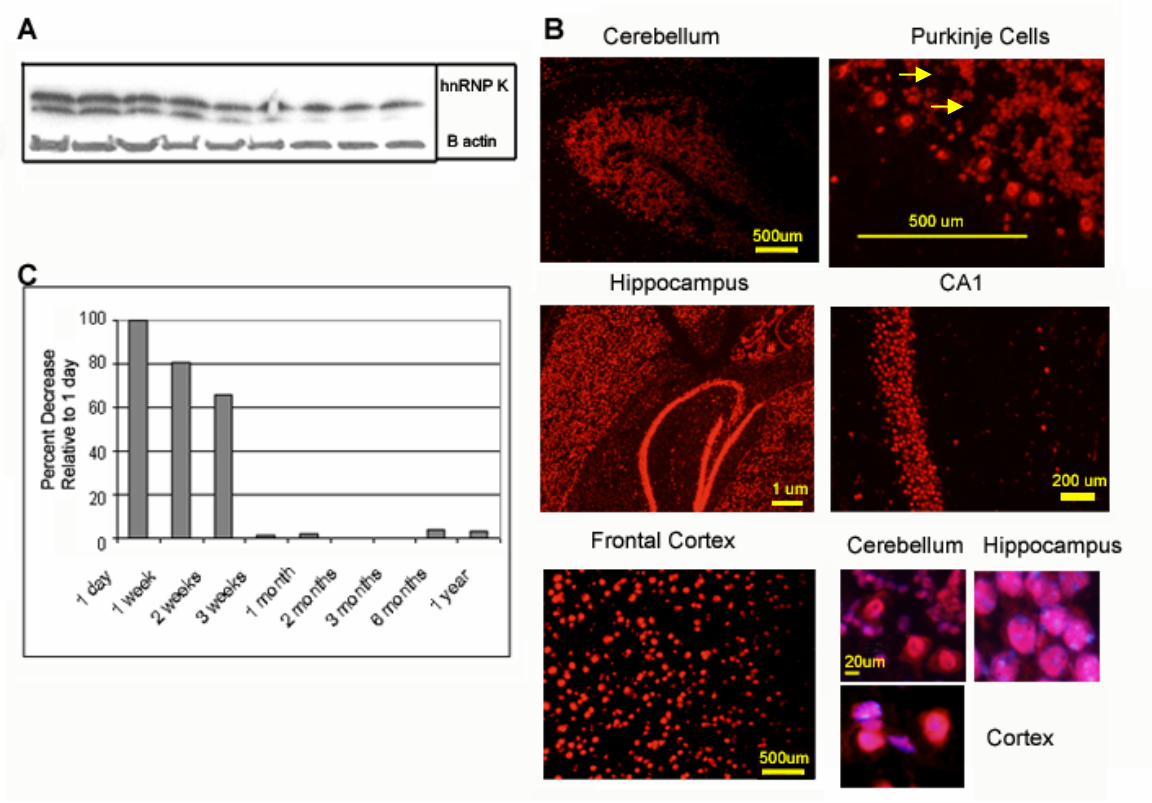

A. Developmental Western blot of protein extracted from whole rat brain showing hnRNP K at 1 day, 1 week, 2 weeks, 3 weeks, 1 month, 2 months, 3 months, 6 months, and 12 months. β-actin was used as a loading control. B. Quantification of hnRNP K levels as visualized by Western blot. C. hnRNP K expression evaluated in brain by immunohistochemistry. High levels are seen in the cerebellum, specifically Purkinje cells and granular cells. Some cells in the granular layer of the cerebellum show virtually no expression (arrow). High expression is seen in the hippocampus. Mid-high expression is seen in cortex. The last panel illustrates overlay of hnRNP K (red) with DAPI (Blue), demonstrating at the cellular level hnRNP K is highly expressed in the nucleus, but also seen in the cytoplasm of the Purkinje cells.

Table 5.1. Ataxin-10 and hnRNP K Expression in Mouse Brain

Regions of Brain	Mouse ATXN10	Mouse hnRNP K
Olfactory Bulb	++	++
Cerebral Cortex	0/+	++
Striatum	0/+	++
Locus Ceruleus	+	++
Substantia Nigra	0	++
Midbrain Raphe	++	+/++
Nuclei Pontis	++/+++	+/++
Nuclei Cuneatus	ND	++
Nuclei Vestibularis	++	++
Nuclei Olivaris	++	++
Nuclei Hypoglossus	ND	++
Purkinje Cells	+/+++	+++
Deep Cerebellar Nuclei	+++	+++
Spinal Motor Neurons	+	ND
Hippocampus	ND	+++
0 - no observable staining + - +++, semi-quantitative staining ND- not determined		

Modified from Marz *et al* (Marz et al., 2004).

rat brain at various ages ranging from one day to twelve months. *ATXN10* transcripts were found to vary throughout the course of a year with the highest levels expressed at one week and the lowest levels expressed at six and twelve months (Figure 5.3A). Thus,

unless AUUCU repeat collect cumulatively throughout the life of the mice, the level of ataxin-10 transcript is unlikely to offer an explanation for the late onset.

AUUCU Aggregates More Prevalent in Older Brain Tissue

While *ATXN10* transcripts were found to decrease with age, it is possible that AUUCU aggregates increase with age. In DM1, CUG repeat aggregates within patient-derived cells in culture have been shown to be dynamic, continuously forming and disappearing (data not published). However, the fate of the AUUCU aggregates is unknown in SCA10. To investigate the formation of aggregates in aging mouse brain, we used SCA10 transgenic mice expressing a transgene containing expanded ATTCT repeat (Chapter III, Figure 3.1). F2 mice were sacrificed at 3 days, 2 weeks, 1 month, 3 months, and 6 months to compare presence of AUUCU aggregates at various ages. Sagittal brain sections underwent fluorescent *in situ* hybridization with a Cy3-$(AGAAU)_{10}$ riboprobe. AUUCU foci were not present in F2 brains at 3 days or 1 month (Figure 5.3B). However, aggregates were visualized in brains of 3 month F2 mice, 6 month F2 mice, and older F1 and founder mice. (Figure 5.3C) The quantity of aggregates did not appear to change (as counted) in cortex, hippocampus, cerebellum, and pontine nuclei of the 3 month F2, 6 month F2, or older F1 and founder mice. These results suggest that AUUCU foci become more prevalent with age in the brains of transgenic mice. Correlating the increased presence of AUUCU foci with the decreased expression of hnRNP K further supports the sequestration hypothesis.

Figure 5.3. *ATXN10* Transcript Decreases with Age, but AUUCU Foci Increase with Age

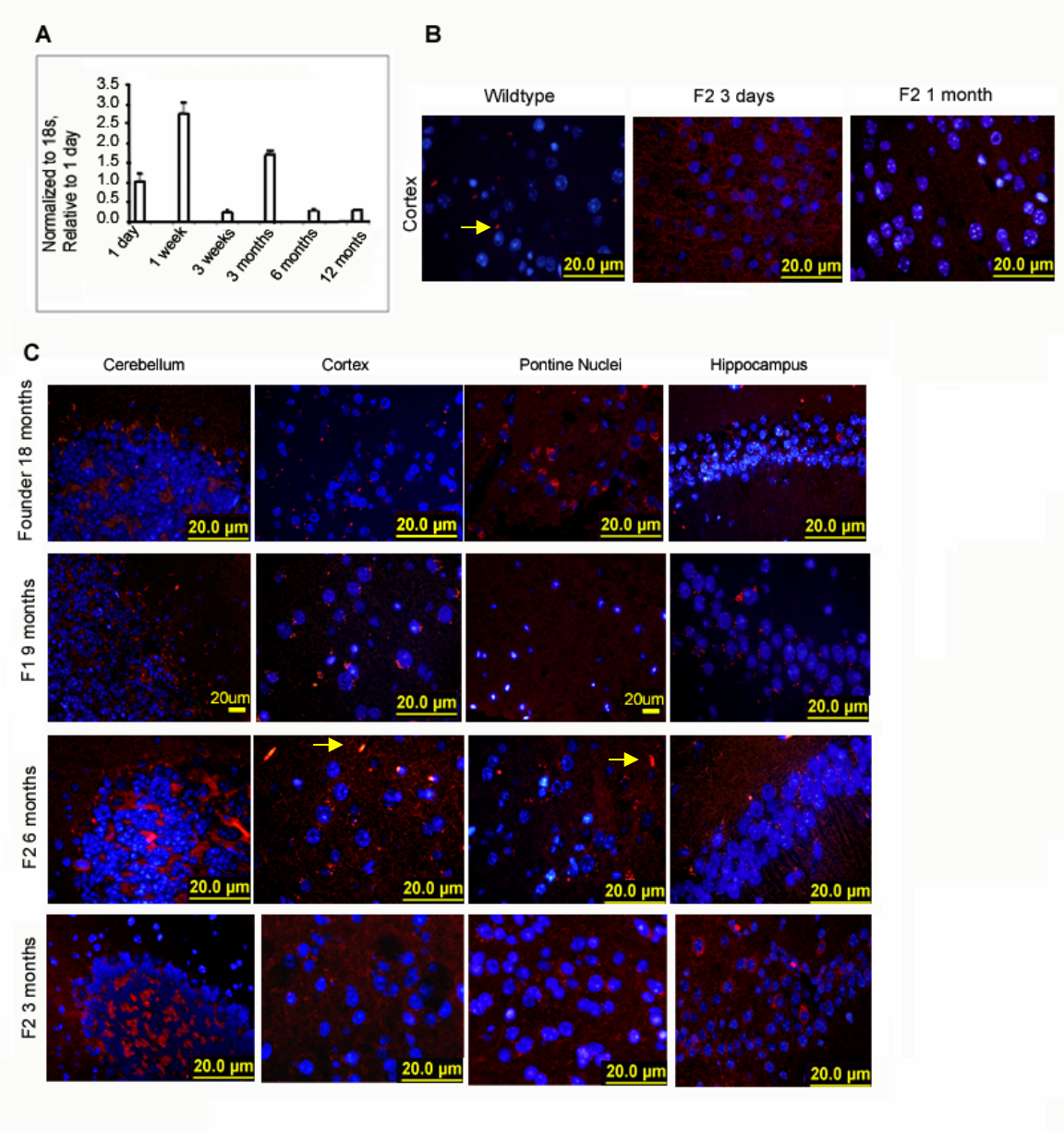

A. Quantitative RT-PCR of total RNA from whole rat brain normalized to 18s RNA and relative to 1 day. B. *FISH* with Cy3-$(AGAAU)_{10}$ probe of sagitally sectioned brains from wildtype, 3 days, and 1 month. No AUUCU aggregates are seen. C. *FISH* on 3 months and 6 months of F2 mice, 9 months in F1, and 18 months Founder. Foci are shown by punctuate dots. Very bright streaks are paraffin accumulations (arrow).

DISCUSSION

The mechanism presented in Chapter II and III is all or none, with caspase-3 activation bringing about cell death. However, SCA10 patients do not start experiencing symptoms until adulthood, making SCA10 a highly transmissible genetic disease. While it is not fully understood why aggregates were not present in the brain samples of the mice younger than three months old, it is not an uncommon concept. The role of aggregates within neurodegenerative disorders has been debated. Both in Huntington and Alzheimer's Disease, behavioral abnormalities in transgenic mice were found to supersede aggregations in histological analysis (Nguyen et al., 2006). In the vast majority of the repeat-expanded neurodegenerative disorders containing aggregates, aggregates are not present early in life; with aging, aggregations become more prevalent (Gatchel and Zoghbi, 2005; Lee and Kim, 2006). It has been suggested that the increased number of aggregates is not due to an increased quantity of aggregates, but possibly to an decrease in the clearing of the aggregates (Meriin and Sherman, 2005). Chaperones are known to clear aggregates through the ubiquitin-proteasomal pathway. One possible mechanism suggests that a senescence-like effect occurs with the clearing of aggregates, such that chaperones no longer activate the proteasomal pathway, the cell is bombarded by abnormal aggregates, and undergoes cell death (Meriin and Sherman, 2005).

To further investigate the SCA10 mechanism, specifically an answer for the late onset, we evaluated the protein levels of hnRNP K and *ATXN10* transcripts throughout life. The decreased levels of hnRNP K in aged mice, as well as the low level of expression of hnRNP K in some cerebellar cells, suggests that with age, hnRNP K reaches a critical level within the cerebellum. When hnRNP K is sequestered to the

AUUCU aggregates, the levels of hnRNP K are not enough to perform cellular functions and result in the PKCδ-mediated activation of caspase-3. Alternatively, a high level of hnRNP K and a large amount of AUUCU aggregates may result in a larger amount of PKCδ translocation to the mitochondria, targeting tissues which are both high in hnRNP K and *ATXN10*, such as Purkinje cells. The *ATXN10* transcript levels were found to decrease with age, contrarily to the formation of AUUCU aggregates within brain. AUUCU aggregates were evaluated at 3 days, 1 month, 3 months, and 6 months, and found to contain an increasing number of aggregates with age, with aggregates first appearing around 3 months. An increase in the presence of aggregates as well as a decrease in the level of hnRNP K could provide the basis for onset of SCA10 phenotypes.

MATERIALS AND METHODS

Developmental Western Blot

The developmental Western blot samples were purchased from Novagen, Inc. Whole brain protein was extracted from various aged mice. Blots were blocked in 5% milk in TBST for one hour before probing with mouse monoclonal antibody to hnRNP K 1:5000 (from Acris) overnight at 4˚C with gentle agitation. The membrane was washed 3 times, 10 minutes each in TBST with agitation. Hybridization with secondary HRP-anti-mouse antibody 1:5000 and ECL was used to visualize expression of hnRNP K.

Quantitative RT-PCR

Primers were designed in the coding region of rat *ATXN10* by the Quantitative RT-PCR core lab at University of Texas Medical Branch. Total RNA was purchased from Novagen, Inc. and extracted from whole Rat brain at various ages.

FISH and Sagittal Sections

Sagittal sections of transgenic brain were obtained by perfusion as described in Chapter III. *FISH* also was performed as described in Chapter III.

Ladder PCR

Ladder PCR was performed using 140ng of genomic DNA extracted from mouse tail as described in Chapter III.

hnRNP K Immunohistochemistry

hnRNP K immunohistochemistry was performed as previously described in Chapter III on sagittally sectioned wildtype mouse brain.

Chapter VI:

Conclusion

The work described in this dissertation provides a direct mechanism from the beginning, expansion of an intronic ATTCT repeat, to the end, the final fate of apoptosis. The possible finding of autophagy in the transgenic mouse brains provides support for both sides in the autophagy versus apoptosis neurodegeneration debate. Apoptosis readily was apparent in induced cell culture models, but signs of autophagy were seen in the transgenic brains, suggesting the two methods of programmed cell death may work concertedly. The finding of a mechanism in SCA10 that results in apoptosis provides hope that through further investigation, therapeutical intervention in the apoptotic pathway will be possible.

THE MECHANISM

As reported in Wakamiya *et al,* the expanded ATTCT repeat is properly transcribed into an expanded AUUCU transcript and spliced from the coding region (Wakamiya et al., 2006). Fluorescent *in situ* hybridization to the AUUCU repeat in fibroblasts derived from SCA10 patients revealed aggregations of AUUCU as distinct foci within the cell. The aggregates were inducible in cell culture by endogenously expressed expanded ATTCT, as well as in mouse brains of transgenic animals expressing expanded ATTCT transcripts. *In vitro*, AUUCU was found reproducibly to bind hnRNP K in bead-binding pull down experiments. Subsequently, hnRNP K was shown to bind

Figure 6.1. Model for Role of hnRNP K and PKCδ in SCA10.

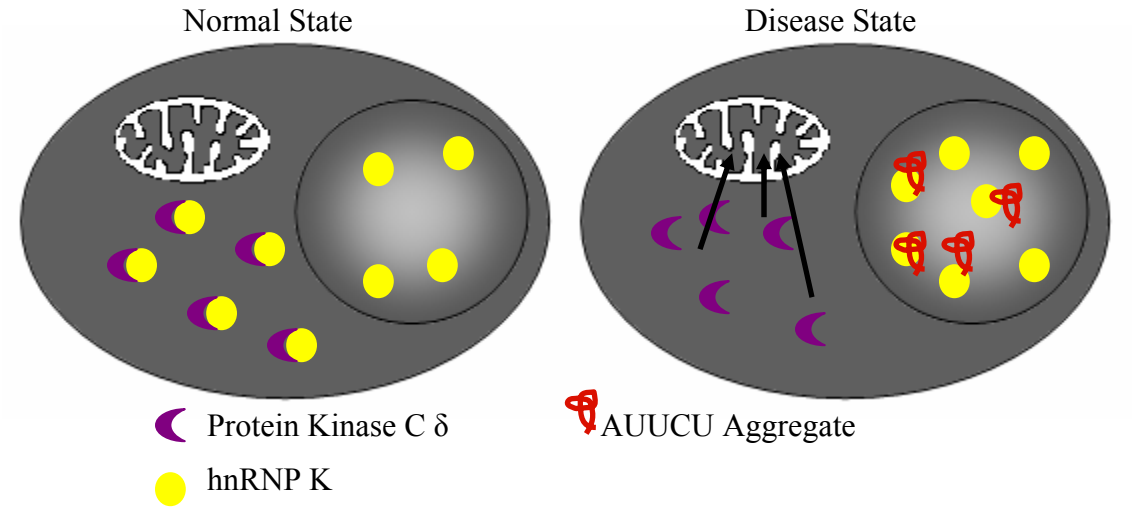

In a normal state, PKCδ and hnRNP K are constitutively bound. However, in SCA10, hnRNP K is sequestered to the AUUCU aggregates within the nucleus, leaving unbound PKCδ. PKCδ is theorized to translocate to the mitochondria where it is known to release cytochrome C and result in the activation of apoptosis.

AUUCU foci in the brains of transgenic animals. Thus, a mechanism leading to cell death through sequestration of hnRNP K was investigated.

hnRNP K is a K homology domain protein containing three KH domains, with the first two KH domains relatively close to each other and the third KH domain separated by a K interactive region. The only other known proteins with this similar layout of KH domains are the Nova proteins, Nova-1 and Nova-2. Nova1 is the implicated protein in another devastating ataxia disorder, paraneoplastic opsoclonus myoclonus ataxia (POMA) (Buckanovich et al., 1993). POMA is usually seen with a breast or uterine cancer which results in an antibody that recognizes tumors as well as Nova-1 and Nova-2. When the autoimmune response targets the Nova proteins, the activity of Nova-1 and Nova-2 are inhibited, and result in the movement disorder phenotype (Buckanovich et al.,

1993). Based upon this finding, and the similarity of the purported decreased activity of hnRNP K, we were convinced that hnRNP K was somehow involved in SCA10. Moreover, point mutations in PKCγ have been implicated in SCA14 (Klebe et al., 2005). It is currently not understood how the point mutations in the coding region of PKCγ result in the progressive decline of cerebellar function and ataxia. However, the similarities between PKCγ and PKCδ, as well as the known interaction between PKCδ and hnRNP K, prompted our focus.

Upon investigation into a mechanism involving PKCδ, we discovered that PKCδ translocated to mitochondria when fibroblasts were transfected with either expanded ATTCT repeat, or small interfering hnRNP K. The transfection of repeat as well as the inactivation of hnRNP K was accompanied with activation of caspase-3-mediated apoptosis. Further investigation into fibroblasts derived from SCA10 patients and transgenic mouse brain revealed that PKCδ was abnormally expressed in mitochondria, where it is only known to be localized during activation of apoptosis. Subsequent studies revealed that hnRNP K expression levels decrease with age in protein extracted from whole rat brain. Additionally, hnRNP K expression in the brain is variable, specifically in expression in cerebellum, where degeneration is known to occur. Based upon these findings, as well as the finding that AUUCU aggregates increase with age and length of repeat, we concluded that the late onset of SCA10 may result from decreased levels of hnRNP K and increased levels of toxic, AUUCU aggregates.

Transgenic animals were analyzed for both histological and behavioral abnormalities. The stability of the repeat was found to vary, as in the human disorder, with both expansion and contraction occurring regardless of sex of transmission. The mice demonstrated a hind claw withdrawal reflex, gait abnormalities, abnormal

exploratory behavior and decreased movement. Histologically, the brains contained expanded AUUCU aggregates which sequestered hnRNP K. Regions of the brain, hippocampus and cerebellum, had extensive translocation of PKCδ to mitochondria as well as regions of the brain that showed no overtly abnormal PKCδ localization. These findings are thought to represent the tightly regulated interaction between the AUUCU aggregates, hnRNP K, and PKCδ (Figure 6.1). It appears that a critical level of hnRNP K must be sequestered before adverse cellular phenotypes, such as translocation of PKCδ to mitochondria, occur. The aggregates found in transgenic brain were present at the nuclear membrane and in the cytoplasm, rather than in the nucleus and the nuclear membrane in SCA10 fibroblasts. The difference between the location of the aggregates in the transgenic and in the fibroblasts is likely to result from an intronic repeat expansion within the fibroblasts of human patients and a 3' UTR repeat expansion within the transgene of the transgenic mice. Further investigation revealed that the aggregates were sometimes present in the mitochondria, resulting in hnRNP K, PKCδ and AUUCU aggregates colocalized in the mitochondria. It is unknown the importance of the pathway that results in the triple translocation to the mitochondria, or if the triple translocation is present in human SCA10. Additionally, cytoplasmic vacuoles were seen in the brains of the transgenic animals. The vacuoles stained positive for periodic acid Schiff, indicating glycogen storage, and possibly autophage. These results suggest that autophagy may be activated in the brains of the transgenic animals.

Finally, we investigated a method of rescue for the SCA10 cellular phenotype, specifically a decreased activation of caspase-3 or translocation of PKCδ from the mitochondria. When the level of *Ataxin 10* transcript was abrogated with small interfering RNA, PKCδ translocated from the mitochondria into the cytoplasm.

Additionally, overexpression of GFP-labeled hnRNP K revealed that SCA10 fibroblasts which were transfected successfully with the hnRNP K "treatment" translocated PKCδ from mitochondria, while SCA10 fibroblasts not overexpressing hnRNP K still had extensive PKCδ in the mitochondria. Neuroblastoma cells were used to measure the induction of caspase-3 via the endogenous expression of expanded ATTCT repeat. Cells which were pre-transfected with full-length hnRNP K, as well as cells which were pre-transfected with K homology domain 3, showed decreased caspase-3 activation. These findings suggest that translocation to mitochondria and the activation of caspase-3 are reversible, and may provide viable treatment options upon further investigation.

FUTURE STUDIES

The mechanism presented here by no means is meant to be the only active mechanism present in SCA10. The expanded AUUCU repeat is likely to sequester other proteins, resulting in other pathways of pathogenesis. Furthermore, the SCA10 repeat expansion is reportedly interrupted (Matsuura et al., 2006), thus is likely to form alternative secondary structures within the cell, and sequester additional proteins. Given the variable phenotypes found in SCA10 patients, it is possible that the variably sequestered protein could result in alternative phenotypes in patients. Moreover, the sequestration of hnRNP K is likely to result in a cascade of cellular effects. Since hnRNP K is ubiquitously expressed in the cell and has a montage of functions, it would be presumptuous to believe that decreased activity of hnRNP K would only affect PKCδ.

Future studies should focus on fully defining the hnRNP K/PKCδ mechanism, as well as finding alternative mechanisms resulting from a decreased availability of hnRNP K. Multiple cellular factors are known to activate PKCδ and result in mitochondrial

translocation and cleavage of caspase-3, but it is not understood what results in the activation of PKCδ in SCA10. Based upon the interaction of p53 with both hnRNP K and PKCδ, efforts should be placed to determine if the ATTCT repeat expansion is recognized as DNA damage and results in a cascade involving p53, hnRNP K, and PKCδ. Additionally, further defining interruptions of expanded ATTCT repeats is needed. Variable phenotypes, specifically the additional phenotype of epilepsy, are perplexing. If repeat variability only occurs in the affected Mexican population, which is known to have interrupted repeat, it is possible that the other affected populations not expressing epilepsy may have pure repeat expansion. The pure and interrupted repeat expansions should be further analyzed in bead pull-down experiments to determine if alternative binding proteins are found.

Bibliography

Al-Mahdawi, S., Pinto, R. M., Ruddle, P., Carroll, C., Webster, Z., and Pook, M. (2004). GAA repeat instability in Friedreich ataxia YAC transgenic mice. Genomics 84, 301-310.

Alonso, I., Jardim, L. B., Artigalas, O., Saraiva-Pereira, M. L., Matsuura, T., Ashizawa, T., Sequeiros, J., and Silveira, I. (2006). Reduced penetrance of intermediate size alleles in spinocerebellar ataxia type 10. Neurology 66, 1602-1604.

Ashizawa, T., and Wells, R.D. (2006). Genetic Instabilities and Neurological Disorders (Burlington, MA: Elsevier).

Auweter, S. D., Oberstrass, F. C., and Allain, F. H. (2006). Sequence-specific binding of single-stranded RNA: is there a code for recognition? Nucleic Acids Res 34, 4943-4959.

Backe, P. H., Messias, A. C., Ravelli, R. B., Sattler, M., and Cusack, S. (2005). X-ray crystallographic and NMR studies of the third KH domain of hnRNP K in complex with single-stranded nucleic acids. Structure 13, 1055-1067.

Basu, A. (2003). Involvement of protein kinase C-delta in DNA damage-induced apoptosis. J Cell Mol Med 7, 341-350.

Bomsztyk, K., Denisenko, O., and Ostrowski, J. (2004). hnRNP K: one protein multiple processes. Bioessays 26, 629-638.

Boy, J., Leergaard, T. B., Schmidt, T., Odeh, F., Bichelmeier, U., Nuber, S., Holzmann, C., Wree, A., Prusiner, S. B., Bujard, H., *et al.* (2006). Expression mapping of tetracycline-responsive prion protein promoter: digital atlasing for generating cell-specific disease models. Neuroimage 33, 449-462.

Bredesen, D. E., Wiedau-Pazos, M., Goto, J. J., Rabizadeh, S., Roe, J. A., Gralla, E. B., Ellerby, L. M., and Valentine, J. S. (1996). Cell death mechanisms in ALS. Neurology 47, S36-38; discussion S38-39.

Brodie, C., and Blumberg, P. M. (2003). Regulation of cell apoptosis by protein kinase c delta. Apoptosis 8, 19-27.

Buckanovich, R. J., Posner, J. B., and Darnell, R. B. (1993). Nova, the paraneoplastic Ri antigen, is homologous to an RNA-binding protein and is specifically expressed in the developing motor system. Neuron 11, 657-672.

Burgess, D. L., Matsuura, T., Ashizawa, T., and Noebels, J. L. (2000). Genetic localization of the Ca2+ channel gene CACNG2 near SCA10 on chromosome 22q13. Epilepsia 41, 24-27.

Charroux, B., Angelats, C., Fasano, L., Kerridge, S., and Vola, C. (1999). The levels of the bancal product, a Drosophila homologue of vertebrate hnRNP K protein, affect cell proliferation and apoptosis in imaginal disc cells. Mol Cell Biol 19, 7846-7856.

Chu, C. T. (2006). Autophagic stress in neuronal injury and disease. J Neuropathol Exp Neurol 65, 423-432.

Clark, R. M., De Biase, I., Malykhina, A. P., Al-Mahdawi, S., Pook, M., and Bidichandani, S. I. (2007). The GAA triplet-repeat is unstable in the context of the human FXN locus and displays age-dependent expansions in cerebellum and DRG in a transgenic mouse model. Hum Genet 120, 633-640.

Crawley, J. N. (2000). What's Wrong with my Mouse? (New York: John Wiley and Sons, Inc.).

Cuervo, A. M. (2004). Autophagy: many paths to the same end. Mol Cell Biochem 263, 55-72.

Davis, B. M., McCurrach, M. E., Taneja, K. L., Singer, R. H., and Housman, D. E. (1997). Expansion of a CUG trinucleotide repeat in the 3' untranslated region of myotonic dystrophy protein kinase transcripts results in nuclear retention of transcripts. Proc Natl Acad Sci U S A 94, 7388-7393.

Dejgaard, K., and Leffers, H. (1996). Characterisation of the nucleic-acid-binding activity of KH domains. Different properties of different domains. Eur J Biochem 241, 425-431.

Du, W., Thanos, D., and Maniatis, T. (1993). Mechanisms of transcriptional synergism between distinct virus-inducible enhancer elements. Cell 74, 887-898.

Duenas, A. M., Goold, R., and Giunti, P. (2006). Molecular pathogenesis of spinocerebellar ataxias. Brain 129, 1357-1370.

Fischer, M., Rulicke, T., Raeber, A., Sailer, A., Moser, M., Oesch, B., Brandner, S., Aguzzi, A., and Weissmann, C. (1996). Prion protein (PrP) with amino-proximal deletions restoring susceptibility of PrP knockout mice to scrapie. Embo J 15, 1255-1264.

Fortune, M. T., Vassilopoulos, C., Coolbaugh, M. I., Siciliano, M. J., and Monckton, D. G. (2000). Dramatic, expansion-biased, age-dependent, tissue-specific somatic mosaicism in a transgenic mouse model of triplet repeat instability. Hum Mol Genet 9, 439-445.

Garrido, C., Galluzzi, L., Brunet, M., Puig, P. E., Didelot, C., and Kroemer, G. (2006). Mechanisms of cytochrome c release from mitochondria. Cell Death Differ 13, 1423-1433.

Gatchel, J. R., and Zoghbi, H. Y. (2005). Diseases of unstable repeat expansion: mechanisms and common principles. Nat Rev Genet 6, 743-755.

Gatto, E. M., Gao, Rui, White, Misti C, Uribe Roba, Marcela C, Etcheverry, Jose L, Persi, Gabriel, Poderoso, Juan J, Ashizawa, Tetsuo (in press). Spinocerebellar Ataxia Type 10: Description of a family from Argentina. Neurology.

Goldberg, Y. P., Kalchman, M. A., Metzler, M., Nasir, J., Zeisler, J., Graham, R., Koide, H. B., O'Kusky, J., Sharp, A. H., Ross, C. A., *et al.* (1996). Absence of disease phenotype and intergenerational stability of the CAG repeat in transgenic mice expressing the human Huntington disease transcript. Hum Mol Genet 5, 177-185.

Gunter, C., Paradee, W., Crawford, D. C., Meadows, K. A., Newman, J., Kunst, C. B., Nelson, D. L., Schwartz, C., Murray, A., Macpherson, J. N., *et al.* (1998). Re-examination of factors associated with expansion of CGG repeats using a single nucleotide polymorphism in FMR1. Hum Mol Genet 7, 1935-1946.

Handa, V., Yeh, H. J., McPhie, P., and Usdin, K. (2005). The AUUCU repeats responsible for spinocerebellar ataxia type 10 form unusual RNA hairpins. J Biol Chem 280, 29340-29345.

Ho, T. H., Bundman, D., Armstrong, D. L., and Cooper, T. A. (2005). Transgenic mice expressing CUG-BP1 reproduce splicing mis-regulation observed in myotonic dystrophy. Hum Mol Genet 14, 1539-1547.

Holmes, S. E., O'Hearn, E. E., McInnis, M. G., Gorelick-Feldman, D. A., Kleiderlein, J. J., Callahan, C., Kwak, N. G., Ingersoll-Ashworth, R. G., Sherr, M., Sumner, A. J., *et al.* (1999). Expansion of a novel CAG trinucleotide repeat in the 5' region of PPP2R2B is associated with SCA12. Nat Genet 23, 391-392.

Idriss, H., Kumar, A., Casas-Finet, J. R., Guo, H., Damuni, Z., and Wilson, S. H. (1994). Regulation of in vitro nucleic acid strand annealing activity of heterogeneous nuclear ribonucleoprotein protein A1 by reversible phosphorylation. Biochemistry 33, 11382-11390.

Ito, K., Sato, K., and Endo, H. (1994). Cloning and characterization of a single-stranded DNA binding protein that specifically recognizes deoxycytidine stretch. Nucleic Acids Res 22, 53-58.

Jellinger, K. A., and Stadelmann, C. H. (2000). The enigma of cell death in neurodegenerative disorders. J Neural Transm Suppl, 21-36.

Johnson, C. L., Lu, D., Huang, J., and Basu, A. (2002). Regulation of p53 stabilization by DNA damage and protein kinase C. Mol Cancer Ther 1, 861-867.

Kanthasamy, A. G., Anantharam, V., Zhang, D., Latchoumycandane, C., Jin, H., Kaul, S., and Kanthasamy, A. (2006). A novel peptide inhibitor targeted to caspase-3 cleavage site of a proapoptotic kinase protein kinase C delta (PKCdelta) protects

against dopaminergic neuronal degeneration in Parkinson's disease models. Free Radic Biol Med 41, 1578-1589.

Klebe, S., Durr, A., Rentschler, A., Hahn-Barma, V., Abele, M., Bouslam, N., Schols, L., Jedynak, P., Forlani, S., Denis, E., *et al.* (2005). New mutations in protein kinase Cgamma associated with spinocerebellar ataxia type 14. Ann Neurol 58, 720-729.

Klesert, T. R., Cho, D. H., Clark, J. I., Maylie, J., Adelman, J., Snider, L., Yuen, E. C., Soriano, P., and Tapscott, S. J. (2000). Mice deficient in Six5 develop cataracts: implications for myotonic dystrophy. Nat Genet 25, 105-109.

Koch, K. S., and Leffert, H. L. (1998). Giant hairpins formed by CUG repeats in myotonic dystrophy messenger RNAs might sterically block RNA export through nuclear pores. J Theor Biol 192, 505-514.

Lancaster, H. O. (1990). Expectations of Life: A study in the Demography, Statistics, and History of World Mortality (New York: Springer Verlag).

Larsen, K. E., and Sulzer, D. (2002). Autophagy in neurons: a review. Histol Histopathol 17, 897-908.

Lasfer, M., Davenne, L., Vadrot, N., Alexia, C., Sadji-Ouatas, Z., Bringuier, A. F., Feldmann, G., Pessayre, D., and Reyl-Desmars, F. (2006). Protein kinase PKC delta and c-Abl are required for mitochondrial apoptosis induction by genotoxic stress in the absence of p53, p73 and Fas receptor. FEBS Lett 580, 2547-2552.

Lee, M. H., Mori, S., and Raychaudhuri, P. (1996). trans-Activation by the hnRNP K protein involves an increase in RNA synthesis from the reporter genes. J Biol Chem 271, 3420-3427.

Lee, S. T., and Kim, M. (2006). Aging and neurodegeneration. Molecular mechanisms of neuronal loss in Huntington's disease. Mech Ageing Dev 127, 432-435.

Li, L., Lorenzo, P. S., Bogi, K., Blumberg, P. M., and Yuspa, S. H. (1999). Protein kinase Cdelta targets mitochondria, alters mitochondrial membrane potential, and

induces apoptosis in normal and neoplastic keratinocytes when overexpressed by an adenoviral vector. Mol Cell Biol 19, 8547-8558.

Lin, X., and Ashizawa, T. (2003). SCA10 and ATTCT repeat expansion: clinical features and molecular aspects. Cytogenet Genome Res 100, 184-188.

Lin, X., and Ashizawa, T. (2005). Recent progress in spinocerebellar ataxia type-10 (SCA10). Cerebellum 4, 37-42.

Lynch, M., Chen, L., Ravitz, M. J., Mehtani, S., Korenblat, K., Pazin, M. J., and Schmidt, E. V. (2005). hnRNP K binds a core polypyrimidine element in the eukaryotic translation initiation factor 4E (eIF4E) promoter, and its regulation of eIF4E contributes to neoplastic transformation. Mol Cell Biol 25, 6436-6453.

Majumder, P. K., Mishra, N. C., Sun, X., Bharti, A., Kharbanda, S., Saxena, S., and Kufe, D. (2001). Targeting of protein kinase C delta to mitochondria in the oxidative stress response. Cell Growth Differ 12, 465-470.

Majumder, P. K., Pandey, P., Sun, X., Cheng, K., Datta, R., Saxena, S., Kharbanda, S., and Kufe, D. (2000). Mitochondrial translocation of protein kinase C delta in phorbol ester-induced cytochrome c release and apoptosis. J Biol Chem 275, 21793-21796.

Mankodi, A., Urbinati, C. R., Yuan, Q. P., Moxley, R. T., Sansone, V., Krym, M., Henderson, D., Schalling, M., Swanson, M. S., and Thornton, C. A. (2001). Muscleblind localizes to nuclear foci of aberrant RNA in myotonic dystrophy types 1 and 2. Hum Mol Genet 10, 2165-2170.

Manley, K., Pugh, J., and Messer, A. (1999). Instability of the CAG repeat in immortalized fibroblast cell cultures from Huntington's disease transgenic mice. Brain Res 835, 74-79.

Marz, P., Probst, A., Lang, S., Schwager, M., Rose-John, S., Otten, U., and Ozbek, S. (2004). Ataxin-10, the spinocerebellar ataxia type 10 neurodegenerative disorder protein, is essential for survival of cerebellar neurons. J Biol Chem 279, 35542-35550.

Matsuura, T., Achari, M., Khajavi, M., Bachinski, L. L., Zoghbi, H. Y., and Ashizawa, T. (1999). Mapping of the gene for a novel spinocerebellar ataxia with pure cerebellar signs and epilepsy. Ann Neurol 45, 407-411.

Matsuura, T., and Ashizawa, T. (2002). Polymerase chain reaction amplification of expanded ATTCT repeat in spinocerebellar ataxia type 10. Ann Neurol 51, 271-272.

Matsuura, T., Fang, P., Lin, X., Khajavi, M., Tsuji, K., Rasmussen, A., Grewal, R. P., Achari, M., Alonso, M. E., Pulst, S. M., *et al.* (2004). Somatic and germline instability of the ATTCT repeat in spinocerebellar ataxia type 10. Am J Hum Genet 74, 1216-1224.

Matsuura, T., Fang, P., Pearson, C. E., Jayakar, P., Ashizawa, T., Roa, B. B., and Nelson, D. L. (2006). Interruptions in the expanded ATTCT repeat of spinocerebellar ataxia type 10: repeat purity as a disease modifier? Am J Hum Genet 78, 125-129.

Matsuura, T., Yamagata, T., Burgess, D. L., Rasmussen, A., Grewal, R. P., Watase, K., Khajavi, M., McCall, A. E., Davis, C. F., Zu, L., *et al.* (2000). Large expansion of the ATTCT pentanucleotide repeat in spinocerebellar ataxia type 10. Nat Genet 26, 191-194.

Meriin, A. B., and Sherman, M. Y. (2005). Role of molecular chaperones in neurodegenerative disorders. Int J Hyperthermia 21, 403-419.

Michelotti, E. F., Michelotti, G. A., Aronsohn, A. I., and Levens, D. (1996). Heterogeneous nuclear ribonucleoprotein K is a transcription factor. Mol Cell Biol 16, 2350-2360.

Montermini, L., Andermann, E., Labuda, M., Richter, A., Pandolfo, M., Cavalcanti, F., Pianese, L., Iodice, L., Farina, G., Monticelli, A., *et al.* (1997). The Friedreich ataxia GAA triplet repeat: premutation and normal alleles. Hum Mol Genet 6, 1261-1266.

Moseley, M. L., Zu, T., Ikeda, Y., Gao, W., Mosemiller, A. K., Daughters, R. S., Chen, G., Weatherspoon, M. R., Clark, H. B., Ebner, T. J., *et al.* (2006). Bidirectional

expression of CUG and CAG expansion transcripts and intranuclear polyglutamine inclusions in spinocerebellar ataxia type 8. Nat Genet 38, 758-769.

Mosemiller, A. K., Dalton, J. C., Day, J. W., and Ranum, L. P. (2003). Molecular genetics of spinocerebellar ataxia type 8 (SCA8). Cytogenet Genome Res 100, 175-183.

Moumen, A., Masterson, P., O'Connor, M. J., and Jackson, S. P. (2005). hnRNP K: an HDM2 target and transcriptional coactivator of p53 in response to DNA damage. Cell 123, 1065-1078.

Nguyen, H. P., Kobbe, P., Rahne, H., Worpel, T., Jager, B., Stephan, M., Pabst, R., Holzmann, C., Riess, O., Korr, H., *et al.* (2006). Behavioral abnormalities precede neuropathological markers in rats transgenic for Huntington's disease. Hum Mol Genet 15, 3177-3194.

Ostrowski, J., Kawata, Y., Schullery, D. S., Denisenko, O. N., Higaki, Y., Abrass, C. K., and Bomsztyk, K. (2001). Insulin alters heterogeneous nuclear ribonucleoprotein K protein binding to DNA and RNA. Proc Natl Acad Sci U S A 98, 9044-9049.

Ostrowski, J., Klimek-Tomczak, K., Wyrwicz, L. S., Mikula, M., Schullery, D. S., and Bomsztyk, K. (2004). Heterogeneous nuclear ribonucleoprotein K enhances insulin-induced expression of mitochondrial UCP2 protein. J Biol Chem 279, 54599-54609.

Paziewska, A., Wyrwicz, L. S., Bujnicki, J. M., Bomsztyk, K., and Ostrowski, J. (2004). Cooperative binding of the hnRNP K three KH domains to mRNA targets. FEBS Lett 577, 134-140.

Piano, F., Schetter, A. J., Morton, D. G., Gunsalus, K. C., Reinke, V., Kim, S. K., and Kemphues, K. J. (2002). Gene clustering based on RNAi phenotypes of ovary-enriched genes in C. elegans. Curr Biol 12, 1959-1964.

Potaman, V. N., Bissler, J. J., Hashem, V. I., Oussatcheva, E. A., Lu, L., Shlyakhtenko, L. S., Lyubchenko, Y. L., Matsuura, T., Ashizawa, T., Leffak, M., *et al.* (2003). Unpaired structures in SCA10 (ATTCT)n.(AGAAT)n repeats. J Mol Biol 326, 1095-1111.

Przedborski, S., Vila, M., and Jackson-Lewis, V. (2003). Neurodegeneration: what is it and where are we? J Clin Invest 111, 3-10.

Raji, G. (2002). Clinical features and ATTCT repeat expansion in Spinocerebellar Ataxia Type 10. Archives of Neurology 59, 1285-1290.

Raskin, S., Ashizawa,Tetsuo, Teive, Hélio A.G., Arruda, Walter, Fang, Ping, Gao, Rui, White, Misti, Werneck, Lineu C., and Roa, Benjamin (In press). Reduced penetrance in a Brazilian family with Spinocerebellar Ataxia type 10. Archives of Neurology.

Raskin, S. M., PhD1, Tetsuo Ashizawa, MD2, Hélio A.G. Teive, MD. PhD3, Walter Arruda.MD3, M.D., Ping Fang, PhD4; Rui Gao, MD2, Misti Caudle-White2, Lineu C. Werneck, MD, PhD3 and Benjamin Roa, PhD4; (2006). Reduced penetrance in a Brazilian family with Spinocerebellar Ataxia type 10. Archives of Neurology in press.

Rasmussen, A., Matsuura, T., Ruano, L., Yescas, P., Ochoa, A., Ashizawa, T., and Alonso, E. (2001). Clinical and genetic analysis of four Mexican families with spinocerebellar ataxia type 10. Ann Neurol 50, 234-239.

Salvesen, G. S., and Dixit, V. M. (1997). Caspases: intracellular signaling by proteolysis. Cell 91, 443-446.

Schullery, D. S., Ostrowski, J., Denisenko, O. N., Stempka, L., Shnyreva, M., Suzuki, H., Gschwendt, M., and Bomsztyk, K. (1999). Regulated interaction of protein kinase Cdelta with the heterogeneous nuclear ribonucleoprotein K protein. J Biol Chem 274, 15101-15109.

Shnyreva, M., Schullery, D. S., Suzuki, H., Higaki, Y., and Bomsztyk, K. (2000). Interaction of two multifunctional proteins. Heterogeneous nuclear ribonucleoprotein K and Y-box-binding protein. J Biol Chem 275, 15498-15503.

Siomi, H., Choi, M., Siomi, M. C., Nussbaum, R. L., and Dreyfuss, G. (1994). Essential role for KH domains in RNA binding: impaired RNA binding by a mutation in the KH domain of FMR1 that causes fragile X syndrome. Cell 77, 33-39.

Skalweit, A., Doller, A., Huth, A., Kahne, T., Persson, P. B., and Thiele, B. J. (2003). Posttranscriptional control of renin synthesis: identification of proteins interacting with renin mRNA 3'-untranslated region. Circ Res 92, 419-427.

Steinberg, S. F. (2004). Distinctive activation mechanisms and functions for protein kinase Cdelta. Biochem J 384, 449-459.

Sumitomo, M., Ohba, M., Asakuma, J., Asano, T., Kuroki, T., Asano, T., and Hayakawa, M. (2002). Protein kinase Cdelta amplifies ceramide formation via mitochondrial signaling in prostate cancer cells. J Clin Invest 109, 827-836.

Svitkin, Y. V., Ovchinnikov, L. P., Dreyfuss, G., and Sonenberg, N. (1996). General RNA binding proteins render translation cap dependent. Embo J 15, 7147-7155.

Szallasi, Z., Bogi, K., Gohari, S., Biro, T., Acs, P., and Blumberg, P. M. (1996). Non-equivalent roles for the first and second zinc fingers of protein kinase Cdelta. Effect of their mutation on phorbol ester-induced translocation in NIH 3T3 cells. J Biol Chem 271, 18299-18301.

Taylor, J. P., Hardy, J., and Fischbeck, K. H. (2002). Toxic proteins in neurodegenerative disease. Science 296, 1991-1995.

Teive, H. A., Roa, B. B., Raskin, S., Fang, P., Arruda, W. O., Neto, Y. C., Gao, R., Werneck, L. C., and Ashizawa, T. (2004). Clinical phenotype of Brazilian families with spinocerebellar ataxia 10. Neurology 63, 1509-1512.

Thisted, T., Lyakhov, D. L., and Liebhaber, S. A. (2001). Optimized RNA targets of two closely related triple KH domain proteins, heterogeneous nuclear ribonucleoprotein K and alphaCP-2KL, suggest Distinct modes of RNA recognition. J Biol Chem 276, 17484-17496.

Voss, O. H., Kim, S., Wewers, M. D., and Doseff, A. I. (2005). Regulation of monocyte apoptosis by the protein kinase Cdelta-dependent phosphorylation of caspase-3. J Biol Chem 280, 17371-17379.

Wakamiya, M., Matsuura, T., Liu, Y., Schuster, G. C., Gao, R., Xu, W., Sarkar, P. S., Lin, X., and Ashizawa, T. (2006). The role of ataxin 10 in the pathogenesis of spinocerebellar ataxia type 10. Neurology 67, 607-613.

Wakamiya M, M. T., Liu Y, Schuster GC, Gao R, Xu W, Sarkar P, Lin X, Ashizawa T Neurology (2006). The role of ataxin 10 in spinocerebellar ataxia type 10 pathogenesis. Neurology (in press).

Waragai, M., Nagamitsu, S., Xu, W., Li, Y. J., Lin, X., and Ashizawa, T. (2006). Ataxin 10 induces neuritogenesis via interaction with G-protein beta2 subunit. J Neurosci Res 83, 1170-1178.

Weisman-Shomer, P., Cohen, E., and Fry, M. (2000). Interruption of the fragile X syndrome expanded sequence d(CGG)(n) by interspersed d(AGG) trinucleotides diminishes the formation and stability of d(CGG)(n) tetrahelical structures. Nucleic Acids Res 28, 1535-1541.

Yuan, J., and Yankner, B. A. (1999). Caspase activity sows the seeds of neuronal death. Nat Cell Biol 1, E44-45.

Zu, L., Figueroa, K. P., Grewal, R., and Pulst, S. M. (1999). Mapping of a new autosomal dominant spinocerebellar ataxia to chromosome 22. Am J Hum Genet 64, 594-599.

Vita

Misti Caudle White was born January 1, 1981 to Barbara Helen Caudle and Emmett Dale Caudle in Silver City, New Mexico. She grew up in Abilene, Texas where she attended Cooper High School. After high school she attended college at Texas Christian University where she graduated Magna Cum Laude and was awarded the senior scholar award for her major, biology. Following college, she married Jeff White and began her education at University of Texas Medical Branch in Galveston, Texas. While at UTMB, she was awarded Who's Who among American Colleges and Universities, and served as vice president of the Society for Cell Biology Students, and on a task force committed to change the curriculum of the Cell Biology Students.

Permanent address: 2701 Broken Bough, Abilene, TX, 79606

This dissertation was typed by Misti Caudle White.